SSD

SCIENCE FOR A SUSTAINABLE DEVELOPMENT

ADVANCED EXPLOITATION OF GROUND-BASED MEASUREMENTS FOR ATMOSPHERIC CHEMISTRY AND CLIMATE APPLICATIONS - II

AGACC-II

M. DE MAZIÈRE, H. DE BACKER, J. VANDER AUWERA, E. MAHIEU

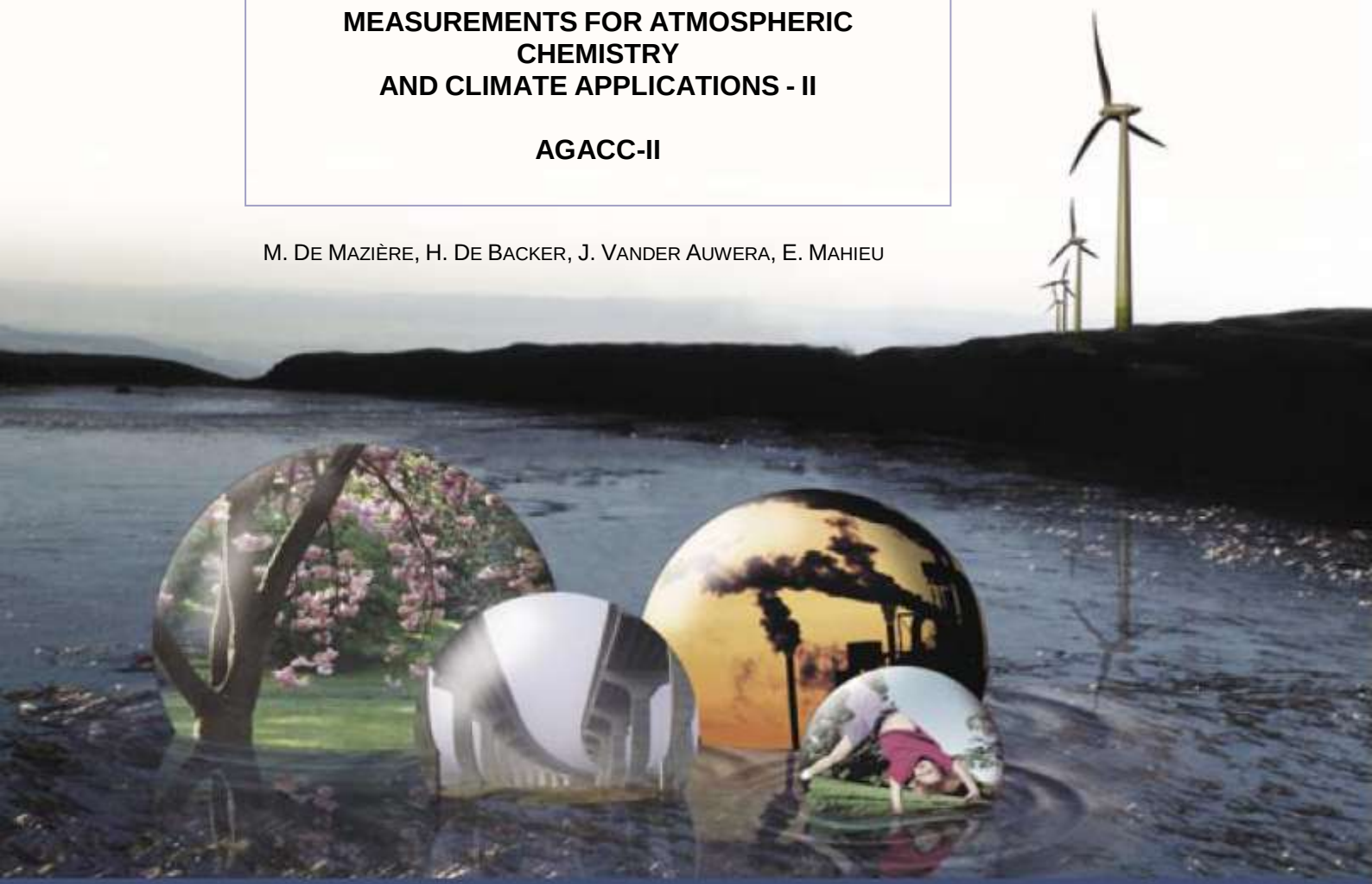

ENERGY

TRANSPORT AND MOBILITY

AGRO-FOOD

HEALTH AND ENVIRONMENT

CLIMATE

BIODIVERSITY

ATMOSPHERE AND TERRESTRIAL AND MARINE ECOSYSTEMS

TRANSVERSAL ACTIONS

.be

SCIENCE FOR A SUSTAINABLE DEVELOPMENT
(SSD)

Climate

FINAL REPORT

AGACC-II:
ADVANCED EXPLOITATION OF GROUND-BASED MEASUREMENTS FOR ATMOSPHERIC CHEMISTRY AND CLIMATE APPLICATIONS - II

SD/CS/07A

Promotors

Belgisch Instituut voor Ruimte Aeronomie (BIRA-IASB)
Ringlaan 3 – 1180 Brussel

Koninklijk Meteorologisch Instituut van België (KMI-IRM)
Ringlaan 3 – 1180 Brussel

Université Libre de Bruxelles (ULB)
Service de Chimie Quantique et Photophysique – C.P. 160/09
50 avenue F.D. Roosevelt – 1050 Bruxelles

University of Liège (ULg)
Quartier Agora
Allée du 6 Août, 19 – 4000 Liège

Authors

Martine De Mazière, Corinne Vigouroux, François Hendrick, Clio Gielen (BIRA-IASB)
Hugo De Backer, Veerle De Bock (KMI-IRM)
Jean Vander Auwera (ULB)
Emmanuel Mahieu (ULg)

Advanced exploitation of Ground based measurements Atmospheric Chemistry and Climate applications

Published in 2017 by the Belgian Science Policy
Avenue Louise 231
Louizalaan 231
B-1050 Brussels
Belgium
Tel: +32 (0)2 238 34 11 – Fax: +32 (0)2 230 59 12
http://www.belspo.be

Contact person: Martine Vanderstraeten
+32 (0)2 238 36 10

M. De Mazière, C. Vigouroux, F. Hendrick, C. Gielen, H. De Backer, V. De Bock, J. Vander Auwera, E. Mahieu. ***AGACC-II: Advanced Exploitation of Ground-Based Measurements for Atmospheric Chemistry and Climate Applications – II. Final Report.*** Brussels: Belgian Science Policy 2017 – 101 p. (Research Programme Science for a Sustainable Development)

TABLE OF CONTENT

SUMMARY

A. Context

AGACC-II supports the development and improvement of various ground-based remote-sensing techniques for the monitoring of the atmospheric composition. Such research is required in the context of the international monitoring networks to which the partners contribute, like the Network for the Detection of Atmospheric Composition Change (NDACC) and the Total Carbon Column Observing Network (TCCON), and in the context of the Copernicus Atmospheric Monitoring Service (CAMS): CAMS requires independent data for validation of the products delivered to the society that are generated through numerical modeling and satellite and in-situ surface data assimilation. AGACC-II includes the essential laboratory spectroscopic research to provide improved reference spectroscopic data: these are indispensable ingredients in the analysis of the remote-sensing data.

B. Objectives

1 To improve or expand the measurement capabilities for greenhouse gases (CO_2, CH_4 and N_2O, as well as CF_4 and CCl_4) with FTIR spectrometers at Jungfraujoch and Ile de La Réunion; to make Ile de La Réunion a site affiliated to the Total Carbon Column Observing Network (TCCON), and to deliver long-term trends of the major greenhouse gases at the Jungfraujoch back to 1976.

2 To extend the measurement capabilities of ground-based FTIR spectrometry to various volatile organic compounds (CH_3Cl, CH_3OH, PAN, acetone) and to some CFC-substitutes, and consequently, using also the results for CCl_4 and CF_4 mentioned above, to establish representative CCl_y and CF_y budgets at the Jungfraujoch, including the contributions from the new AGACC-II halocarbons and of the standard FTIR products (CFC-11 and -12, HCFC-22). It is also planned to revise the time series for C_2H_4, C_2H_6, HCHO based on better laboratory data, at Jungfraujoch and Ile de La Réunion.

3 To provide improved laboratory spectroscopic data in support of the above objectives 1 and 2.

4 To advance our understanding of aerosol characteristics above Ukkel and to estimate the aerosol direct radiative forcing above Ukkel. Therefore the underlying objectives are
   a. to retrieve more information regarding aerosol properties from remote sensing measurements with Brewer and MAXDOAS spectrometers;
   b. to deploy a lidar ceilometer at Ukkel;
   c. to combine the information from all instruments including those from the CIMEL sun photometer, for a more comprehensive evaluation of the aerosol properties at Ukkel;
   d. to derive information about the aerosol sources by modeling with CHIMERE and backtrajectory studies;

5 To implement MAXDOAS measurements in Bujumbura (Burundi, Africa) for the measurement of aerosol and ozone precursors (NO_2, glyoxal, HCHO,…) and to study the export of African emissions to the Indian Ocean (Ile de La Réunion).

6 To make sure that the results of the project are disseminated appropriately and that they are integrated in national and international environmental assessments in support of policy makers.

C. Conclusions

All objectives of the project have been met.

1 The Reunion site has been accepted as a TCCON–compliant operational site in 2012. The absolute calibration of the TCCON data will be performed in the frame of the BRAIN pioneering project UAV_Reunion. The TCCON data are also affiliated to ICOS. Time series of XCO_2, XCH_4, XN_2O, XCO are available starting Sept. 2011 (X stands for the column-averaged dry-air volume mixing ratio).
Homogenized long-term time series of methane and nitrous oxide concentrations back to 1977 have been generated at the Jungfraujoch, including historical grating spectrometer data. They have enabled the evaluation of almost 40-years trends, showing slightly varying increase rates throughout the period.
For CO_2, it has turned out that the historical spectra cannot be exploited, and therefore the timeseries cannot be extended before 1985, i.e., not before the time when regular FTS observations have started.
Other important halogenated greenhouse gases are CCl_4 and CF_4; they contribute significantly to climate forcing and to the organic chlorine and fluorine budgets in the atmosphere. At the Jungfraujch, retrieval strategies for both species have been developed successfully and long-term time series have been derived. CCl_4 has been decreasing over the period 1999-2014, in line with in-situ observations, whereas CF_4 is still increasing, even if the increase rate has slightly slowed down since 1998 as compared to the period 1989-1997.

2 In the course of AGACC-II, it has been demonstrated that several volatile organic species (VOC) can be detected and retrieved at Reunion Island and at the Jungfraujoch. Retrieval strategies have been developed and/or optimized at both sites, taking into account the local conditions of site altitude, humidity and VOC concentrations.
Species that have been retrieved and studied, and in several cases compared to model simulations and/or satellite and in-situ surface data, are carbon monoxide (CO), methanol (CH_3OH), formic acid (HCOOH), formaldehyde (HCHO), ethylene (C_2H_4), and ethane (C_2H_6). For several species, diurnal and seasonal variations as well as their interannual variability (e.g., at Reunion Island linked to biomass burning), have been evaluated.
At Reunion, it has appeared clearly that the move from the Bruker 120M to the Bruker 125HR spectrometer, and then from St. Denis to Maido has improved significantly the signal-to-noise ratio of the spectra and therefore the feasibility of studying the variabilities of geophysical nature.
The FTIR data have supported the identification of a missing source of HCOOH in the atmosphere. Methanol at the Jungfraujoch has shown a stable abundance over the last 17 years; some discrepancies with IMAGESv2 model simulations have been identified. The use of the new linelist for C_2H_4

generated in the laboratory by the ULB partner has improved the retrieval of this species. Also for C_2H_6, new pseudolines based on Xsections published in 2010 and optimized choices of the retrieval microwindows have improved the retrieval quality. Time-series of formaldehyde at the Jungfraujoch covering the 1995-2013 period show a negative trend; the cause of this decrease is still under investigation. An important task has been the comparison between MAXDOAS and FTIR formaldehyde columns at the Jungfraujoch: comparisons with satellite and model data and the investigation of both techniques' sensitivities have confirmed that both datasets are complementary and do not contradict each other.
At both sites, methylchloride (CH_3Cl) has also been studied. At Reunion Island, it turns out that more reliable results are obtained at Maido, and that we need some more years to confirm the seasonal variation. At Jungfraujoch, thanks to recent spectroscopic improvements, CH_3Cl has been retrieved with good quality and a time series spanning the 2000-2014 period has been derived, showing a good agreement with in situ data, year-to-year variations and a small positive trend.
Attempts to retrieve PAN (peroxyacetilenitrate) and acetone have not been successful for acetone, because of the lack of appropriate spectroscopic data; they have also not been successful for PAN at the Jungfraujoch; at Reunion Island, some results have been obtained but improvements are certainly required to generate more reliable data.
At Jungfraujoch, it has been demonstrated that retrievals of HCFC-142b are possible, and a time series covering the 2000-2012 period has been generated, confirming the strong increase rate also observed by the AGAGE in-situ network.

Thanks to the derivation of CCl_4, CF_4 and HCFC-142b concentrations, the total budgets of organic chlorine and fluorine have been updated: CCl_y is found to decrease over the period 2000-2014 by 0.23%/yr, whereas CF_y is found to still increase at a rate of 0.6%/yr over the same time period.

3 New spectroscopic data for line intensities and self-broadening coefficients for the υ_7 band observed in the 10 μm region of the ethylene spectrum have been acquired and an update to the corresponding data in HITRAN 2012 was generated. Use of these update data in the inversion of atmospheric solar absorption spectra recorded at the Jungfraujoch and at Ile de La Reunion have led to a systematic reduction of the C_2H_4 columns by (4.1 $\pm$ 0.1) % and (4.6 $\pm$4.2) %, resp. This same spectral region also includes weaker absorption bands coupled to υ_7: a combined frequency and intensity analysis of these bands has been performed. A HITRAN-formatted list of parameters for 65420 lines of the υ_{10} / υ_7 / υ_4 / υ_{12} bands has been built. It provides a consistent description of the 620 – 1525 cm^{-1} spectral region of the $^{12}C_2H_4$ spectrum and constitutes an improvement over the information currently available in the HITRAN and GEISA databases.
Experimental determination of line intensities for formaldehyde near 3.4 μm (2600 – 3100 cm^{-1} region) can be affected by the easy polymerization of the molecule. Therefore a special set-up was conceived, involving simultaneous measurements in specific ranges of the target IR region using a tunable diode

laser (TDL) and of pure rotational lines in the far-infrared (FIR; 0 – 400 cm^{-1} range) using a high resolution Fourier transform spectrometer. Because of the limited quality of the recorded TDL spectra, only a confirmation of the uncertainty of 5–10% estimated for the intensities of strong lines provided in HITRAN could be obtained.
Ethane remote-sensing measurements in the earth atmosphere use the 3.3 μm spectral region. The plan was to improve the reference line positions and intensities. Laboratory spectra have been taken and a theoretical model of the vibration-rotation structure was used to analyse them. At present, the results are unsatisfactory. Another rotational analysis, without relying on a model, was therefore initiated. Although the results are limited up to now, this work is an important step in the understanding of the very complicated spectrum of ethane.

4 Various types of aerosol measurements have been performed at Ukkel: Brewer and sunphotometer measurements of total Aerosol Optical Depth (AOD), MAXDOAS and ceilometer measurements in the lower troposphere of the AOD and aerosol extinction profile, and backscatter profile, resp., as well as aethalometer and nephelometer in-situ data at ground-level.
All these datasets have been optimized and exploited together and in combination with modeling tools (backtrajectories and Chimere).
For the Brewer spectrometer, the cloud screening method has been improved, resulting in a more automatic procedure for deriving the AOD at 340 nm from Brewer sun scan measurements. This new cloud screening method has also been applied to Brewer direct sun measurements in the UV. In parallel, a new inversion method has been developed to extract the aerosol single scattering albedo from Brewer UV measurements. However, this method requires further improvements before delivering reliable results. The AOD and/or SSA measurements from the Brewer will be implemented in the UV-index forecast model in the future.
Also for the MAXDOAS measurements, cloud-screening has proven to be very important to obtain reliable aerosol extinction profiles: a new method based on the colour index has been developed. The method has been validated by comparing the MAXDOAS data with correlative and complementary data from the sunphotometer and an infrared pyranometer available at Ukkel. Ceilometer data about the aerosol backscatter profiles are obtained through an iterative inversion approach constrained by the sunphotometer data. The ceilometer data also deliver the mixing layer height (with a retrieval procedure developed at KMI-IRM), and these measurements have been validated against the values computed by ECMWF and ALARO7, and against radio-soundings data. The agreement was shown to be good except under specific conditions; therefore a quality flagging method has been developed to automatically detect the failure of the retrieval.
The success of the ceilometer developments has led to the installation of three more ceilometers in Belgium, with near-real-time delivery of data on a dedicated Website.

The chemical transport model CHIMERE has been used together with the OPAC software package to model the optical properties of aerosols based on

their chemical composition. One of the uncertainties in this study comes from the fact that CHIMERE chemical aerosol categories do not correspond directly to the aerosol categories present in OPAC which is used to convert the chemical properties of the aerosol in the output of CHIMERE into optical properties that are comparable then to the remote-sensing and in-situ observational data. At present, the agreements between direct observations and modeled observations of AOD (via CHIMERE and OPAC) are rather poor and more research is needed.
Another study looks for the source regions using the APTRA parcel trajectories model available at ECMWF, and meteorological parameters like wind direction and speed, and humidity. The current results indicate that it is not possible to develop a model based on meteorological parameters only, to forecast AOD.

Simultaneous measurements of the erythemal UV dose, global solar radiation, total ozone column and AOD at 320.1 nm are now available for a period of 23 years (1991-2013): they have been used to determine the mutual relationships between the four parameters. Linear trends have been determined, a change point analysis has been carried out, and a multiple linear regression method has been used to explore the correlations on a daily and seasonal scale. The conclusions of these analyses are multiple and have been published in De Bock et al. (2014). Among the conclusions is the fact that the UV irradiance changes are impacted by changes in aerosol and cloud properties, and that the latter have changed over the past 23 years.

5 A MAXDOAS and sunphotometer instrument have been installed in Bujumbura in November 2013: both instruments are operational since then and are maintained by E. Nzendako from the University of Burundi, who was trained in Brussels during late 2012 up to end of February 2013.
The data analysed up to now (AOD, NO_2 and HCHO vertical profiles and columns) have been used for the validation of the GOME-2A, GOME-2B and OMI satellite data. It is found that the use of the MAXDOAS measured vertical profiles as a priori in the satellite retrievals has a significant effect on the resulting columns and improves the agreement between both datasets. Diurnal cycles are being investigated. Also the retrieval of glyoxal (CHOCHO) has been improved, leading to agreements with satellite data within the error bars.

D. Contribution of the project in a context of scientific support to a sustainable development policy

The project contributes to a better knowledge of the atmospheric composition and its variability, in particular its long-term evolution. This information is important to support policy makers with sound and objective scientific information when they have to design regulations for progressing towards a sustainable socio-economic model.

E. Keywords

Remote-sensing, spectroscopic reference data, NDACC, TCCON, ICOS, greenhouse gases, volatile organic compounds, aerosol, ground-based networks, atmospheric composition, FTIR, MAXDOAS, Brewer, ceilometer, trends.

1. INTRODUCTION

Knowledge about the atmospheric composition (gases and aerosol) and about its long-term evolution is of major importance in the investigation of current environmental issues such as climate change and air quality. This knowledge must come from observations, preferably long-term and of high quality and consistency, theoretical and numerical modelling studies, and laboratory experiments. Remote sensing of the atmospheric composition is one of the available observation techniques, in which the AGACC-II partners have a strong, internationally recognized expertise; it is used from airborne, ground- and space-based platforms.
Advances in our knowledge continuously raise new questions, and to answer these, the observations must be improved as to precision, accuracy, and detection capabilities, and the available time series must be extended in time and space, and possibly be updated and homogenized to match the current state-of-the-art. These are the essential goals of AGACC-II.

A first specific objective has been to improve or expand the measurement capabilities for greenhouse gases (CO_2, CH_4 and N_2O, as well as CF_4 and CCl_4) with FTIR spectrometers at Jungfraujoch and Reunion Island, and to deliver long-term trends of the major greenhouse gases at the Jungfraujoch back to 1976.
The second aim has been extending the measurement capabilities of ground-based FTIR spectrometry to various volatile organic compounds (CH_3Cl, CH_3OH, PAN, acetone) and to some CFC-substitutes, and consequently, using also the results for CCl_4 and CF_4 mentioned above, to establish representative CCl_y and CF_y budgets at the Jungfraujoch, including the contributions from the new AGACC-II halocarbons and of the standard FTIR products (CFC-11 and -12, HCFC-22). It was also planned to revise the time series for C_2H_4, C_2H_6, HCHO based on better laboratory data, at Jungfraujoch and Reunion Island.

A third major objective has been to improve the capabilities for aerosol detection and characterization, and to use various observational techniques supported by model studies (backtrajectory studies and regional chemistry-transport modeling) to advance our understanding of the aerosol occurrences above Ukkel.

The fourth specific objective has been to start new ground-based remote sensing atmospheric measurements in Africa, namely in Bujumbura in Burundi, with a focus on air quality. They are also extremely wanted for satellite validation.

The optical remote sensing measurements performed in AGACC-II are of spectrometric nature. As such, they entirely depend on the availability of reference spectroscopic information for the target species, measured in the laboratory. This information is of utmost importance: be it absent, optical remote sensing measurements can not be made. Although such an information exists, its completeness and accuracy for instance do not necessarily meet the requirements of current atmospheric research and may introduce biases in the results obtained and conclusions drawn. Reference spectroscopic information is bound to evolve because it can be very difficult to measure accurately in the laboratory and such activities are intimately linked with technological progress and financial support. Therefore, in parallel with its main objectives, AGACC-II aimed to improve reference spectroscopic information for a number of minor or

trace gaseous constituents of the atmosphere, in spectral regions actually used to probe them using optical remote sensing techniques. Specific regions of the infrared spectrum of three species, namely formaldehyde (HCHO), ethylene (C_2H_4) and ethane (C_2H_6), were identified as targets. These choices were guided by the quality of the reference spectroscopic information available, either possibly biased (ethylene and formaldehyde) or providing a too approximate description of the spectrum of the target molecule (ethane).

In addition, we measured improved reference spectroscopic information for carbon dioxide (CO_2) and contributed to the improvement of a spectroscopic model for that species aiming to reach the needs to quantify and map the sources and sinks of CO_2 (Crisp et al., 2004; Crisp et al., 2009).

The AGACC-II partners contribute to international global observation networks and to the spectroscopy community and submit their data to the associated international databases (NDACC, TCCON, WOUDC, HITRAN, …).

Therefore the achievements realized in AGACC-II must be considered in this international context in which expertise and data are exchanged for the benefit of all. The partners are also involved with satellite observations and have direct links to modeling teams, strengthening the dissemination and exploitation of the results.

In addition, they contribute regularly to the scientific literature and symposia for communication of the outcomes of the project.

Their results are also picked up in policy-oriented environmental assessments such as the MIRA-T reports at the Belgian/regional level and the WMO Assessment of Ozone Depletion at the international level.

2. METHODOLOGY AND RESULTS

WP1: Exploitation of FTIR spectra to derive useful geophysical information for a suite of GHGs (CO_2, CH_4, N_2O, CF_4, CCl_4)

Task 1.1. Produce time series for the major GHGs CO2, CH4 and N2O

Task 1.1.1 Analyse historical grating spectra at the Jungfraujoch between 1976 and 1989, merge them with more recent data and derive long-term trends of the major greenhouse gases CO2, CH4 and N2O above the Jungfraujoch.

METHODOLOGY

Historical solar spectra recorded at the Jungfraujoch with a high-resolution grating spectrometer have been re-analyzed to derive total columns of a series of atmospheric gases. This instrument was used in the sixties and seventies to record two solar spectrum atlases extending from the near-ultraviolet to the near-infrared (from ~300 to ~1200 nm). From 1977 to 1989, it was also regularly and intentionally used to record narrow spectral intervals in the mid-infrared, encompassing absorption lines of gases of atmospheric interest, e.g. CH_4, HF, HCl. More than ten thousand spectra were recorded during this period.

In the past, the plotted grating spectra were analyzed by manually measuring the equivalent width (integrated surface of an absorption line) of the target gas lines with a high-precision Coradi planimeter. They were never analyzed with fitting programs, which did not exist at that time. In AGACC-II, a first significant effort consisted in their transfer from tapes to accessible modern supports, to the cautious and thorough inventory of all available observations, to the identification and solving of internal inconsistencies (e.g. mismatch between the hour and geometry of observation), to the calibration of the spectra in cm^{-1}, to the generation of a dedicated database and to the modification of our fitting chain to accept these early observations. It was then possible to cautiously and consistently re-analyze and valorize these pioneering observations with modern spectral fitting tools, in particular SFIT-2 which is the standard retrieval code in the NDACC Infrared Working Group.

Then, all available observational subsets (various diffraction orders and slit widths were used, resulting in spectral resolution from about 7 to 13 mK) have been investigated to identify suitable lines allowing total column determination of CH_4, N_2O or CO_2.

Strategies were set up for the retrieval of CH_4 and N_2O, for all available observational subsets. Details on the strategies used to retrieve CH_4 total columns from the grating spectra can be found in Bader et al. (2011a) and in Bader (2011b). As to nitrous oxide investigations, several N_2O lines located in the 2481 – 2483 and 2537 – 2540 cm^{-1} spectral intervals were used. These subsets were then harmonized among them.N_2O intercomparisons between columns derived from coincident homemade FTS and grating observations, as well as between grating spectra, showed very good agreement, with ratios of (1.00±0.01) and (1.00±0.02), respectively, allowing to directly combine all ensembles.

For CH_4, the total columns derived from the grating spectra have been combined – after careful intercalibration using common observation days– with the FTIR columns derived at the Jungfraujoch since the mid-1980s, in order to produce consistent datasets and to derive the temporal evolution of methane since 1977.

Table I lists the intervals which include at least an exploitable CO_2 line for its total column retrieval from the grating spectra. It immediately appears that the earlier relevant observation was recorded in November 1983, but this interval spans a weak CO_2 line, preventing reliable retrieval of this GHG in early spectra. All other windows have been systematically recorded from 1985 onwards, i.e. after the start of regular operation of the homemade FTS. Therefore and unfortunately, their exploitation does not allow extending the Jungfraujoch CO_2 total column time series back in time.

Table I: Available spectral ranges and time periods for the retrieval of CO_2 from grating observations at Jungfraujoch.

Spectral range (cm^{-1})	Time period	# days (spectra)	Comment
2481.3-2484.9	11/1983 – 07/1985	24 (61)	Weak feature
2437.2-2442.1	08/1985 – 10/1989	119 (789)	
2416.0-2419.9	10/1985 – 09/1989	93 (1016)	
2386.8-2394.3	10/1985 – 09/1989	74 (412)	

RESULTS

Long-term time series for CH_4 and N_2O above Jungfraujoch, combining in a consistent way the data from three successive instruments, have been obtained.

For CH_4, the trend analysis indicates four consecutive regimes, with relative yearly increase rates close to 0.8% over 1983-1992, 0.4% over 1993-1999, 0% over 2000-2004 and 0.4% over 2005-2010. This is in good agreement with CHASER model results, except over the last years. This latter disagreement points to the need for the model to include updated emissions for that period, e.g. the anomalous emission of methane from wetlands in 2007. Very good agreement is also observed when comparing with *in situ* trends from the AGAGE station of Mace Head in Ireland (see Bader, 2011b).

A recent study has focused on the methane trend after the 2000-2004 plateau, using observations from 10 NDACC sites as well as a tagged model simulation by the GEOS-Chem model, informing on the contribution of the various emission sources (coal, biomass burning, rice cultures…) and sinks (soil absorption, OH oxidation) to the methane budget. The NDACC time series indicate an average trend of 0.30±0.05 %/yr over 2005-2012 (using the 2005.0 columns as reference), with all sites showing a significant increase at the 2σ level of uncertainty. The GEOS-Chem simulation is able to reproduce the observed trends, identifying the anthropogenic emissions from coal, oil and gas as the main drivers for the renewed increase of CH_4 (Bader et al., 2015).

For N_2O, a more regular accumulation is revealed by our three-decadal time series. Nevertheless, we can distinguish between two regimes, with yearly increase rates of (0.39±0.02)% for 1983-1995 and (0.24±0.01)% for 1996-2011 (2-σ), indicating a significant slowing down of the N_2O build up over the last fifteen years (Demoulin et

al., 2011). The latter value is confirmed when including the most recent measurements, with a trend over the 1996-2014 time period of (0.23±0.01)%/yr.

Task 1.1.2 Implement TCCON-compliant measurements at Ile de La Reunion for the measurement of CO_2, CH_4 and N_2O.

TCCON (Total Carbon Column Observing Network) compliant measurements of CO_2, CH_4, N_2O and CO in St. Denis on Reunion Island started in September 2011. In 2012 the site was recognised as an official station of the TCCON. The data are submitted on a regular basis to the TCCON database at Caltech. The data are publicly available three months after acquisition.
In 2014, a new version of the GFIT retrieval software has been delivered (GFIT14) and the whole timeseries has been re-analysed and submitted in netCDF format to the TCCON archive which has been relocated to CDIAC (http://tccon.ornl.gov/). The data are accompanied by the required documentation.
The TCCON data are a primary validation source for GOSAT, OCO-2, SCIAMACHY, and the future Carbonsat satellite data.
Since the launch of OCO-2 in July 2014, the Reunion site is targeted on a regular basis by the OCO-2 instrument. We then perform coincident TCCON measurements when weather and instrument conditions allow so. These TCCON data are then uploaded to Caltech within 6 weeks after acquisition.

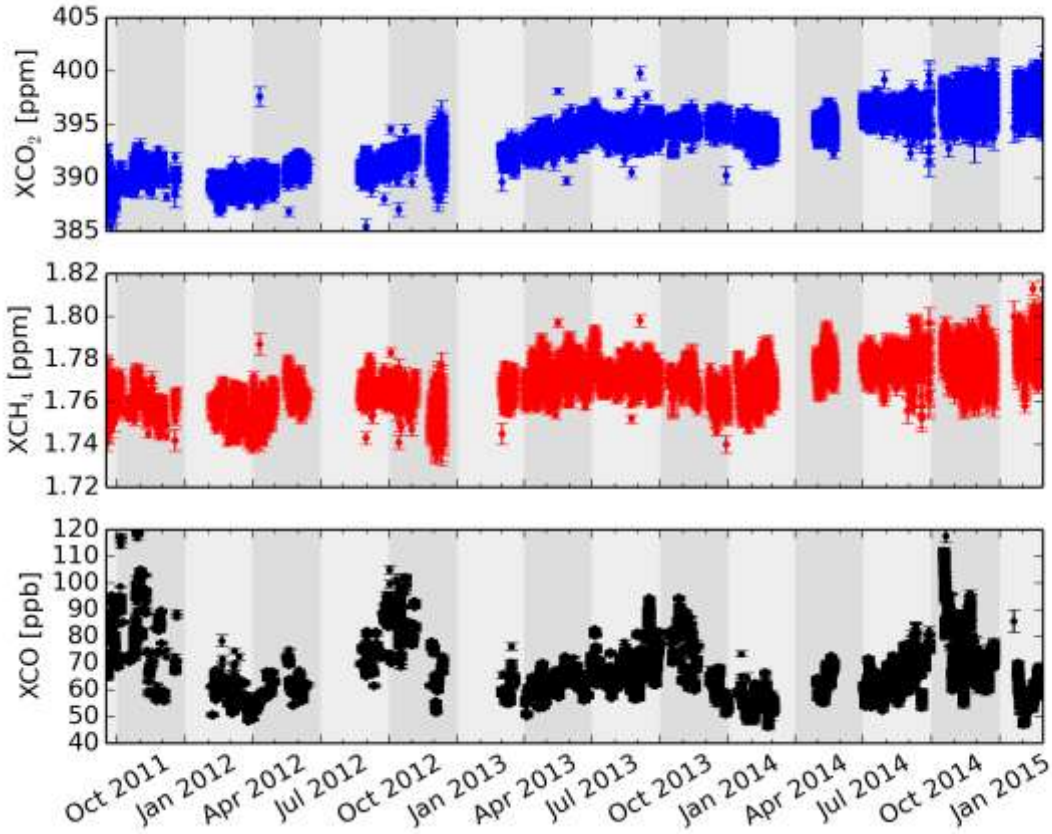

Figure 1: Timeseries of (from top to bottom) XCO_2, XCH_4 and XCO individual observations at Reunion-St Denis since the start of the TCCON measurements (Sept 2011) up to now (Feb. 2015).

Figure 1 shows the whole time series of XCO_2, XCH_4 and XCO measurements at Reunion Island; X points to the column-averaged dry-air column of the gas. Gaps in the time series occur when we met instrumental problems.

We achieve a precision (1 sigma) of 0.1% for XCO_2, 0.1%: for XCH_4, 0.5% for XN_2O, and 2% for XCO, compliant with the TCCON requirements.

One aspect in which we are not yet fully compliant with TCCON is the absolute calibration of the data. This is done usually by taking above the site an in-situ aircraft profile calibrated to the WMO standard, and comparing the integrated profile with the TCCON column. It is hardly possible to do that at Reunion Island. Therefore, we are developing a technique with a balloon-borne aircore and a gliding wing or parafoil that brings the aircore back to a pre-determined location on the Island – for analysis with an in-situ gas analyzer (PICARRO instrument); this is one of the objectives of the ongoing BRAIN pioneer project 'UAV_Reunion'. The hope is to get the technique validated in autumn 2015, during a campaign in Sodankyla, and then to perform a calibration flight at Reunion Island in the first or second quarter of 2016.

The Reunion TCCON site is also included in the EU ICOS_Inwire project (www.icos-inwire.lsce.ipsl.fr) which required the following developments:
(1) High-speed data delivery, not only of in-situ surface concentrations, but also of total columns as measured in TCCON
(2) Development of integrated data products (integration of surface and column measurements) to support validation of satellite data

The first objective has been achieved: an automatic procedure has been developed that enables us to deliver the TCCON data within 3 weeks after data acquisition. The automated TCCON data uploads to ICOS-INWIRE started in November 2014. Figure 2 below shows the data analysis and upload time schedule.

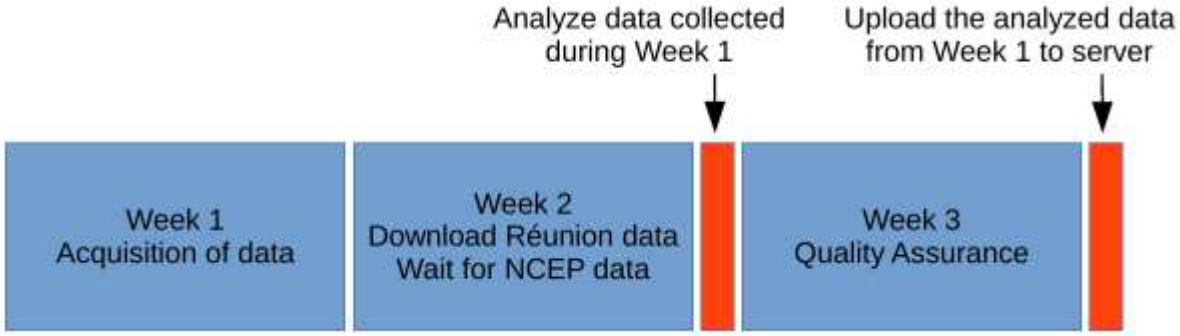

Figure 2: Data analysis and upload time schedule

Work is ongoing regarding the second objective.
The BIRA-IASB PICARRO instrument has been installed at Maido in January 2015 and is operational since then.

As such, Reunion Island is now ready to deliver both in-situ and remote sensing greenhouse gas data also to the ICOS Thematic Data Center.

Task 1.1.3 CH_4 in the near infrared (NIR) versus mid-infrared (MIR) region.

This task comprises the comparison of the retrievals in the near- and mid-infrared. Figure 3 shows the X_{gas} results of the CH_4 retrievals from the TCCON (near-infrared) and NDACC (mid-infrared) measurements at St. Denis. Each datapoint in the plot represents the mean value of the measurements during a 6-hour interval.

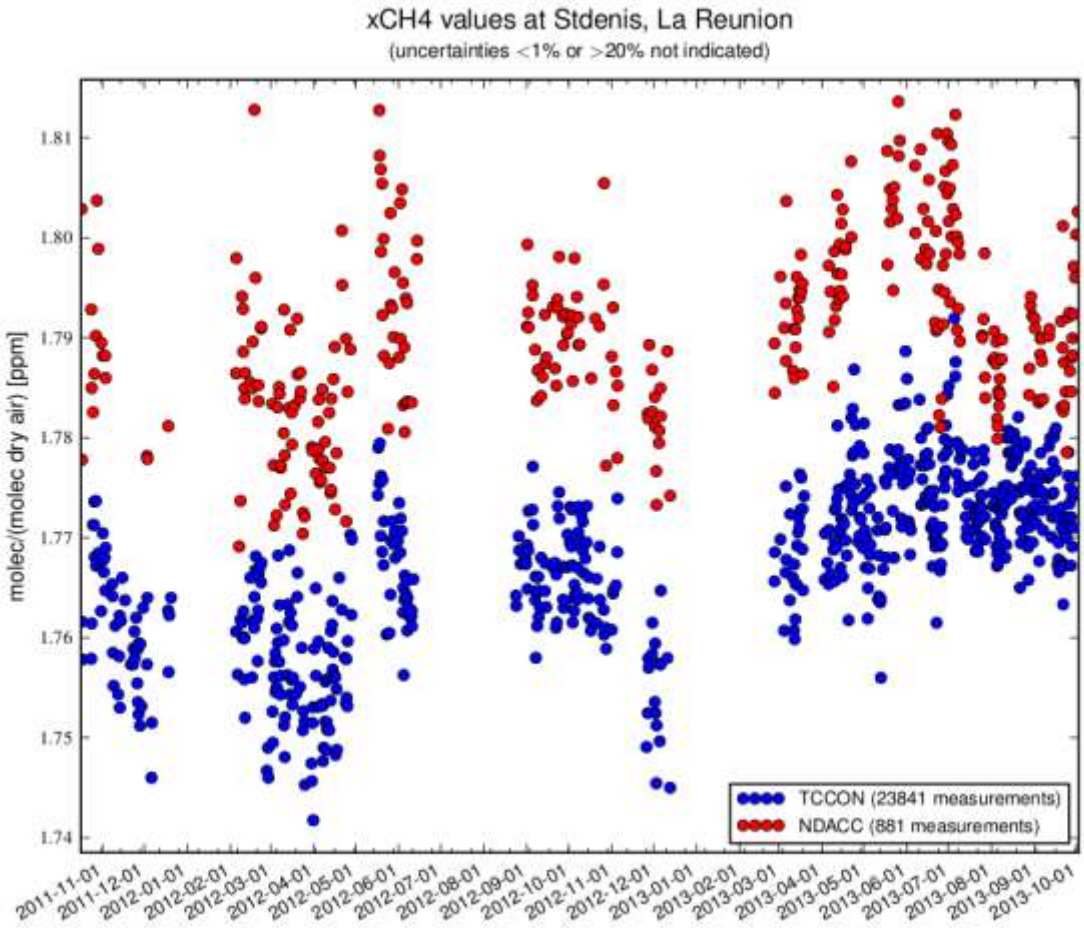

Figure 3: A comparison of the retrievals of XCH_4 in the NIR (TCCON) and MIR (NDACC).

Although the same events are captured in the timeseries of the NIR and MIR measurements, there is a bias of 1.3% between the results from the different spectral domains. It should be noted that this bias depends on the NDACC strategy that is used. There are different strategies for CH_4 retrievals in the NDACC, these differ in their choice of microwindows, spectroscopy, modelling of the instrument response and retrieval method. It is principally the choice of microwindows and spectroscopy which has an influence on the results of the retrievals. In Figure 3, a strategy proposed by Frank Hase (based on the strategy proposed in the discussion of Sussmann *et al.,* 2011) is used for the retrieval; when another strategy is used (proposed by Sussmann *et al.,* 2011), the bias changes to 1.6%.
The choice of microwindows and the spectroscopy of the absorption lines has a clear influence on the bias.

Dedicated laboratory work on the spectroscopy of methane has been performed by Darko Dubravica et al., and will be released in 2015. As soon as this updated spectroscopy is available, which possibly is in June 2015, the comparison exercise will be repeated using the latest version of the retrieval software, SFIT4, and this spectroscopy.

Task 1.2 Investigate additional GHGs: CCl_4 and CF_4

Carbon tetrachloride (CCl_4)

METHODOLOGY

The carbon tetrachloride (CCl_4) molecule is a key component of the stratospheric chlorine budget as well as a potent greenhouse gas, with a global warming potential relative to CO_2 of 1400 on a 100-year horizon. Its atmospheric monitoring is therefore of relevance to both the Kyoto and the Montreal Protocols.

The most appropriate feature for the retrieval of CCl_4 from ground-based FTIR spectra is the strong ν_3 band near 12.7µm. However, such retrievals have been hampered by a nearby CO_2 Q-branch affected by spectroscopic line-mixing. Neglecting this effect resulted in large systematic residuals (see frame B of Figure 4), with negative influence on the retrieval of CCl_4 and on its error budget.

We have therefore implemented in the SFIT-2 algorithm a routine of J.-M. Hartmann (LISA, IPSL, Paris) to account for line-mixing effects in the CO_2 Q branch at 792 cm^{-1}. Improvement in the residuals is obvious when comparing frame A and B of Figure 4.

A retrieval strategy further accounting for interferences by water vapor and ozone has been set up, with the fitted microwindow extending from 785 to 807 cm^{-1}. Careful error budget evaluations have indicated for a single fit a total random error of less than 7%, a total systematic error of less than 11%, the latter being essentially influenced by the uncertainty on the CCl_4 spectroscopic line parameters.

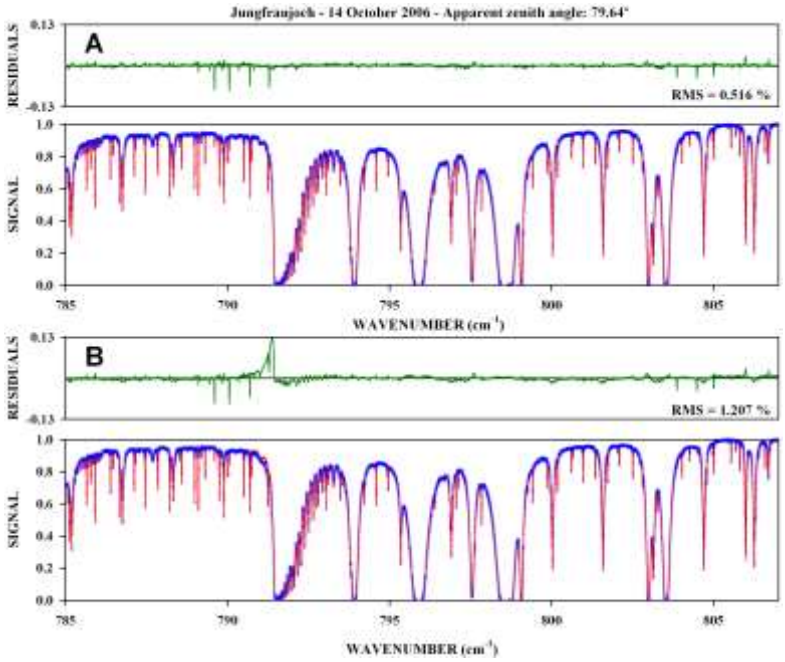

Figure 4. Sample fits to a spectrum recorded on October 14, 2006 at the Jungfraujoch station. The observed and fitted spectra are reproduced in red and blue, respectively. Frame A displays in green the observed minus calculated residuals when accounting for the line mixing in the CO_2 Q-branch. This corresponds to a significant improvement when compared to the residuals which were obtained when neglecting this spectroscopic effect (see frame B).

RESULTS

The study of CCl_4 has been finalized and published (Rinsland et al., 2012). The main findings are: (i) neglecting line-mixing in a strong CO_2 Q-branch interference results in CCl_4 columns biased high by (15±2) %, (ii) the CCl_4 abundance decreases at –(1.1±0.1)%/yr over 1999-2012, in good agreement with *in situ* observations, as a consequence of measures adopted by the Montreal Protocol, (iii) CCl_4 remains a significant contributor to the organic and inorganic chlorine budgets.

Since then, the time series have been extended to cover the January 1999 to December 2014 time period. A fit to the CCl_4 daily mean total column data set shows a statistically-significant long-term trend of ($-1.49 \pm 0.06 \times 10^{13}$ molec./cm^2)/yr at the 95 % confidence level. This corresponds to an annual decrease of (-1.31 ± 0.06) pptv for the mean free tropospheric volume mixing ratio, still at the 95 % statistical confidence level. These values are in excellent agreement with trends derived from *in situ* samplings in the Northern hemisphere (WMO2014, Table 1-2). The negative trend of the CCl_4 loading reflects the continued impact of the regulations implemented by the Montreal Protocol and its strengthening amendments and adjustments. However, it is clear that significant unidentified emissions are at play (Liang et al., 2014), leading to a CCl_4 decrease not as rapid as expected. Efforts are ongoing at the international level (as a SPARC activity) to solve this issue, and the CCl_4 strategy developed for the Jungfraujoch is currently being implemented by other FTIR groups (Hannigan et al., 2015) to provide additional time series which, together with ACE-FTS data (Mahieu et al., 2015), will help to complete the picture.

Carbon tetrafluoride (CF_4)

METHODOLOGY

Carbon tetrafluoride (CF_4) is a very long-lived GHG targeted by the Kyoto Protocol, with a lifetime estimated to exceed 50000 years. Combined with a high global warming potential of at least 7390 on a 100-yr time horizon, this compound is a strong greenhouse gas whose anthropogenic emissions are deservedly targeted for regulation under the Kyoto Protocol. A retrieval strategy using ground-based FTIR spectra has been set up for the first time. It is based on an interval spanning 6 CF_4 features of the strong ν_3 band around 1282 cm^{-1}. Numerous interferences have to be accounted for, among which several isotopologues of H_2O, N_2O, $^{13}CO_2$, $ClONO_2$, HNO_3 and H_2O_2. In particular, $H_2{}^{16}O$ and HDO interferences strongly reduce the fitting quality during wet days. Consequently, we had to discard the wettest observations from our data base. Following this approach, a two-decade time series has been produced and analyzed and the results were compared to other CF_4 data sets derived from *in situ* sampling and from solar observations performed from balloon or space platforms.

RESULTS

CF_4 emissions have significantly increased during the last decades of the previous century. The main anthropogenic source is the primary production of aluminum while the only identified natural sources are lithospheric emissions.

All relevant Jungfraujoch spectra available from 1989 onwards have been analyzed. The resulting daily mean time series has allowed deriving the CF_4 trend and corresponding emissions. Our data set reveals a mean linear increase of (1.14±0.04) x 10^{13} molec./cm^2/yr (2-sigma), or (13.2±0.4) Gg/yr between 1989 and 2012. When looking into more details, two successive regimes are identified, with emissions of (15.8±1.3) Gg/yr and (11.1±0.2) Gg/yr, for 1989-1997 and 1998-2012, respectively (Mahieu et al., 2014). Comparisons with results obtained in situ by the AGAGE network (including at the Jungfraujoch station), or from balloon- or space- platforms have shown a very consistent picture for the CF_4 atmospheric build up over the last 30 years, when accounting for the uncertainties associated to the various techniques involved. All data sets and techniques involved therefore confirm the slowing down in the accumulation of CF_4 in the atmosphere, attributed to efforts undertaken by the aluminum industry to limit its emissions despite increasing Al production. Nevertheless, CF_4 is still on the rise at a rate of ~1%/yr and this is a serious issue in the context of the Earth's global warming considering its very long lifetime and large global warming potential.

Task 1.3 laboratory spectroscopic data for CO_2

We measured improved reference spectroscopic information for carbon dioxide and contributed to the evaluation of improvements made to an accurate modelling of the absorption coefficient of that species in air at atmospheric pressures. These two activities are described here after.

In the frame of an experimental and theoretical study of self collisional effects on the spectrum of the $\nu_1+3\nu_2^1$ band of carbon dioxide observed near 3340 cm^{-1} (Daneshvar *et al.*, 2014), we recorded 10 spectra of pure CO_2 at pressures from 3 to 903 hPa (with 55 meters absorption path and at 293 K) using a Bruker IFS 120 to 125 HR upgraded Fourier transform spectrometer. Least squares fitting the 10 spectra simultaneously, we measured the intensities, self broadening and shift parameters, and first-order line-mixing coefficients for R-, P- and Q-branch lines of the $\nu_1+3\nu_2^1$ band, using 3 line shape models. Comparison of our measurements with data available in HITRAN 2012 (Rothman *et al.*, 2013) put forward some discrepancies. For example, if P-branch line intensities available in HITRAN 2012 agree with our measurements, they are about 7% higher in the R- branch, and while the self broadening coefficients agree within 2.5%, self shift coefficients exhibit discrepancies ranging from 5-10% in the R-branch and 20-30% for the P-branch. The discrepancies observed for the line intensities are within the (large) uncertainties reported in HITRAN 2012 (20% or more), and in line with the uncertainties stated for the self shift coefficients. These results seem to indicate that the spectroscopy of carbon dioxide still deserves improvements, especially for weaker bands.

A model (consisting of a database and corresponding software) for the calculation of CO_2-air absorption coefficients taking line-mixing into account has been developed for many years [see (Lamouroux *et al.*, 2014) and references therein]. To test the quality of predictions generated in the 4.3 μm spectral region by the most recent update of this model (Lamouroux *et al.*, 2014), these predictions were compared with Fourier transform spectra of mixtures of 0.25, 0.5 and 1 % of CO_2 in air, for a total pressure of 1 atm, that we recorded at 295 and 223 K in the frame of AGACC-II. These comparisons show that the update is an improvement at 4.3 μm for room temperature conditions, but that residuals on the order of ±0.5% [i.e. larger than the requirements of satellite-based remote sensing of atmospheric CO_2 (Crisp et al., 2004; Crisp et al., 2009)] remain at low temperature (Lamouroux *et al.*, 2014).

WP 2: Volatile Organic Compounds (VOC) and CFC-substitutes in the troposphere

Task 2.1 Methanol (CH_3OH) and methylchloride (CH_3Cl) at Jungfraujoch and La Réunion

2.1.1 Methanol

Methanol was first retrieved from ground-based spectra by Rinsland et al. (JGR, 114, 2009), using a single window spanning the 992-998.7 cm^{-1} interval. This range proved to be unsuccessful for the retrieval of this species from Reunion Island. As a consequence, Vigouroux et al. (2012) developed and used an alternative approach (1029-1037 cm^{-1}). These informations were useful when developing an optimum strategy for the Jungfraujoch, and it turned out that combining both windows (after extension of the first one to 992-1000.3 cm^{-1}) allowed maximizing the information content for this dry site, providing vertical information with a typical DOFS of 1.8.

a) Methanol at Reunion Island (and other VOCs and biomass burning products)

The retrieval strategies of methanol (CH_3OH), and other VOCs and biomass burning products (hydrogen cyanide (HCN), ethane (C_2H_6), acetylene (C_2H_2), and formic acid (HCOOH)) have been optimized at Reunion Island and published in Vigouroux et al., (2012), including the uncertainty budget (e.g. for methanol the mean random uncertainty is 10%). The main difficulties were the weak spectral absorption signatures of the target species and the strong interferences with the water vapor signatures at this humid site. In Vigouroux et al., (2012), we also performed comparisons with the models GEOS-Chem and IMAGESv2. The HCN and CO FTIR total columns have been compared to the chemistry-transport model (CTM) GEOS-Chem, in collaboration with D. Jones and C. Whaley from University of Toronto. The CO, C_2H_6, C_2H_2, CH_3OH and HCOOH total columns have been compared to the CTM IMAGESv2 in collaboration with J. Stavrakou and J.-F. Müller (BIRA-IASB). These comparisons combined with sensitivity tests with both models, have led to improvements of our knowledge about the target species emission budgets.

The FTIR methanol and formic acid time-series at La Réunion were used in emission studies by Stavrakou et al. (2011 and 2012, respectively). The formic acid FTIR total columns were also used in Paulot et al. (2011). Furthermore, the HCN and C_2H_2 FTIR data were used for the validation of IASI products in Duflot et al. (2013, 2015).

The main results of the comparisons with the models discussed in Vigouroux et al. (2012) are the following. First, the fire emission database used in IMAGEsv2 (GFED3; van der Werf et al., 2010) seems to underestimate the pyrogenic emissions, especially in the late September-October period in south-eastern Africa - Madagascar region.
Second, the excellent correlation of CH_3OH and HCOOH with CO between August and November suggests that, despite the dominance of the biogenic source of these compounds on the global scale, biomass burning is their major source at Reunion Island during this period. This was expected for other species such as HCN, C_2H_6 and C_2H_2, but less so for methanol and formic acid given the low contribution of fires to their global budget (2% and 14%, respectively). We show in Figure 5, the FTIR and IMAGESv2 simulations of methanol and formic acid. The optimized IMAGESv2 simulations, using IASI data, are shown in green in Figure 5. We observe that the CH_3OH IASI derived emissions remain too low during the fire season, suggesting that IASI may underestimate CH_3OH in this period in the southeastern Africa-Madagascar region.

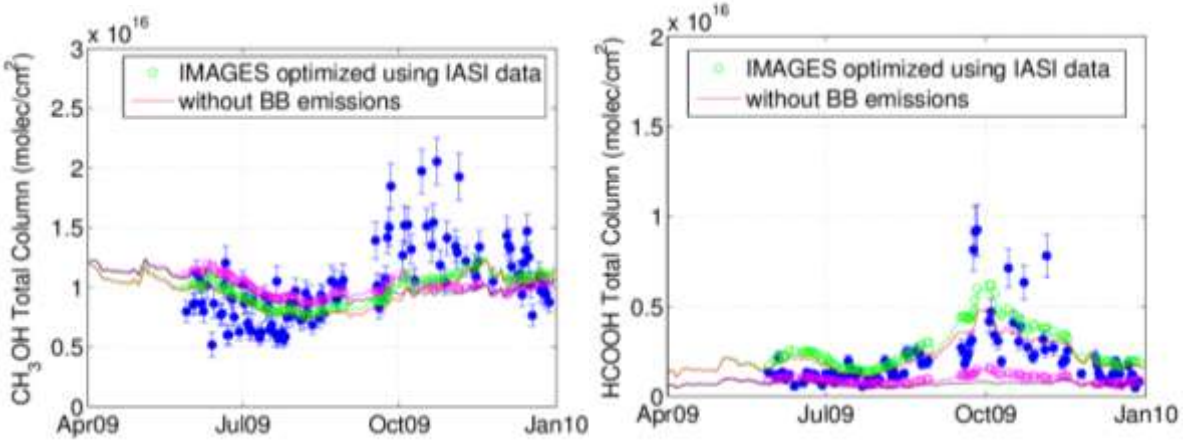

Figure 5: Time-series of daily mean total columns at Reunion Island: CH_3OH (left panel) and HCOOH (right panel). The FTIR data are represented by the blue filled circles, the IMAGESv2 model simulations by the colored lines (magenta for the standard runs; green for the optimized simulations using IASI data), and the model data smoothed with the FTIR averaging kernels with the open circles. The model simulations obtained when the biomass burning (BB) contribution is removed are shown in black for the standard run, and in red for the inversion using IASI data.

From Figure 5, we see that, although the IMAGESv2 optimization of HCOOH sources using IASI data greatly improves the agreement with FTIR data during the fire season (Figure 5, right panel, green curve), the contribution of biomass burning given by IMAGESv2 is only minor (red curve compared to green curve). This specific result at Reunion Island seems to disagree with the conclusion based on FTIR measurements that biomass burning is a dominant source of HCOOH at Reunion Island during the August-November period. On the other hand, the FTIR finding is consistent with the study of Paulot et al. (2011). Indeed, they have shown that a good agreement between the HCOOH columns modeled by GEOS-Chem and the FTIR measurements at Reunion Island can be achieved by assuming that organic aerosol (OA) oxidation generates a diffuse source of formic acid, knowing that the dominant source of OA in the Southern Hemisphere is biomass burning. The different findings from different models highlight the need for ground-based data as provided in AGACC-II.
From Figure 5, we can see that the model IMAGES still underestimates methanol at Reunion Island during the biomass burning season after the optimization using IASI data. Therefore, our ground-based data points out that, even if the satellite data improved the emission budget, there is still a need for model improvement of methanol emissions.

b) Methanol at the Jungfraujoch

The first aim was to select the most suitable microwindow for the Jungfraujoch retrievals among those used this far in the literature. Our tests showed that all lead to very consistent results and that combining them allows to significantly improve the information content. A strategy involving two large windows (992-1008.3 & 1029-1037 cm^{-1}) has been carefully set up and characterized, providing unprecedented information content (note that at Reunion Island, only the second spectral microwindow near 1030 cm^{-1} is used for CH_3OH retrievals). The typical DOFS is equal

to 1.8, with vertical sensitivity spanning the 3.6-15 km altitude range. A complete uncertainty budget has been carefully evaluated, including systematic and random contributions. We found e.g. that typical random errors amount to less than 5% for the total columns, to less than 20% for the tropospheric columns. A final data set has been produced and analyzed for the 1995-2012 time period.

Methanol has been systematically retrieved from all available Bruker spectra with solar zenith angles in the 65-80º range, from 1995 onwards. We evaluated the trend of CH_3OH over these 17 years to (-1.3±2.7) x 10^{13} molec./cm^2, or (-0.2±0.4) %/yr, i.e. a non-significant value at the 2-σ level of confidence. CH_3OH presents a strong seasonal modulation, with minimum total columns and variability in winter (December-February), maximum values in summer (June-August), as a result of important emissions associated with plant growth. The peak-to-peak amplitude amounts to ~130 % of the CH_3OH yearly mean column. The total and lower tropospheric columns have also been compared with IMAGESv2 model simulations provided by BIRA-IASB. There is no systematic bias between the observations and IMAGESv2 but the model underestimates the peak-to-peak amplitude of the seasonal modulations. The diurnal cycle has also been analyzed, showing significant variations characterized by maximum columns at noontime from fall to spring, in contrast with summer (no clear signal during the day), when the CH_3OH variability and columns are by far the largest. Finally, in situ campaign-type measurements performed at the Jungfraujoch in 2005 have been compared with our lower-tropospheric data. These investigations suggest a reasonable agreement, with similar seasonal pattern and data variability for both subsets. It is also clear that significantly higher concentrations are associated to air masses originating from the south, where substantial emissions from biogenic sources occur. More details can be found in Bader et al. (2014).

2.1.2 Methyl Chloride

Methyl chloride is one of the most abundant chlorine-bearing gases in the Earth's atmosphere and a significant contributor to the organic chlorine budget, with mean volume mixing ratio of 550 pptv. Several natural sources have been identified (e.g. dead leaves in tropical regions, biomass burning) while the largest sink is oxidation by OH. Although balanced, its atmospheric budget is still affected by significant uncertainties.

There are numerous but weak features of CH_3Cl near 3µm. Until very recently, attempts to retrieve this species from ground-based FTIR spectra proved unsuccessful because many CH_3Cl features were missing in HITRAN. This was also true for ethane, a species presenting numerous interfering features in this spectral region. Fortunately, pseudoline parameters for ethane have been produced on the basis of Harrison et al. (2010) cross section measurements. Mahieu et al. (2011) have shown that these new parameters allow to significantly improve the quality of the fits in the 2965.7 to 2967.5 cm^{-1} interval, with residuals nearly divided by three in the selected window. Despite this improvement, the retrieval of CH_3Cl from ground-based FTIR spectra was still unsatisfactory at that time: retrieved columns were on average about 50% larger than anticipated. It is only very recently that it was possible

to retrieve sensible total columns of CH_3Cl, using in combination the Harrison parameters for C_2H_6 and the HITRAN 2012 compilation which includes new line parameters for CH_3Cl from Bray et al. (2011).

This approach and settings have been used recently to retrieve CH_3Cl from Reunion and the Jungfraujoch.

a) Methylchloride at Reunion Island

We have performed tests in order to optimize a retrieval strategy for CH_3Cl at Reunion Island. We use the micro-window around 2967 cm^{-1} [Mahieu et al. (EGU2010), also used for ACE satellite retrieval (Rinsland et al., 2007)], where the main interferences are CH_4, H_2O and isotopologues of H_2O. In case of Reunion Island a smaller micro-window is used (2966.87-2967.8 cm^{-1}), to avoid an interference with a water vapor line at 2966.8 cm^{-1}.The spectroscopic signature of CH_3Cl is very weak, so the random error budget due to the signal to noise ratio (SNR) is expected to be very large. Indeed, a very large scatter is seen in the retrieved total columns (see Figure 6, Left). This scatter observed at St-Denis is nicely reduced when the instrumentation has been changed from Bruker 120M (2009-2011) to Bruker 125HR (2012-2013), due to the better quality of the new spectra; the scatter reduced especially since April-May 2013 after optimization of the operational settings (6 scans are co-added per spectrum instead of 4, leading to a higher SNR). At the Maïdo observatory, the scatter is even smaller because the interference with water vapor is smaller thanks to the higher altitude of the site (2200 masl).

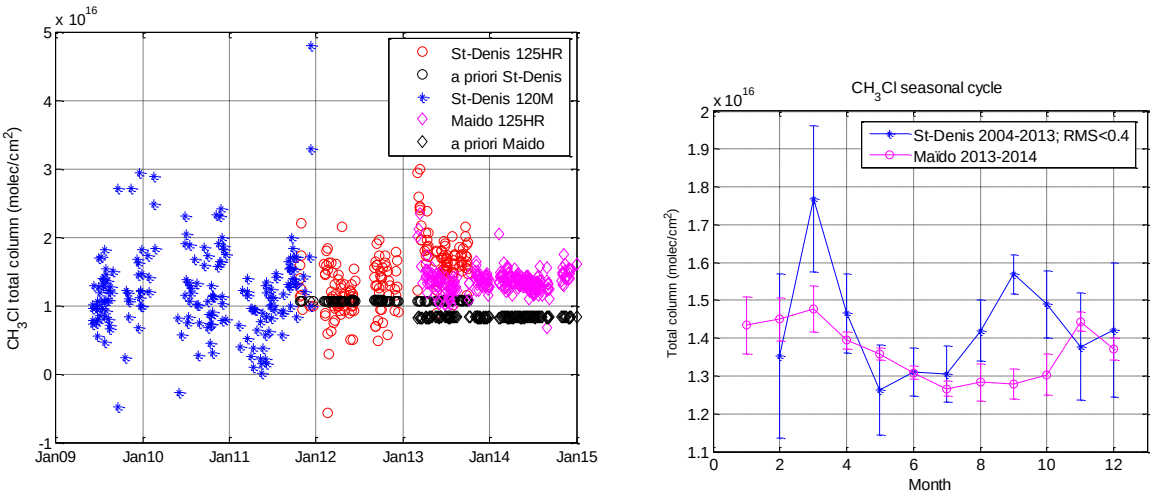

Figure 6: Left: CH_3Cl daily means total columns at St-Denis (blue for Bruker 120M data, red for Bruker 125HR data) and at Maïdo (magenta). The black symbols indicate the a priori values for St-Denis (circles) and Maido (square). Right: CH_3Cl seasonal cycle at St-Denis (only data with RMS residual <0.4 are kept, which represents 70% of the data) and Maïdo. The error bars represent 2 x standard deviation / sqrt(N).

The lifetime of CH_3Cl in the troposphere is more than 1 year, therefore the observed large scatter is not due to natural variability, but to the large random noise. In Figure 6 (right), we show the seasonal cycle derived from our measurements: maximum in

spring for both stations; 2nd maximum in September for St-Denis, and November for Maïdo. These 2nd maxima could be linked to the biomass burning season as found for other species (Vigouroux et al., 2012). The total columns at Maïdo should be lower than at St-Denis, due to the higher altitude of Maïdo (2.2 km), which is not the case for some months. Considering the large scatter in St-Denis total columns and the difference in the seasonal cycles at both stations, it might be safer to only exploit the Maido CH_3Cl data in the future. However, future NDACC data at St-Denis might be exploitable if a similar SNR as in Apr-Nov 2013 is achieved.
The seasonal cycle at Maïdo (Figure 6, right) is roughly in phase with the one obtained from AURA satellite measurements at 150hPa altitude in the 15°S-30°S region which show a maximum in December-January and a minimum in September, with an amplitude of about 30% (Santee et al., 2013). It would be interesting to check the seasonal cycle at Reunion Island from a chemistry-transport model, but neither IMAGES nor the standard GEOS-chem runs provide CH3Cl.

b) Methyl chloride at Jungfraujoch

A CH_3Cl time series spanning the 2000-2014 time period has been retrieved for Jungfraujoch using the Hitran2012 parameters, combined with the pseudolines for C_2H_6. (see grey symbols in Figure 18). A mean column close to 7.7 E+15 is determined, corresponding to an average mixing ratio of 550 ppt, in good agreement with in situ measurement for the northern hemisphere. Year-to-year changes are obvious, consistent with those identified by the AGAGE in situ network (see figure 1-1 in WMO2014) and a small positive trend is derived over the last 15 years (0.23 ± 0.03 %/yr).

Task 2.2 Re-analysis of C_2H_4, C_2H_6 and HCHO data at Jungfraujoch and La Réunion with improved spectroscopic data

Task 2.2.1 provide improved laboratory spectroscopic data for $^{12}C_2H_4$,$^{12}C_2H_6$ and $H_2{}^{12}C^{16}O$

On parallel with its main activities, AGACC-II aimed to improve reference spectroscopic information for a number of minor or trace gaseous constituents of the atmosphere, in spectral regions used to probe them using optical remote sensing techniques. The activities carried out in this context are described here.

Ethylene ($^{12}C_2H_4$)

Optical remote sensing of ethylene relies on the 10 μm spectral region, dominated by the strong ν_7 band. The reference intensity information available in databases such as HITRAN (Rothman *et al.*, 2013) and GEISA (Jacquinet-Husson *et al.*, 2011) was generated by matching relative line intensities, calculated for the whole band using appropriate modelling of the vibration-rotation motion of the molecule (Rusinek *et al.*, 1998), to the intensities of 13 lines located between 942 and 970 cm^{-1} (i.e. the central region of the band), measured using tunable diode laser spectroscopy (Blass *et al.*, 2001). So, apart from these 13 lines and 4 other lines observed in the same spectral range (Reuter and Sirota, 1993; Brannon and Varanasi, 1992), line intensities were actually never measured in the 10 μm spectral region of the ethylene

spectrum. The aim of the work completed within AGACC-II was to check the line intensities existing in databases against actually measured information.

We recorded 6 high-resolution Fourier transform absorption spectra of the 10 µm region of ethylene, at pressures from 1.5 to 101 hPa. These 6 FTS spectra were simultaneously least squares fitted to measure the intensities of 1221 ν_7 band lines of $^{12}C_2H_4$. This is the first time that such an extensive intensity information was measured for that band. As Figure 7 shows, line intensities measured in this work exhibit systematic discrepancies with the line intensities available in HITRAN 2012 (Rothman *et al.*, 2013). Note that these discrepancies are within the stated uncertainty of the line intensities in HITRAN (5–10%). We believe that they come from an incomplete modelling of the rotational dependence of the line intensities in HITRAN, provided by the model used at the time to generate them (Rusinek *et al.*, 1998). Relying on the comparison shown in Figure 7, the line intensities for the ν_7 band of $^{12}C_2H_4$ available in HITRAN 2012 were corrected. We estimated that the uncertainties on these corrected line intensities are in the 2–5% range. The impact of these improved line intensities on retrievals of atmospheric ethylene in the 949 – 952 cm^{-1} spectral range was evaluated by the ULg AGACC-II partner using a subset of ground-based high-resolution Fourier transform infrared solar spectra recorded at the Jungfraujoch station. The use of HITRAN 2012 with line intensities modified to match the present measurements led to a systematic reduction of the measured total columns of ethylene by –4.1 ± 0.1% (Vander Auwera *et al.*, 2014).

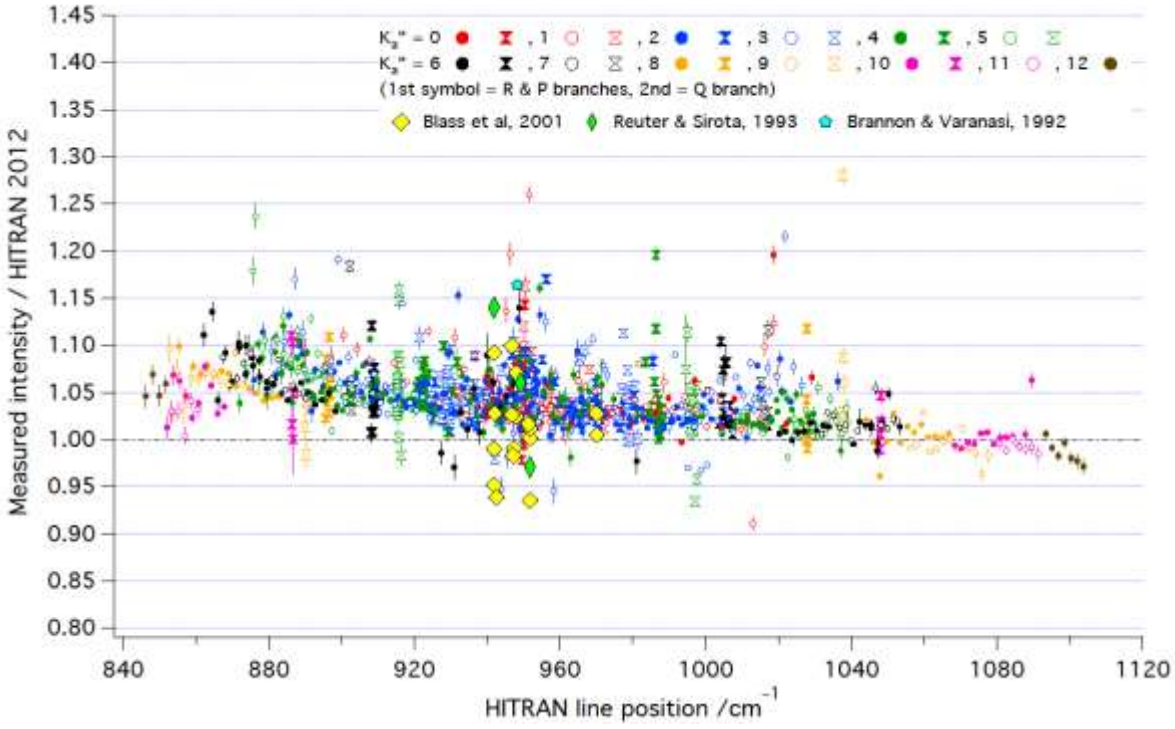

Figure 7: Ratio of line intensities measured in this work and in the literature for the ν_7 band of $^{12}C_2H_4$ with those available in HITRAN 2012 (Rothman *et al.*, 2013). K_a is a rotational quantum number. Note that the line intensities in HITRAN were generated by scaling calculated relative intensities (Rusinek *et al.*, 1998) with some average of the intensities reported in (Blass *et al.*, 2001).

Line intensities are correlated with the line broadening coefficients. Accurate measurements of line intensities therefore require that self-broadening coefficients are known. Such information was limited for $^{12}C_2H_4$ and only default values are available in HITRAN (Rothman *et al.*, 2013). Among the 6 spectra included in the present analysis of the line intensities were 3 FTS spectra of pure ethylene at pressures of 25, 51 and 101 hPa. Such higher pressure spectra allowed precise measurements of self-broadening coefficients of 1221 $^{12}C_2H_4$ lines to be made, simultaneously with their intensities. Although not of direct interest for atmospheric measurements, the self-broadening coefficients of all the ethylene lines available in HITRAN were also updated with information calculated using expressions determined with the 1221 self-broadening coefficients measured (Vander Auwera *et al.*, 2014).

The work carried out for ethylene in the frame of AGACC-II therefore resulted in a list of improved line parameters. This list is the information available for ethylene in HITRAN 2012 (Rothman *et al.*, 2013), with the line intensities of the ν_7 band and self broadening coefficients of all the lines modified to match the present measurements (Vander Auwera *et al.*, 2014).

Additionally, AGACC-II initiated an in-depth study of the 10 μm spectral range of ethylene, of more fundamental nature. Although dominated by the ν_7 band, this spectral range also involves weaker bands, coupled to ν_7, namely the ν_{10}, ν_4 and ν_{12} bands observed near 826, 1026 and 1442 cm^{-1}, respectively. Relying on 11 FTS spectra of ethylene and a collaboration with two French research teams [at the *Université de Reims Champagne Ardenne* (Prof. M. Rotger, Reims) and at the *Université de Bourgogne* (Dr V. Boudon, Dijon)] who developed a theoretical model describing the vibration-rotation motion of the ethylene molecule (Wenger *et al.*, 2005), a combined frequency and intensity analysis of the ν_{10} / ν_7 / ν_4 / ν_{12} band system has beenperformed (Alkadrou et al., 2015). Parameters of the theoretical model have been determined through fitting of 10737 line positions and 1870 line intensities measured in the 4 bands. These parameters and model were then used to generate the positions and intensities of 65420 lines in the 620 – 1525 cm^{-1} spectral region. Self broadening coefficients from our other contribution (Vander Auwera et al., 2014) and information from the literature (air broadening coefficients and their temperature dependence exponent, and air-shift coefficients) were added to provide a linelist in HITRAN format. Figure 8 shows an example of the improved modelling of the lower energy range of the 10 μm ethylene spectrum provided by this linelist. A similar work is in progress for the 3 μm spectral region of ethylene (the main bands are ν_9 and ν_{11} near 3105 and 3012 cm^{-1}, respectively). Although not of direct interest in the context of the atmosphere of the Earth but rather for other planets such as Mars, it will also lead to an improvement of spectroscopic parameters for ethylene.

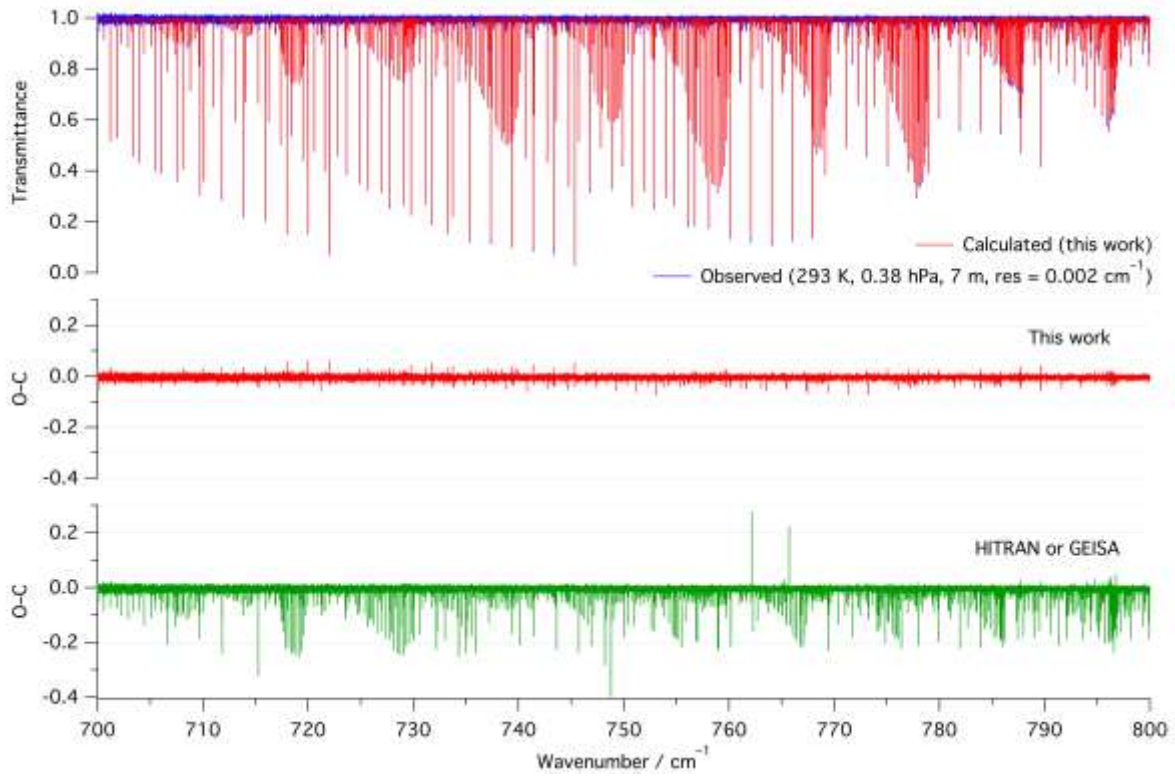

Figure 8: Comparison of an observed spectrum (blue in the upper panel) of the P branch of the ν_{10} band of ethylene with spectra calculated for $^{12}C_2H_4$ using results of the present work (red in the upper panel) and the HITRAN (Rothman et al., 2013) or GEISA (Jacquinet-Husson et al., 2011) databases. The corresponding residuals between the observed and calculated spectra are presented in the middle and lower panels, respectively.

Ethane ($^{12}C_2H_6$)

Optical remote sensing measurements of ethane in the atmosphere can rely on the 3.3 μm spectral region (Rinsland *et al.*, 2000). This part of the ethane spectrum indeed provides increased sensitivity because of the presence of prominent Q branches of the ν_7 band (Harrison *et al.*, 2010). However, apart from the $^pQ_3$ and $^rQ_0$ branches that have been studied at sub-Doppler resolution (Pine and Stone, 1996), the reference spectroscopic information available for ethane (Rothman *et al.*, 2013) provides a rather poor modelling of this spectral range. Within AGACC-II, we proposed the difficult task to try and improve the reference line positions and intensities to more accurately and consistently model the 3.3 μm spectral region of ethane.

We recorded 4 high-resolution Fourier transform absorption spectra of that spectral range and relied on a theoretical model developed in the group of C. di Lauro (*Università di Napoli Federico II*, Naples) to analyse them. This model attempts to describe the network of vibration-rotation levels predicted to be observed at 3.3 μm, taking into account the effects of the internal rotation of the CH_3 groups. However, because of the complexity of the problem, only 572 line positions belonging to the ν_7 band and to two other, weaker bands could be fitted with a quite large standard deviation of 0.018 cm^{-1} (Lattanzi *et al.*, 2011). A list of positions and relative intensities was nevertheless generated for 4969 lines in the range 2900–3071 cm^{-1}.

Yet, as could be expected from the rather poor fit, spectra predicted using these line parameters exhibit large discrepancies with observed spectra.

In view of these unsatisfactory results, we tried to carry out another rotational analysis, focused on the ν_7 band and not relying on a modelling of the vibration-rotation structure of the molecule to avoid biasing the results with an inaccurate model. We only relied on the positions of R and P branch lines (and Q branch lines when resolved) observed in the recorded spectra and from the literature, and assigned them using information from previous work. These assignments were then checked using ground state combination differences. With such a procedure, we were able to extend the rotational assignments in the ν_7 band. However, a lot of work remains to be done before the spectroscopic information gathered so far, still resulting in significant discrepancies with observed spectra for the cold band and completely missing the hot bands, would provide a satisfactory description of the 3.3 μm spectral region of ethane.

Although limited, the results that we obtained during the work carried out in the frame of AGACC-II is another step toward the understanding of this very complicated spectrum. Currently, the best approach to modelling this spectral region is still to use absorption cross sections (Harrisson *et al.*, 2010).

Formaldehyde

As formaldehyde easily polymerizes or degrades, the main difficulty faced in the laboratory to measure reference line intensities for this species is the determination of its particle density in the vapour phase. Indeed, this latter information being commonly obtained from measurements of the total pressure in the cell, it can be affected by non-monomeric formaldehyde or decomposition products possibly present in unknown quantities in the gas phase. Within AGACC-II, we aimed to evaluate the importance of such an effect on infrared (IR) line intensities available in HITRAN, determined using the measured total pressure in the cell (Perrin *et al.*, 2009). For that purpose, we aimed to compare HITRAN line intensities with the same information derived relying on the particle density of formaldehyde measured using intensities of far infrared (FIR) pure rotation lines and the accurately known electric dipole moment of the molecule (Fabricant *et al.*, 1977). Such a comparison would in particular involve IR spectral ranges used for remote sensing measurements of formaldehyde (Vigouroux *et al.*, 2009). To be able to use the particle density determined in the far infrared to obtain line intensities in the infrared region, the IR and FIR spectra had to be recorded simultaneously.

Spectra of formaldehyde were recorded at ULB simultaneously in the FIR range (0–400 cm^{-1}), using a Bruker IFS 120 to 125 HR upgraded Fourier transform spectrometer (FTS), and in the IR region (near 3.4 μm), using a tunable diode laser (TDL) spectrometer available in the group of Prof. M. Lepère (*Université de Namur*) and installed at ULB. Figure 9 shows the arrangement of the two spectrometers during the measurements. The formaldehyde sample (about 0.15 Torr diluted in about 10 Torr of N_2) was contained in a cross-shaped stainless-steel cell (shown in the inset in Figure 9) located inside the evacuated FTS. A total of six experiments were conducted at 296 K with six different formaldehyde samples. Each experiment lasted about 8 hours, which was the time needed to record one high-resolution FIR

spectrum in the range 0–400 cm^{-1}. In the meantime, about 30 IR spectra were recorded around 3.4 μm using the TDL spectrometer, each requiring about 1 minute to be obtained. The recording of the FIR spectrum was then extended overnight, to yield a high-resolution spectrum with improved signal-to-noise ratio. Figure 10 presents a portion of the pure rotation spectrum of formaldehyde, recorded during one of the experiments.

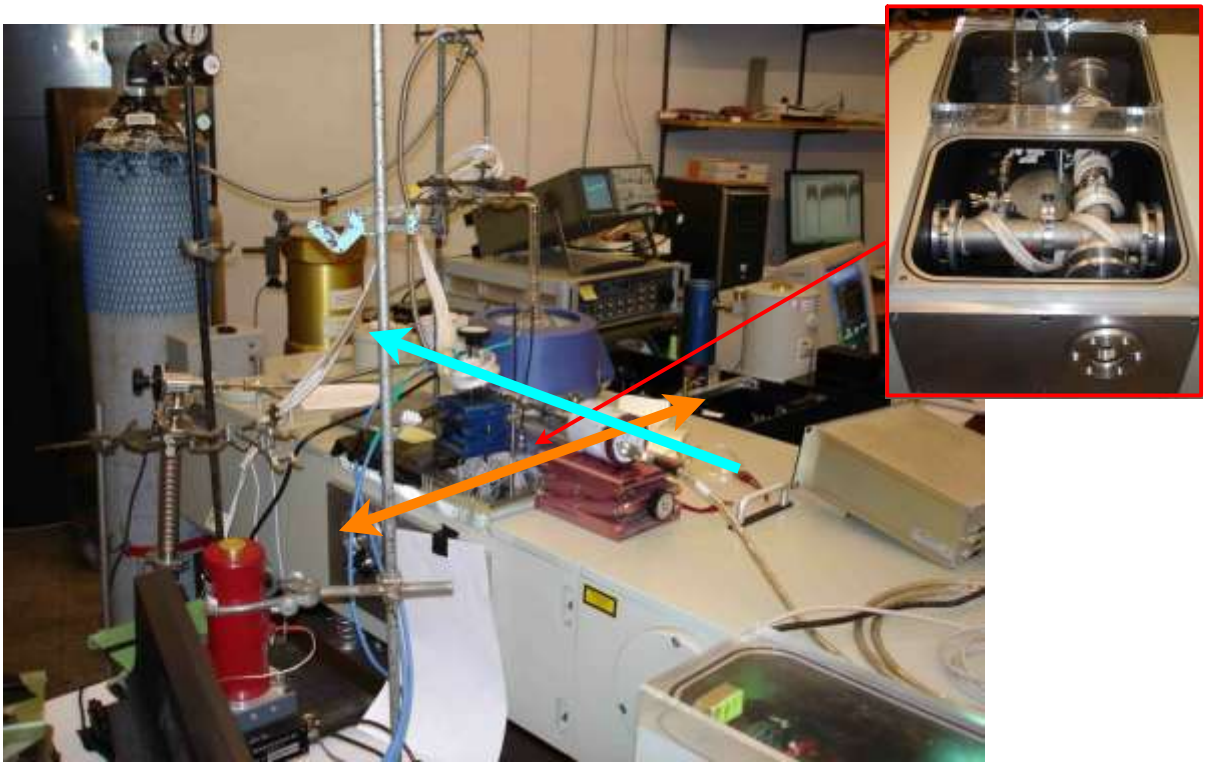

Figure 9: View of the laboratory at ULB during the simultaneous recording of FIR and IR spectra of the same sample of formaldehyde using a Bruker IFS125HR FTS and a TDL spectrometer, respectively. The cross-shaped stainless steel cell containing the sample and located inside the evacuated FTS is shown in the inset. The FIR and IR beams are represented by cyan and orange arrows (the latter double passing in the cell), respectively.

The analysis of the FIR spectra recorded simultaneously with the TDL-IR measurements to determine the particle density of formaldehyde was relatively straightforward. It was carried out in the 29–55 cm^{-1} range, corresponding to the R(11) to R(21) pure rotation transitions of formaldehyde. The particle density of formaldehyde was determined from the ratio of the integrated absorption coefficients of these pure rotation lines, measured by least squares fitting the observed line shapes to a Voigt function, and their integrated absorption cross sections, calculated using the accurately known electric dipole moment of HCHO (Fabricant *et al.*, 1977). Note that we investigated the possible existence of a Herman-Wallis dependence of the pure rotation line intensities of HCHO using the high-resolution FIR spectra recorded overnight. Such dependence would indeed affect the particle density of the species inferred from the pure rotation line intensities. None could be observed.

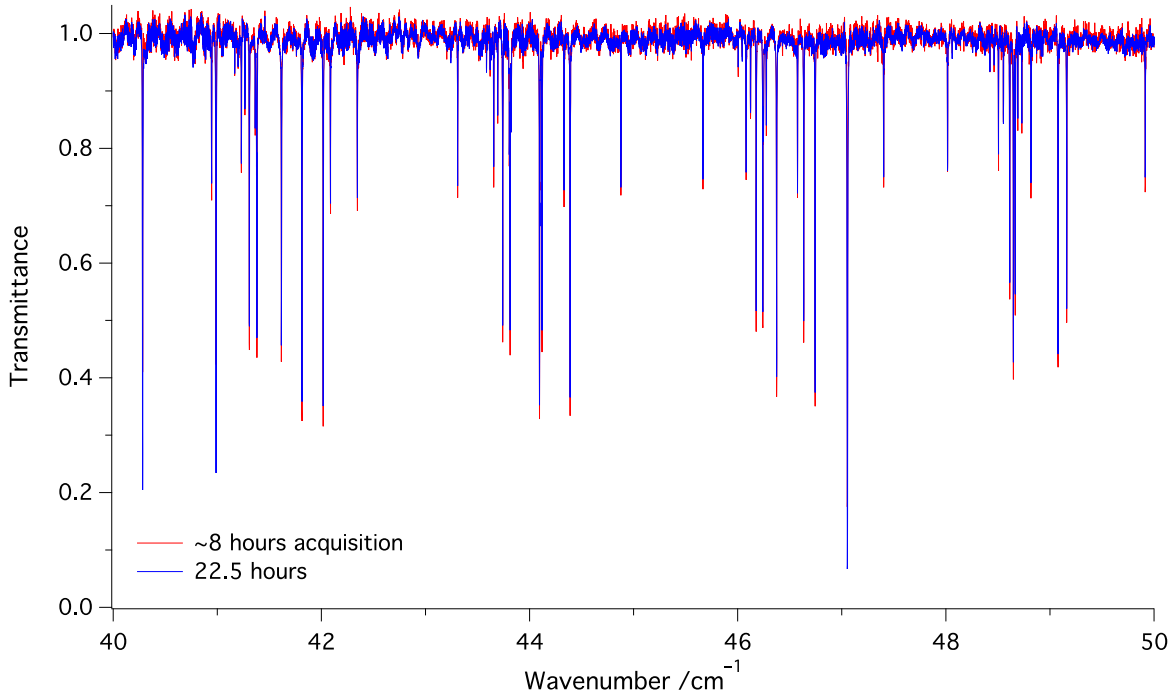

Figure 10: Part of the high-resolution pure rotation spectrum of formaldehyde (about 0.17 Torr in about 9 Torr N_2) recorded simultaneously with the IR tunable diode laser spectra (red) and extended overnight (blue). Most of the observed lines belong to formaldehyde and correspond to R(16) to R(19). A few lines due to water vapour are also observed.

The analysis of the TDL spectra proved to be a much more involved process. The six sets of IR spectra probe five different, ~0.6 cm^{-1} wide regions of the HCHO spectrum. To linearize these TDL spectra (i.e. determine the exact spectral range probed in these spectra and associate a wavenumber scale to them), we had to record high-resolution FTS spectra of the same region (actually of the whole ν_1 / ν_5 band system, between 2500 and 3200 cm^{-1}). It then turned out that most of the TDL spectra were affected by what could be interpreted as a non-linear response of the HgCdTe detector or amplifier(s) used. We modelled that non linear response with functions involving one or two parameter(s), the value(s) of which being determined by matching relative intensities of weaker and stronger HCHO lines measured in the corrected TDL spectra and in the high-resolution FTS spectra of the whole ν_1 / ν_5 band system. With this method, we managed to correct two sets of TDL spectra probing the same spectral range (2911.40 – 2912.25 cm^{-1}). Indeed, the HCHO lines observed in that spectral region were the only ones to have intensities sufficiently different to allow measuring their integrated absorption coefficients with some confidence. Comparison of the line intensities thus determined in this limited range with HITRAN showed an agreement in line with the estimated uncertainty of 5–10% provided in HITRAN. A similar agreement was obtained when comparing the intensities of strong lines measured in the high-resolution FTS spectra of the whole ν_1 / ν_5 band system with the line intensities provided in HITRAN.

Task 2.2.2. Re-analyze the data for C_2H_4, C_2H_6 and HCHO with new spectroscopic data at Jungfraujoch and Reunion Island.

The idea behind this task was to verify new, improved spectroscopic data as they became available in the course of the project.
As seen above, the work on the spectroscopy of formaldehyde has encountered several unforeseen difficulties and has therefore not yet been finalized. So the retrievals have been optimized with currently available HITRAN2008 data.

As to ethane, it was in the past impossible to combine the three main features (i.e. the $^{P}Q_3$, $^{P}Q_1$ and $^{R}Q_0$ branches near 2976, 2983 and 2986 cm^{-1}, respectively, due to spectroscopic inconsistencies for the C_2H_6 parameters. Bader et al. (EGU2012) showed that pseudoline parameters derived by G.C. Toon (NASA-JPL) from Harrison et al. (JQSRT, 2010) laboratory spectra helped solving that issue, with a significant improvement of the information content. The 3-window strategy was then successfully applied to Eureka spectra (Viatte et al., 2014) and Jungfraujoch spectra (Franco et al., 2015), while for Reunion, the strategy had to be limited to a 2-window approach, because of important interferences by water vapor in the 2986 cm^{-1} interval (Vigouroux et al., 2012).

For ethylene, the new spectroscopic linelist generated in the project (see above) has been used.

HCHO at Reunion Island

The retrieval strategy for HCHO was optimized and published prior to the AGACC-II project, in Vigouroux et al. (2009). In this study, comparisons were made with MAXDOAS measurements at Reunion Island in 2004, showing a good agreement between both techniques. Small changes in the retrieval strategy have been made since then: the micro-windows for the preliminary retrievals of the interfering gas H_2O and HDO have been changed. The micro-window for HDO being now the 2855.65-2856.4 cm^{-1}, it has been removed from the previous set of HCHO micro-windows used in Vigouroux et al. (2009). We give in Figure 11 the new HCHO time-series at Reunion Island, Saint-Denis, and the comparisons with the IMAGES model.

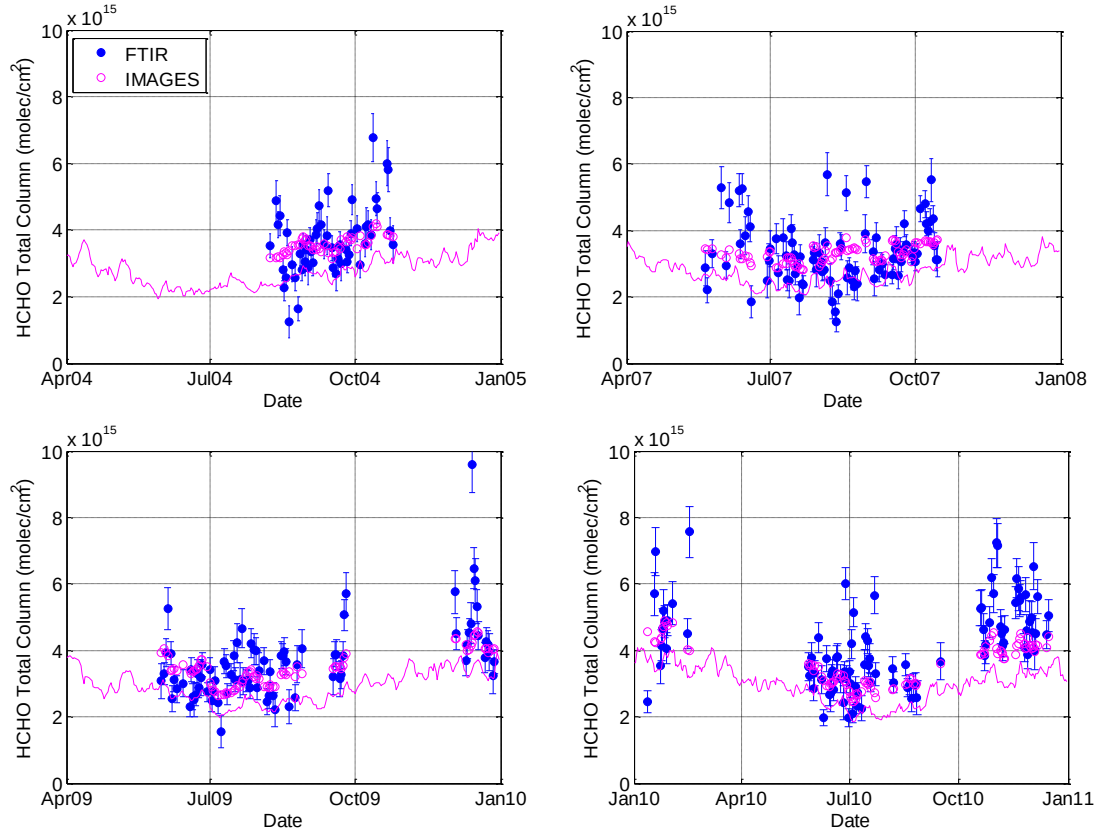

Figure 11: **Daily mean total columns of HCHO at Reunion Island, Saint-Denis. Blue: FTIR; Magenta line: IMAGES model; Magenta circle: IMAGES model smoothed by the FTIR averaging kernels.**

The HCHO diurnal cycle obtained from these time series has been used in recent satellite (De Smedt et al. 2015) and model (Stavrakou et al., 2015) studies. Indeed, the diurnal cycle is not available from current satellite measurements (GOME-2 measures only at about 9:30 local time, and OMI at 13:30). A positive bias is observed between OMI and GOME-2 HCHO total columns above Reunion Island (De Smedt et al., 2015), and ground-based observations were crucial to conclude that the bias is due to the diurnal cycle and not to the uncertainties on the satellites data.

HCHO at Jungfraujoch

Two HCHO retrieval strategies have been tested for the Jungfraujoch station, where the HCHO absorption generally does not exceed 1%. The first one focuses on one microwindow (2833.07 – 2833.35 cm^{-1}) only, which is covered by a tunable bandpass optical filter since December 2005. Using a larger diaphragm aperture (1.45 mm) on a narrow spectral range (2810 – 2850 cm^{-1}), it provides solar spectra with very high signal-to-noise ratio helping for the HCHO fitting. The second HCHO retrieval strategy corresponds to a modified version of the method implemented by Vigouroux et al. (2009) for Réunion Island (see previous section), fitting simultaneously 4 of the 6 microwindows in the 2760 – 2860 cm^{-1} spectral domain, not covered by the tunable optical filter.

The 4-microwindows retrieval strategy described in Franco et al. (AMT, 2015) has been selected to produce a HCHO long-term time series covering the 1988 – 2014 (Figure 12), showing strong intra-annual variations characterized by the largest

columns and variability during summertime and by regular minimum and compact columns in winter. This multidecadal data set allows identifying three consecutive periods characterized by statistically different trends (see insert in Fig. 11). GEOS-Chem multi-year sensitivity simulations indicate that the long-term evolution of HCHO above Jungfraujoch is mainly driven by the CH_4 oxidation, with a maximum contribution of 25% from anthropogenic NMVOCs during wintertime (see Franco et al., ACPD, 2015).

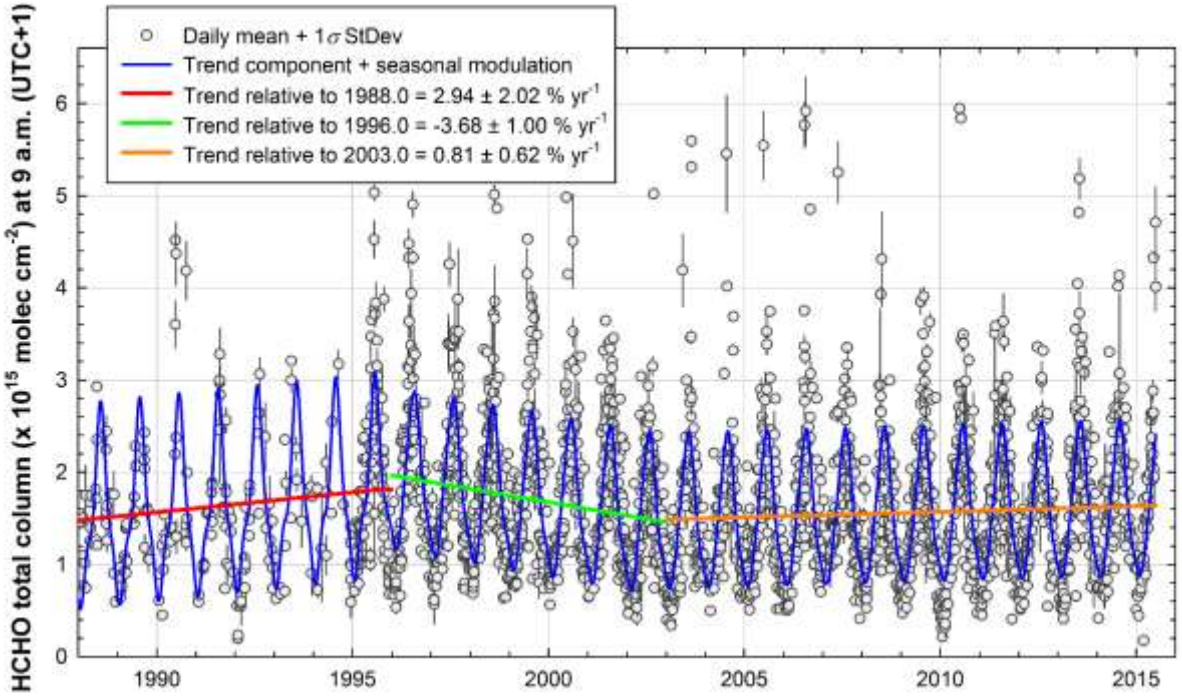

Figure 12: Long-term FTIR time series of formaldehyde above Jungfraujoch (Franco et al., ACPD, 2015).

C_2H_6 at Reunion Island

The retrieval strategy for C_2H_6 has been optimized for Reunion Island during AGACC-II. The spectral micro-windows are 2976.66-2976.95 cm^{-1} and 2983.20-2983.55 cm^{-1}. Due to the strong interference with water vapor line, the third micro-window around 2986 cm^{-1} is not recommended at Reunion Island. We show in Figure 13 and Figure 14 the C_2H_6 time series (2004-2010) published in Vigouroux et al. (2012), and the updated time series with new measurements at both stations St-Denis and Maido, respectively.

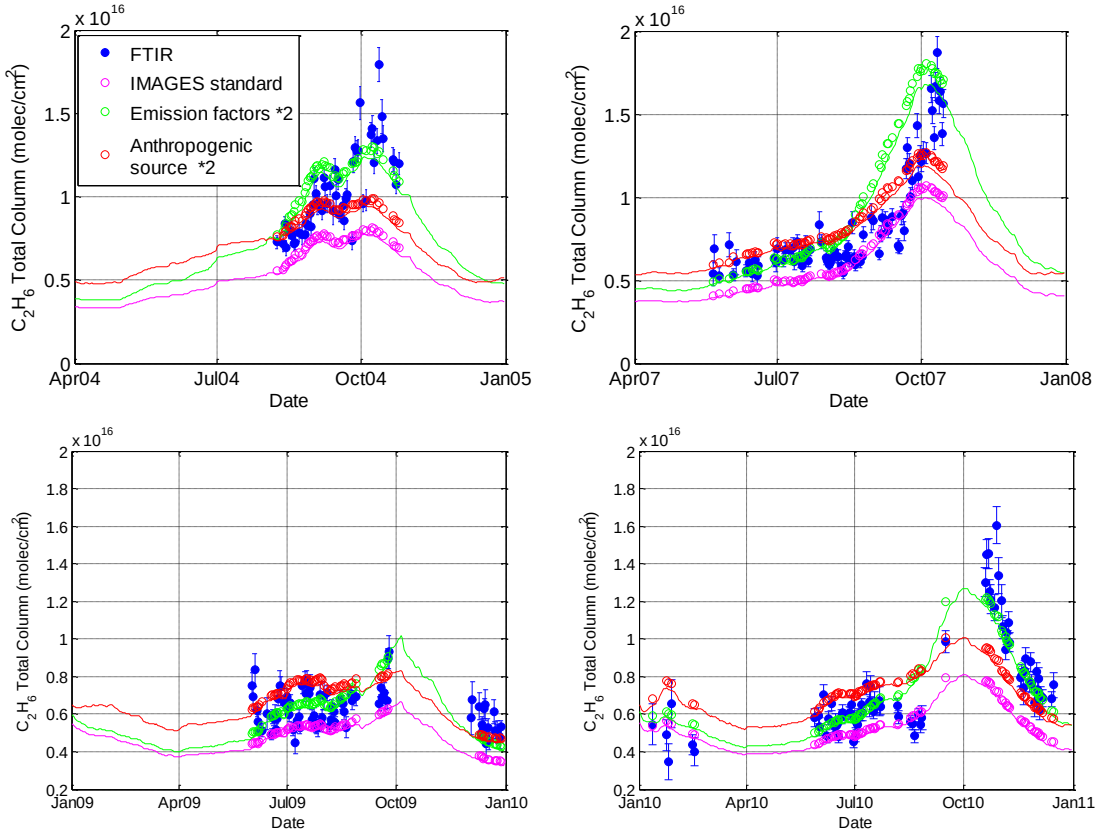

Figure 13: Daily mean total columns of C_2H_6 at Reunion Island, Saint-Denis used in Vigouroux et al. (2012). Blue: FTIR; Magenta line: IMAGES model; Magenta circle: IMAGES model smoothed by the FTIR averaging kernels. Green and red: sensitivity tests performed in IMAGES to study the impact of different emission sources (Green: the biomass burning emission factors are multiplied by a factor 2 in IMAGES; Red: the anthropogenic source is multiplied by a factor 2).

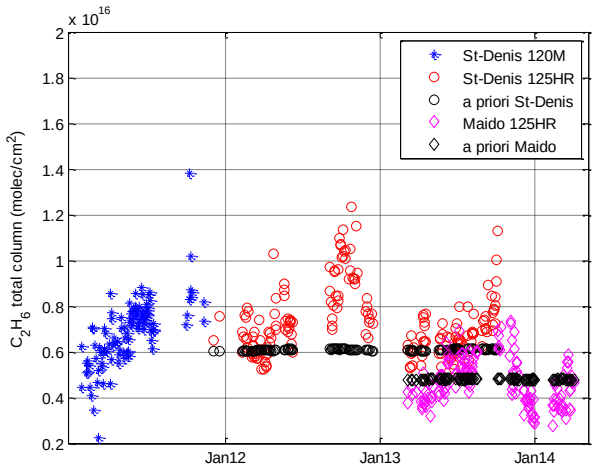

Figure 14: Updated time series of daily mean total columns of C_2H_6 at Reunion Island. Blue: measurements at St-Denis with the Bruker 120M in 2011; Red: measurements at St-Denis with the Bruker 125HR; Magenta: measurements at Maïdo observatory.

C_2H_6 at Jungfraujoch

The retrieval strategy for ethane has been completely revisited, after implementation of very recent C_2H_6 line parameters (Harrison et al., JQSRT, 2010) and for CH_3Cl (Bray et al., JQSRT, 2011). Our investigations showed that combining three windows around 2976, 2983 and 2986 cm^{-1} is now possible and that the new parameters help to significantly reduce the fitting residuals. The DOFS is also strongly improved, from 1.4 with the previous approach to more than 2 with the new one.

Using the optimized 3-window retrieval strategy, we have produced a 20-year long-term time series of C_2H_6 abundance above Jungfraujoch from 1994 onwards. After a 1994 – 2008 decrease of the C_2H_6 amounts, which is very consistent with prior major studies and with our understanding of global C_2H_6 emissions, trend analysis using a bootstrap resampling tool reveals a C_2H_6 upturn and statistically-significant sharp burden increase from 2009 onwards. We hypothesize that this observed recent increase in C_2H_6 could affect the whole Northern Hemisphere and may be related to the recent massive growth in the exploitation of shale gas and tight oil reservoirs. This hypothesis is supported by measurements derived from solar occultation observations performed since 2004 by the Atmospheric Chemistry Experiment – Fourier Transform Spectrometer (ACE-FTS) instrument. Indeed, the recent trend characterizing the ACE-FTS version 3.5 partial columns above North America is consistent in magnitude and sign with the one derived from the FTIR measurements at Jungfraujoch. Investigating both the cause and impact on air quality of the C_2H_6 upturn should be a high priority for the atmospheric chemistry community (Franco et al., 2015) . Follow-up investigations involve FTIR observations from North America, and Canada in order to quantify –with support from dedicated model simulations– the emissions responsible for the ethane increase after 2009 (Franco et al., EGU2015) and its possible impact on air quality degradation.

C_2H_4 at Reunion Island

The spectroscopic signatures of C_2H_4 are very weak and close to the detection limit. The main C_2H_4 signature is at the edge of a strong CO_2 line (around 949.5 cm^{-1}). Therefore, as for CH_3Cl, a large scatter is observed in the total columns, due to the large random noise error. This scatter is improved at the Maïdo observatory (Figure 15, Left), due to the better instrumentation (Bruker 125HR) and to the lower interferences with other molecules. The data shown in Figure 15 have been filtered with RMS<0.45, however there are still negative columns.

The use of the new spectroscopy from ULB has an impact of -4.6+/-4.2% on total columns at Maïdo when only positive columns are taken into account. The spectral signatures are so weak that a possible impact of the new spectroscopy on the RMS is not observed. The RMS is dominated by the SNR and the interfering species fit.

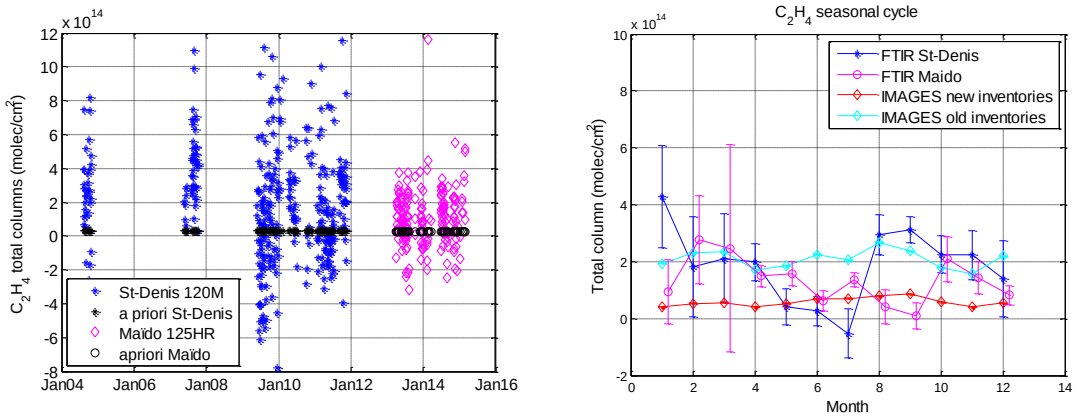

Figure 15: Only data with RMS<0.45 are shown. Left: C_2H_4 daily means total columns at St-Denis (blue) and at Maïdo (magenta). Right: C_2H_4 seasonal cycle at St-Denis (blue) and Maïdo (magenta);. The error bars are 2* standard deviation / sqrt(n). The IMAGES seasonal cycles from new (red) and old (cyan) inventories are also shown.

We compare in Figure 15 (right), the seasonal cycles obtained at St-Denis and Maïdo, and with the model IMAGES. There is a reasonable agreement between St-Denis and Maïdo in Oct-Apr. The too low monthly values at St-Denis in May-July (St-Denis columns should be larger than the Maïdo ones due to the lower altitude of St-Denis) are due to the negative values in 2009. The columns at Maïdo are minimum in Aug-Sept, which is not seen at St-Denis and by the model. This needs to be studied, and more years of data can help to determine if this is due to real variability or to large systematic errors due to e.g. the interfering species. The FTIR data are in reasonable agreement with the older version of inventories (in cyan) used in IMAGES, especially for the Aug-Apr and Oct-May periods at St-Denis and Maïdo, respectively. The new inventories (in red) which relied on aircraft measurements in the Pacific and United-States to decrease the biogenic and oceanic emissions of C_2H_4, are in better agreement with Maïdo when the columns are minimum (Dec-Jan; Jun-Sep), but they do not reproduce the maxima in Spring and Oct-Nov. The Oct-Nov months are a period of biomass burning in Madagascar. Some biomass burning sources (fires from agriculture) are still missing in the GFED3 inventory used by IMAGES, and are included in the next GFED4 inventory which still need to be implemented in IMAGES.

C_2H_4 at Jungfraujoch

Absorption by ethylene in Jungfraujoch spectra is very weak, on the order of a few tenths of a percent for background conditions, and the production of a complete time series has not been successful thus far, using the window around 949.5 cm^{-1}. This is the reason why only a subset of spectra providing maximum C_2H_4 abundance were used to study the impact of the new line parameters produced by ULB (see Vander Auwera et al., 2014).

Task 2.2.3: comparison between FTIR and MAX-DOAS and with model simulations.

Comparisons between FTIR and MAX-DOAS data have revealed an underestimation of the HCHO total columns produced by the single-microwindow FTIR retrieval strategy, especially during summertime, which has been confirmed by further

comparisons with ACE-FTS v.3.5 measurements as well as GEOS-CHEM and IMAGES simulations. In contrast, the multi-windows retrieval approach has provided HCHO data in good agreement with MAX-DOAS, ACE-FTS and both models. Further tests using the HITRAN 2012 line list parameters (implementing enhanced broadening coefficients of the HCHO features) have also been performed, leading to much lower total columns, thus significantly degrading the agreement between the FTIR, MAX-DOAS and model time series. Hence, the multi-microwindow approach and the HITRAN 2008 lime parameters were used to produce an unprecedented long-term time series of HCHO spanning more than 25 years.

In-depth comparisons between MAX-DOAS and FTIR measurements of formaldehyde at the unpolluted site of the Junfgraujoch have been performed and analyzed by Franco et al. (2014). With the support of GEOS-CHEM 2° x 2.5° and IMAGES 2.5° x 2.5° model simulations, it was possible to demonstrate a very good agreement between both techniques, despite their contrasted sensitivity, for a species presenting a very short lifetime of a few hours and strong intra-day variability. Using the CTMs outputs as intermediate, FTIR and MAX-DOAS retrievals have indeed shown consistent seasonal modulations of HCHO throughout the investigated period of common measurements (2010-2012), characterized by summertime maximum and wintertime minimum. Such comparisons have also highlighted that FTIR and MAX-DOAS provide complementary products for the HCHO retrieval above the Jungfraujoch station.

Task 2.3 Retrieval feasibility studies

Task 2.3.1: Feasibility of retrieval of PAN and acetone at Jungfraujoch and La Réunion

Acetone

The acetone cross-sections have been released in the HITRAN 2012 database, but no pseudo-lines that can be used in the retrieval softwares SFIT2 or SFIT4 have been delivered to the IRWG community. Therefore it was not possible to make the feasibility study of acetone retrieval at both stations.

PAN

At Jungfraujoch,

Thus far, the search for PAN in Jungfraujoch spectra has not been successful.

At Reunion Island

We have tested the 2 most intense bands of PAN, centered at 794 cm^{-1} and at 1163 cm^{-1} (Glatthor et. al, 2007). Unfortunately, the most intense one at 794 cm^{-1} is in a spectral region where our FTIR spectra are more noisy, at the edge of the band pass filter. Also strong saturated water vapor lines are absorbing in the region, even in the Maïdo spectra. Therefore, the PAN columns obtained using this spectral region were unrealistic. The second band at 1163 cm^{-1} looks more promising, even if a large

scatter and some negative values are observed (Figure 16, left), especially the expected maximum in October due to the biomass burning season at Madagascar is observed (Figure 16, right). Note that no data passed the quality criteria of RMS<0.4 in January and November (another month with expected higher PAN values due to biomass burning). More years of data will help to determine the complete seasonal cycle. The strong H_2O lines in the spectral window are not perfectly fitted; therefore there is probably some room for improvement in the future if a better spectroscopy for H_2O lines becomes available.
We show in Figure 16 (right) the seasonal cycle obtained at Maïdo.
The retrievals at St-Denis are not done yet, because it requires some technical changes in our S/W, due to the very large window needed to fit the broad absorption cross-section of PAN (more than 20 cm^{-1}).

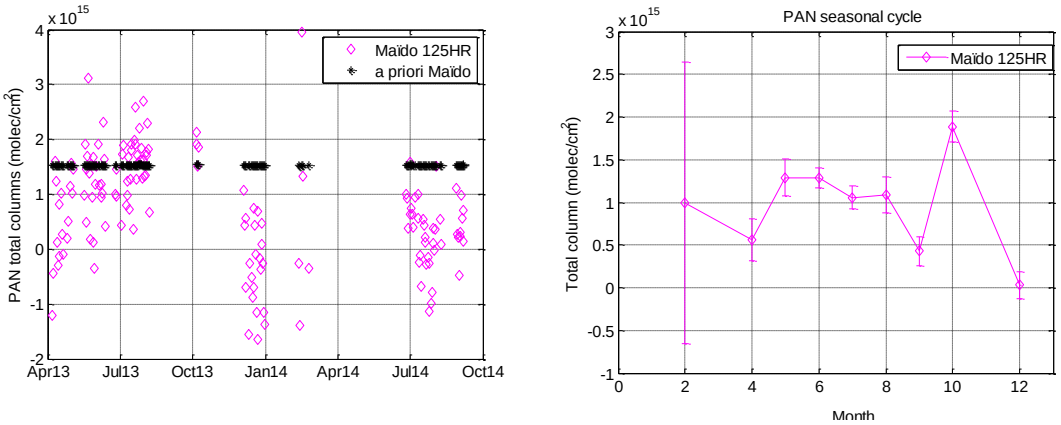

Figure 16: Only data with RMS<0..40 are shown. Left: PAN daily means total columns at Maïdo. Right: PAN seasonal cycle at Maïdo. The error bars are 2* standard deviation / sqrt(n).

Task 2.3.2 search for absorption features of CFC substitutes

We have been seeking for signatures of two CFC-substitutes, HCFC-142b (CH_3CClF_2) and HFC-134a (CH_2FCF_3), respectively. We were able to detect weak systematic residuals (0.5-1.0%) when assuming no HCFC-142b or HFC-134a in the atmosphere. Pseudolines are not available for the latter, hence it was not possible to perform any retrieval.

We have carefully evaluated the possibility to retrieve HCFC-142b (CH_3CClF_2), a CFC-substitute, from Jungfraujoch spectra, in four candidate windows (900-906, 965-970, 1132-1136 and 1191-1196 cm^{-1}). It turned out that only two domains could be used, the 900-906 and 1191-1196 windows, the two others being affected by strong interferences by CO_2, O_3 and H_2O. Moreover, systematic and independent fits to both domains have revealed that the adoption of the second interval led to the determination of total columns that are too large by about a factor of 2, possibly resulting from missing interferences in HITRAN 2008 and/or inconsistent cross section parameters for HCFC-142b. Therefore, the 900-906 feature has been selected to produce a HCFC-142b data set, using all available low sun spectra for the 2000-2014 time frame. Uncertainties on the total columns have been evaluated to

<8% and <12% for the total random and systematic contributions. Figure 17 shows the contribution of the interferences (shifted vertically for clarity) as well as the weak HCFC-142b feature (pink trace). The upper panel allows comparing the fitting residuals, in green when including HCFC-142b in the retrieved species, in red when assuming no HCFC-142b in the atmosphere.

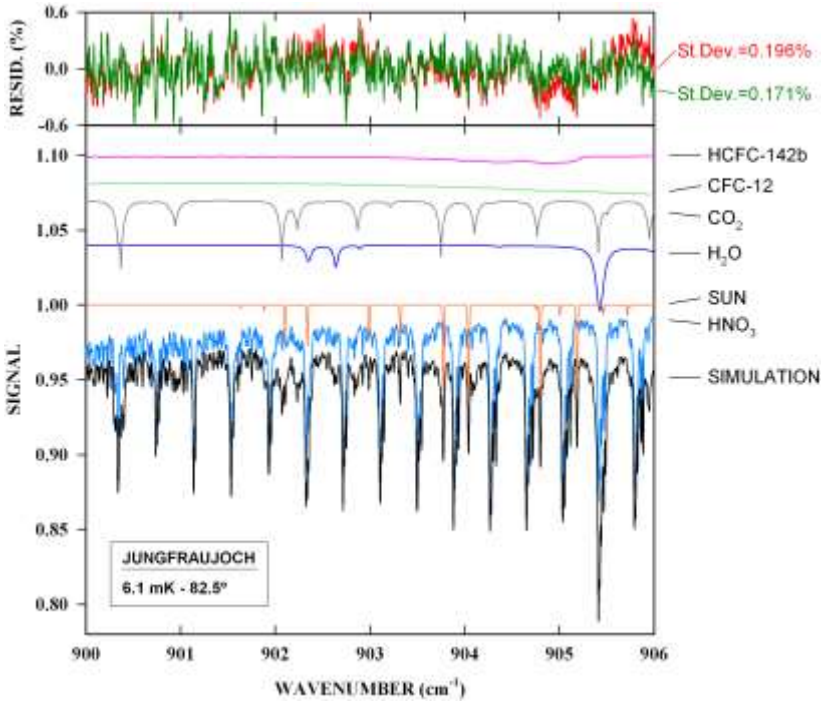

Figure 17: Selected microwindow for the retrieval of HCFC-142b from the Jungfraujoch station.

The 2000-2012 total column data set of HCFC-142b is characterized by a strong increase, from about 1.6 to 2.8 x10^{14} molec./cm^2 over 13 years, i.e. a relative rate of change of 6.5%/yr. This is commensurate with the trend derived by the AGAGE network at Mace Head (53ºN). Comparison of surface mixing ratio suggests that the FTIR data are lower by 5% on average, i.e. well below the systematic uncertainty upper limit of 12% evaluated in our study (Mahieu et al., 2013).

Task 2.4 Production of the CCl_y and CF_y budgets for Jungfraujoch.

Retrieval strategies have been revisited for CFC-11, CFC-12 and HCFC-22, in order to derive some vertical information from the spectra and optimize the total column determinations. Typical DOFS amount to 1.6, 1.9 and 1.5, respectively. Final time series have been produced from 2000 onwards. They have been combined with the HCFC-142b (CH_3CClF_2) and with the CCl_4 or CF_4 weighted contributions to generate CCl_y and CF_y total column budgets, respectively. Hence, the CCl_y^* and CF_y^* proxies include the following contributions:

$$[CCl_y]^* = 3 \times [CCl_3F] + 2 \times [CCl_2F_2] + [CHClF_2] + [CH_3CClF_2] + 4 \times [CCl_4] + [CH_3Cl]$$

$$[CF_y]^* = [CCl_3F] + 2 \times [CCl_2F_2] + 2x [CHClF_2] + 2 \times [CH_3CClF_2] + 4 \times [CF_4]$$

Figure 18 shows the time series of 6 halogenated source gases monitored at the Jungfraujoch station over the last fifteen years. Five species are relevant to establish the evolution of the CCl_y^* budget. All together, they correspond to ~87% of the total CCl_y budget for the year 2004. The CCl_y* trend over 2000-2014 shows a constant decrease at rates close to –(0.23±0.05)%/yr (see Figure 19). It is important however to realize that the largest negative contribution of CFC-11 is currently canceled by the steady accumulation of HCFC-22.

A corresponding budget has been established for organic fluorine, including the contributions from CFC-11 and -12, HCFC-22 and -142b as well as of CF_4. In contrast to CCl_y, CF_y is still characterized by a positive rate of increase, of (0.60 ± 0.03) %/yr.

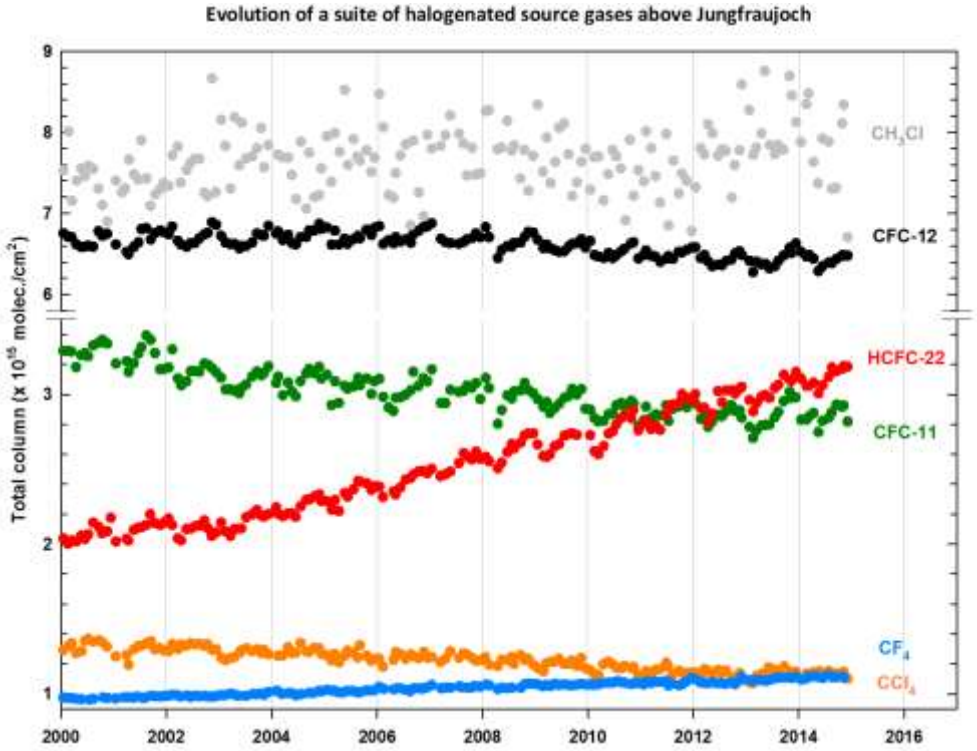

Figure 18: Evolution of a suite of halogenated source gases above Jungfraujoch over the last 15 years. Investigations performed within the framework of AGACC-II have allowed doubling the list of species, with the addition of CCl_4, CF_4, CH_3Cl and HCFC-142b (note that the HCFC-142b time series is not visible in this figure, with columns ranging from ~ 1.5 to 3 E14 molec./cm2).

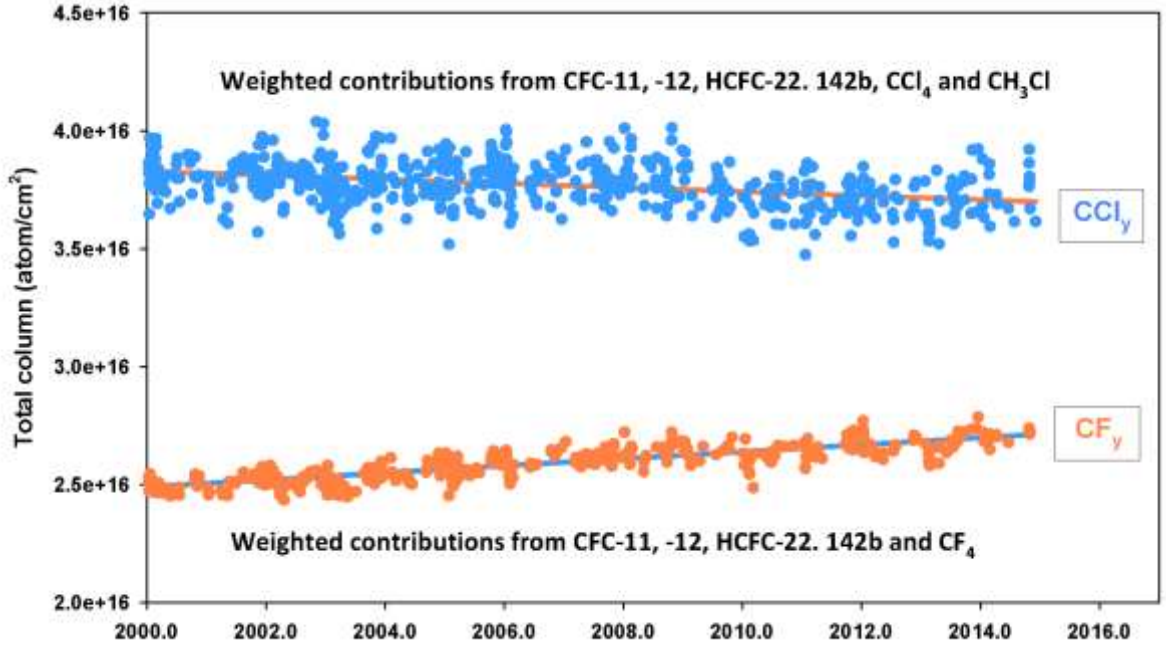

Figure 19: Evolution of the organic chlorine and fluorine budgets above Jungfraujoch over the last fifteen years (Mahieu et al., EGU2015).

WP 3: Aerosol properties and radiative forcing at Ukkel

Task 3.1 Improve algorithms for aerosol characterization from ground-based spectral measurements

Task 3.1.1 Develop a better cloud screening method for deriving the AOD at 340nm from the Brewer measurements

During the previous AGACC project (SD/AT/01B), a method was developed that allowed the retrieval of Aerosol Optical Depth (AOD) at 340nm from sun scan measurements of Brewer#178 at Ukkel (De Bock et al. 2010). At that time, an initial cloud screening algorithm was developed to remove cloud perturbed AOD measurements from the results. Analysis of the cloud screened data indicated that the performance of this screening technique was not optimal. Therefore it was decided to develop an ***improved cloud screening*** method. This new cloud screening method (Figure 20) makes use of sunshine duration data and is also based on the assumption that the variability of the AOD in the course of one day is either lower than 10% or lower than 0.08 AOD units. The advantages of this new method are (1) the removal of the arbitrary maximum level of AOD values, and (2), it runs completely automatic (whereas the old one needed manual verification afterwards).

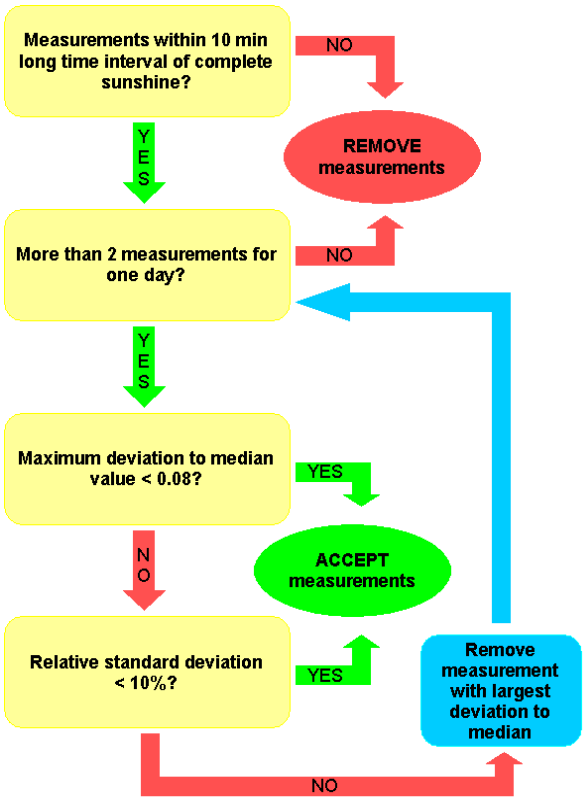

Figure 20: Overview of the improved cloud screening method.

The AODs obtained with the improved cloud screening method are compared to quasi-simultaneous CIMEL sunphotometer level 2.0 values (with a maximum time difference of 3 minutes) for a period from August 2006 until May 2014. For this period, 979 individual AOD values were compared and the correlation coefficient, slope and intercept of the regression line are 0.979, 0.993 +/- 0.007 and 0.072 +/- 0.002 respectively (Figure 21). These values are similar to the ones calculated based on the shorter time period (2006-2010) and show that the cloud screened Brewer AOD agree very well with the CIMEL data. The newly developed cloud screening method has now also been applied to the Brewer AOD retrieval using direct sun measurements at 306, 310, 313, 316 and 320nm.

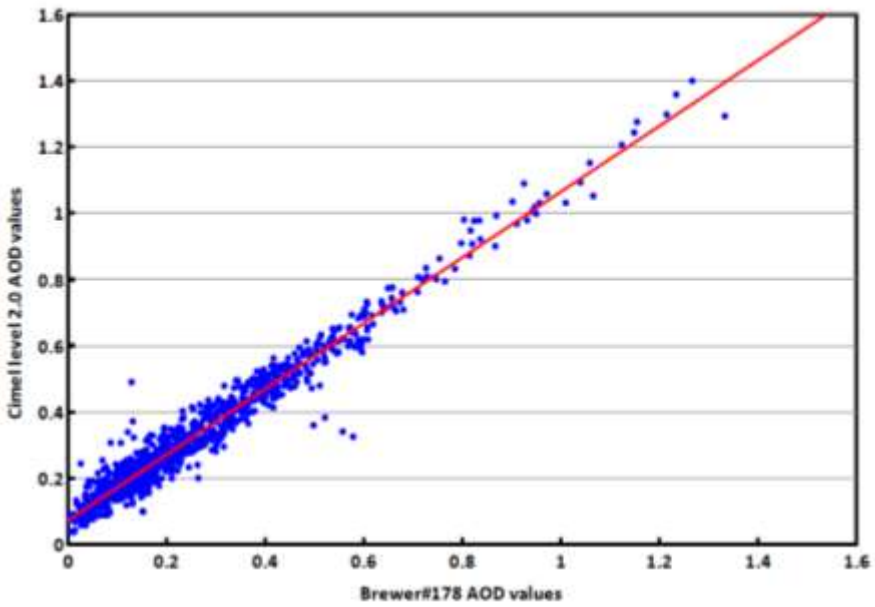

Figure 21: Comparison of the cloud screened (improved method) Brewer and CIMEL AOD values at Ukkel at 340nm for the 2006-2104 period.

Task 3.1.2 Develop an inverse modeling system to extract aerosol single scattering albedo information from Brewer data

We have developed an algorithm to extract single scattering albedo (SSA) values using Brewer spectrophotometer data, based on the comparison between measured and modelled UV irradiances. The measured irradiances are provided by Brewer#016 (from 290 to 325nm). The radiative transfer model TUV version 3.0 (Madronich, 1993), was used to model UV irradiances for cloudless days. The "SSA retrieval algorithm" consists of different steps:

1) Choose a UV scan measurement (the time of this scan = the time for which the TUV model is run)
2) Choose the wavelength at which you want to determine the SSA
3) Select AOD and ozone for input of TUV model (i.e. Brewer measurements of ozone and AOD (at the selected wavelength) closest to the UV scan measurement time)
4) Run the TUV model with an initial SSA value
5) Compare the modeled and measured UV irradiances at the chosen wavelength:
    a. If the difference between the two is less than 1%: accept the SSA value + increase or decrease the SSA value + run the TUV model again
    b. If the difference between the two is more than 1%: increase or decrease the SSA value + run the model again

We have modeled SSA ranges (calculated for a time around 12UT) for 84 cloudless days between September 2006 and December 2010. From the results, it is clear that the SSA range becomes very large when the input AOD value is low. There is also a clear relationship between the input AOD and the mean modelled SSA value, with higher AOD values leading to higher and more reliable SSA values (Figure 22). SSA values modelled for AOD values below 0.5 are very unrealistic. From these results,

we can conclude that the method to retrieve SSA values from Brewer measurements does not perform very well, especially under circumstances with low AOD. The sensitivity of the model to different parameters (i.e. measured intensity, measured ozone and measured AOD) has been tested.
The Brewer instruments measure the UV intensity with an average error of about 5%. The difference between the modeled SSA at measured intensity and at an intensity increased/decreased by 5% was therefore analyzed. For ozone, we used the same 5% as uncertainty (although it's actual uncertainty is 1%) while for the AOD measurements the absolute uncertainty is 0.08. The results of this sensitivity study are presented in Table II. They show that the modeled SSA values are highly sensitive to the uncertainties in the input parameters. Due to this high sensitivity of the model to the input parameters, it is not feasible to use the model (at least not in its current form) for SSA retrieval. In the future, we intend to collaborate with the University of Thessaloniki (Greece) in order to investigate other possibilities to derive SSA using radiative transfer models in combination with Brewer measurements.

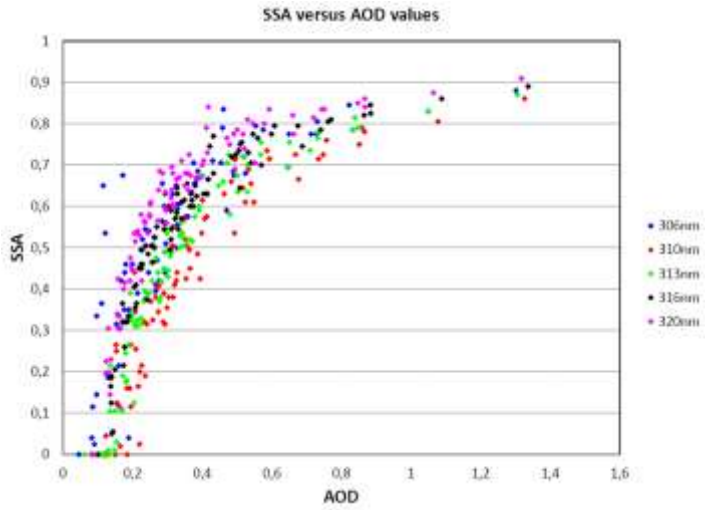

Figure 22: Modeled SSA values versus input AOD at five wavelengths in the UVB region.

Table II: Absolute and relative differences between modeled SSA values caused by changes in input parameters

	Minimum absolute difference	**Maximum absolute difference**	**Minimum % difference**	**Maximum % difference**
Intensity +5%	0.02	0.22	2.20%	181.82%
Intensity -5%	-0.03	-0.25	-3.30%	-91.43%
Ozone + 5%	0.01	0.16	1.10%	103.23%
Ozone -5%	0.01	-0.14	1.49%	-90.91%
AOD + 0.08	0.01	0.41	1.10%	336.36%
AOD -0.08	-0.01	-0.45	-1.01%	-92.63%

Task 3.1.3: Further algorithm developments for retrieval of aerosol properties from MAX-DOAS observations

Retrievals of trace-gas columns and aerosol optical depths (AODs) from MAX-DOAS observations are ideally performed under clear-sky conditions. However, MAX-DOAS

measurements at Uccle, as for other stations, are often strongly affected by clouds, leading to larger uncertainties on the retrievals. To better characterise data taken under cloudy conditions, a cloud-screening method for the MAX-DOAS observations has been developed, based on the colour index (CI, the ratio of the radiance at two different wavelengths, 350 nm and 420 nm in the case of Uccle) of the sky (Gielen et al., 2014).

Using the CI, 3 different sky conditions are defined: bad (=full thick cloud cover/extreme aerosols), mediocre (=thin clouds/aerosols) and good (=clear sky). The presence of broken/scattered clouds is flagged as follows: since the CI shows large drops in value when such clouds pass over, they can be identified by fitting a double-sine functions to the diurnal variation of the CI and determining the outliers, i.e. the MAX-DOAS scans for which the CI differs significantly from the fitted curve.

Removing data under bad-sky and broken-cloud conditions results in a better agreement, in both correlation and slope, between the AERONET and MAX-DOAS AOD retrievals at Uccle (see Figure 23). We find that high MAX-DOAS AODs are removed, as they are now identified as due to clouds (blue crosses in Figure 23 left).

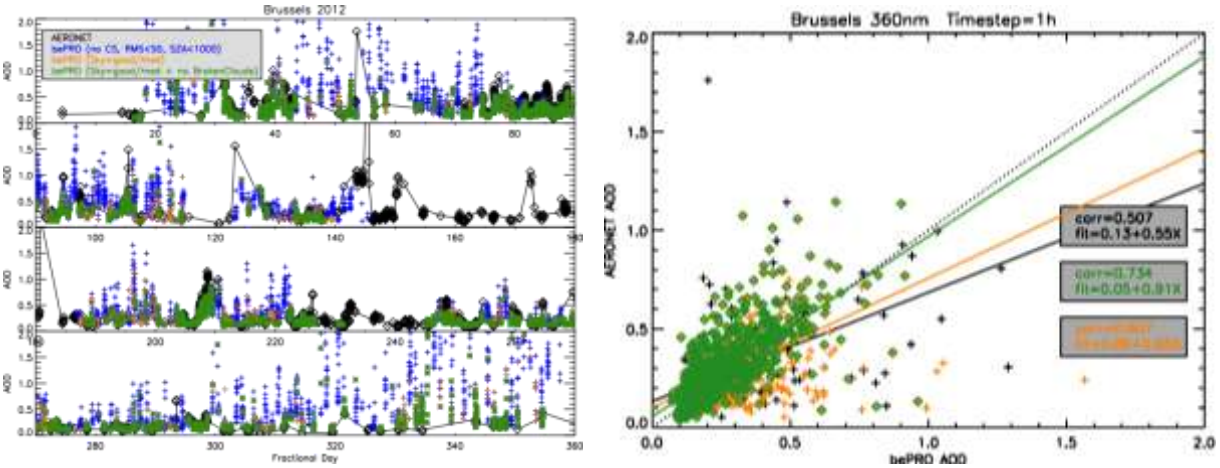

Figure 23: Left: Comparison of AOD retrieved by applying the bePRO profiling tool (Clémer et al., 2010) to MAX-DOAS O_4 measurements at Uccle and co-located AERONET data. In black the AERONET data, blue the non-cloud-screened MAX-DOAS data, orange the cloud-screened data under good/mediocre conditions, green the good/mediocre data with additional removal of data hindered by broken clouds. Right: Corresponding correlation between MAX-DOAS and AERONET AODs. In black the non-cloud-screened MAX-DOAS data, green and orange are defined the same as in the left figure.

In order to validate the cloud screening method, the cloud flagging for Brussels has been compared with thermal-infrared cloud-cover measurements performed in parallel with an infrared pyrometer, which determines the total cloud-cover fraction based on temperature data over a field of view of 6° (Gillotay et al., 2001). The total cloud-cover fraction is defined as the ratio between the observed cloudy solid-angle elements and clear-sky elements. In Figure 24 the total cloud-cover fraction values for an example day can be seen, where our different CI flagging results are colour-marked. High cloud-cover fractions are systematically flagged with a “bad” sky flag, whereas low cloud cover data correspond to “good/mediocre” sky flags, indicating the good reliability of our CI-based cloud screening method.

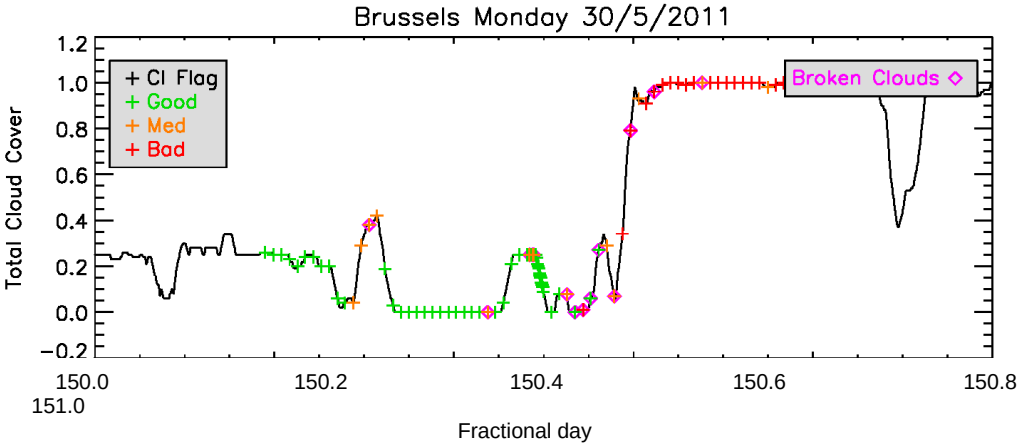

Figure 24: Total cloud-cover values from thermal-infrared measurements are given in black points. Overplotted in coloured crosses are the respective Cl-flag values as derived from our cloud-screening method (green/orange/red=good/med/bad). Data with a broken-cloud flag are marked with a magenta diamond.

Task 3.2 Operate ground-based remote sensing instruments for aerosol characterization at Ukkel

Task 3.2.1 continue the routine operation of the Brewer spectrophotometer and the Cimel sunphotometer at Ukkel, the latter in compliance with the AERONET requirements

The data of both Brewer instruments are continuously stored and regularly checked. Both Brewer instruments were calibrated by Kipp&Zonen in 2012 and 2014. No major problems showed up during the calibration, although the last intercomparison showed that the electronics and parts of the mechanics of Brewer 016 are coming to the end of their life time after more than 30 years of operation.
In November 2011, a campaign was organized to measure the cosine response error of Brewer178 (in collaboration with Mr. David Bolsée of BIRA-IASB). The campaign proved to be a great success since the newly obtained cosine response function is much better than the one that was provided by the manufacturers of the instrument.

At Ukkel, simultaneous measurements of erythemal UV dose, global solar radiation, total ozone column and Aerosol Optical Depth (AOD) at 320.1nm are available for an extensive time series analysis. A time period of 23 years (1991-2013) has been studied, which allows us to determine the mutual relationship between the four parameters. The erythemal UV dose, total ozone column and AOD are retrieved from the Brewer spectrophotometer measurements (Brewer#016) at Ukkel. Global radiation measurements are provided by pyranometers.
Linear trends have been calculated for the monthly anomalies of erythemal UV dose, global radiation, total ozone and AOD at 320.1 nm (Figure 25). The linear trend analysis was also applied to the monthly anomalies of the extreme values (minima and maxima) of the variables. Also, the relative frequency distribution of the daily mean values has been studied for two different time periods: 1991–2002 and 2003–2013. Additionally, the medians for these periods were calculated. In this way, it was

possible to investigate whether there is a shift in the frequency distribution of the variables from the first period to the second one.
From the first part of the study we could conclude the following:

- Erythemal UV dose, global radiation and total ozone all increased over the past 23 years, whereas the AOD values decreased.
- After a period with lower ozone values in the 1990s, it seems that ozone has been recovering over the past 10 years.
- The increase in ozone values does not lead to the expected decrease in erythemal UV values. This indicates that other variables might contribute to the change in erythemal UV dose and that the contribution of ozone might be compensated by the influence of these other variables.
- An increase in the minimum values of global solar radiation shows that the cloud properties (i.e. their amount and/or water content) must have changed over the past 23 years.

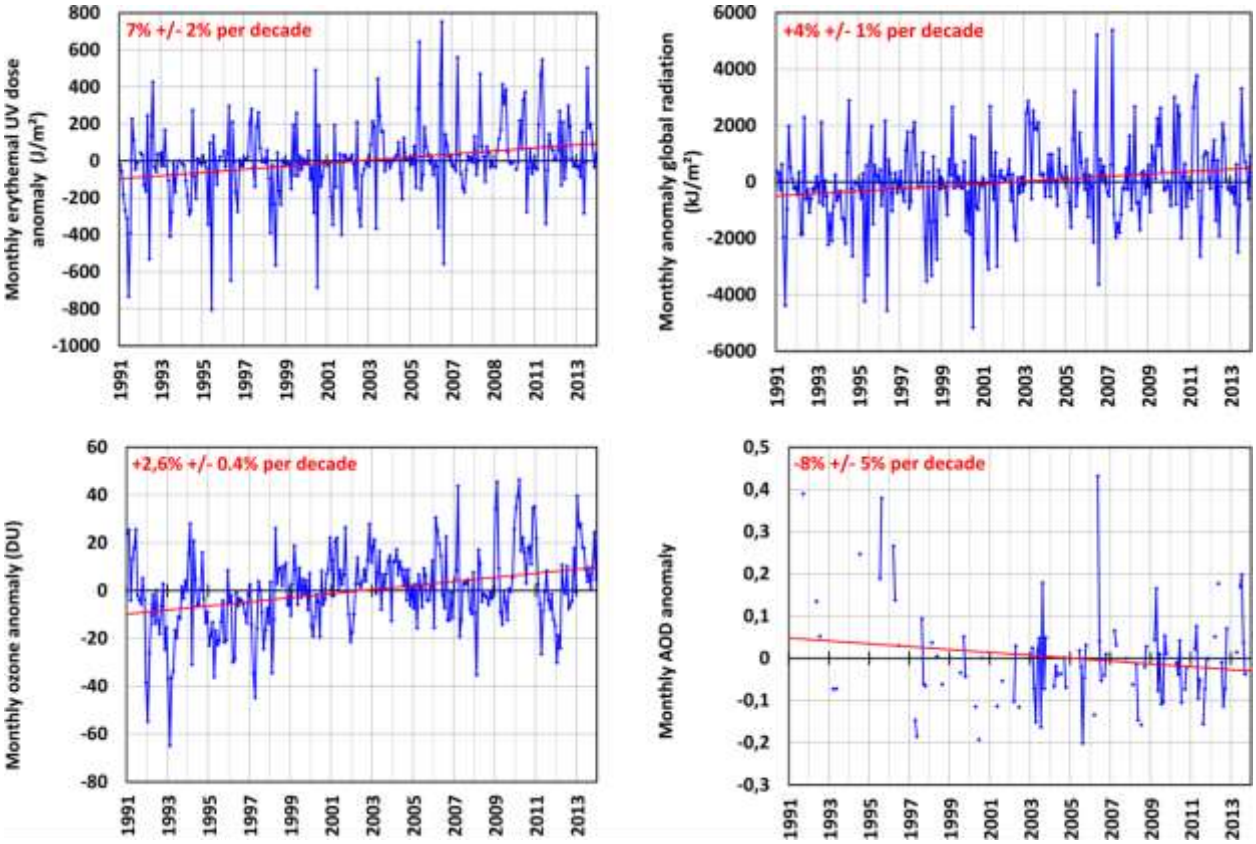

Figure 25: Trends of monthly anomalies at Ukkel for erythemal UV dose (upper left panel), global solar radiation (upper right panel), total ozone column (lower left panel) and AOD at 320.1 nm (lower right panel) for the time period 1991–2013. The blue lines represent the time series, whereas the red lines represent the trend over the time period.

A change point analysis has been performed to determine significant change points in the time series of UV, global radiation, ozone and AOD. Significant change points were detected in the monthly anomalies time series of erythemal UV dose and AOD around February/March 1998. Since we were able to rule out known instrumental causes for the detected change points in both time series, we can assume that they have some natural/environmental cause and are related to each other. The change

point in the ozone time series corresponds with results found in the literature. Recent studies have shown that, for other stations, the ozone recovery started around 1997 (Steinbrecht et al., 2006; Reinsel et al., 2005). Ozone levels seem to follow the change in chlorine concentrations resulting from the regulations of the Montreal Protocol in 1987. When ozone starts to increase, it is expected to have some implications on the UV irradiance as ozone is a strong absorber of UV irradiance in the stratosphere (Wenny et al., 2001). An increase in ozone would normally lead to a decrease in UV irradiance, which is not what was observed at Ukkel, where the UV irradiance levels continue to increase after 1998. Before 1998, the (insignificant) trends in the time series of ozone and erythemal UV dose are opposite, which is what would be expected. However, after 1998, both the (insignificant) ozone and erythemal UV dose are positive. So the behavior of ozone can only partly explain the changes observed in the UV irradiance time series, and other parameters, such as aerosols and cloudiness, might play an important role.

A Multiple Linear Regression (MLR) technique was used to explore whether there is a significant relationship between erythemal UV dose and three explanatory variables (global solar radiation, ozone and AOD) both on a daily and seasonal scale. We used a linear model where the coefficients are determined with the least-squares method. The model was developed based on data from 1991 to 2008. Data from 2009 to 2013 were used for validation of the model. The performance of the model and its parameters were evaluated through different statistical parameters.

The MLR analysis has been applied to 1246 simultaneous daily values of erythemal UV dose (S_{ery}), global solar radiation (S_g), total ozone (QO3) and aerosol optical depth (τ_{aer}) between 1991 and 2008. The resulting regression equation is

$$S_{ery} = 690 + 0.000169 * S_g - 5.10 * QO3 + 70.0 * \tau_{aer} + d + \varepsilon$$

with d representing the constant term and ε the error term. The adjusted R^2 value of the multiple regression is 0.94, which means that S_g, QO3 and τ_{aer} together explain 94 % of the variation in daily S_{ery}. The data from 2009–2013 are used to validate the model. The regression equation between the modeled and measured S_{ery} values (f (x) = 0.93x + 113.45 with x: measured values) and the correlation coefficient (0.96) reveal the good agreement between model and reality. However, in some case negative S_{ery} doses are modeled, which is a sign that the model does not always give realistic results. This is the case only during winter, when the S_g values are much lower than during the other seasons. When moderate to high QO3 values are combined with low S_g values, this leads to negative modeled S_{ery} values according to the regression equation. Also, there is a seasonal cycle present in the residual values. Therefore, we decided to perform the multiple regression analysis on a seasonal scale (Figure 26).

More information on the applied methods and the obtained results of the time series analysis can be found in ***De Bock et al. 2014.***

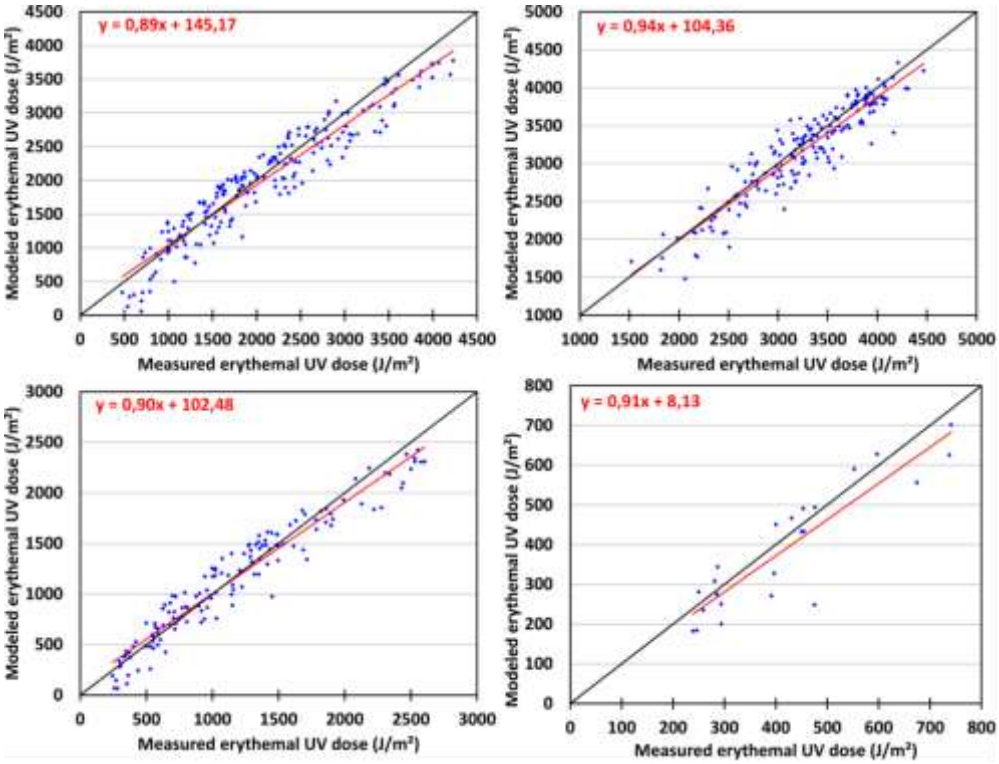

Figure 26: Scatterplots of the measured and modeled erythemal UV doses at Ukkel for the 2009–2013 validation period for spring (upper left panel), summer (upper right panel), autumn (lower left panel) and winter (lower right panel). The red lines represent the regression lines of the data, and the black lines are the f (x) = x lines.

Task 3.2.2 operate an aerosol lidar (ceilometer) at Ukkel and derive the aerosol backscatter ratio profiles and additional parameters (planetary boundary layer height, cloud information)

A Vaisala ceilometer CL 51 was installed in May 2011 at Ukkel. Every 6 seconds, information on the height of the cloud layers is provided. It also generates the backscatter profile. The instrument can be used to determine the cloud base height and the mixing layer height (MLH). Also, the Backscatter to Extinction Ratio (BER) is determined.

The ***cloud base height detection algorithm*** is based on the detection of a strong vertical gradient in the backscatter, combined with a high backscatter signal. It allows for cloud detection every 5 minutes up to 13 km. No cloud detection is possible under circumstances with precipitation or ground-based fog.

For the ***detection of the MLH***, we use a combination of two algorithms. The first algorithm determines the height at which there is a local minimum in the (negative) derivative of the backscatter signal, which means there is a significant vertical gradient at this height. The second algorithm determines the height at which a maximum in the temporal variance of the backscatter profile (within 5 minutes) occurs. If the resulting heights of the two algorithms agree to within 165m, this value is accepted as the MLH. The detection of the MLH is not possible in circumstances with precipitation, ground-based fog, strong convective conditions or too low aerosol concentrations.

The MLH algorithm has been validated by comparing the MLH retrieved by the LIDAR-ceilometer with the MLH retrieved from radio-soundings and with the boundary layer height (BLH) directly computed by the ECMWF and ALARO7 models. Under specific atmospheric conditions, the algorithm fails to retrieve a MLH similar with the values from the other remote sensing retrieval techniques. Therefore, several MLH quality control flags were developed, to automatically detect the failure of the MLH retrieval algorithm. The quality criteria on the MLH observations are crucial for the use of MLH in near real time. Figure 27 shows an example of a plot with the MLH determined from the LIDAR-ceilometer, compared with ALARO7, ECMWF and radio sounding values. The LIDAR-ceilometer MLH values are all quality-flagged and their quality flag values are equal to either 1 (=weak quality) or 2 (=good quality).

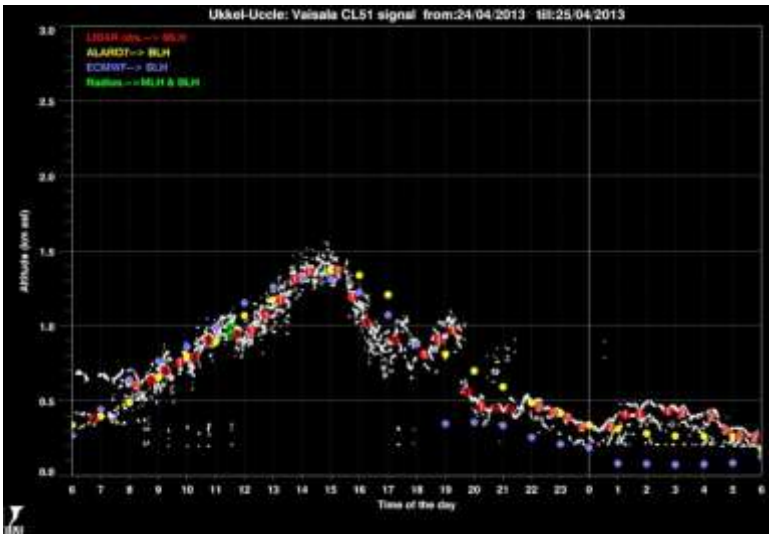

Figure 27: Example of 24 hours of MLH retrieved from LIDAR measurements by the algorithm at Ukkel between 120 and 3000m (white points represent individual MLH values, red points represent the averaged values (over half an hour)). Within the red points there is a number that corresponds to the MLH quality evaluation. The MLH measurements are compared with the Boundary Layer Height (BLH = MLH + entrainment zone) computed by ALARO7 (yellow points) and by ECMWF (blue points) and with the MLH and the BLH retrieved from the temperature profile measured by the radio sounding of Ukkel when it is available (green points).

The lidar can also ***determine the BER*** by using an iterative inversion approach in which the sunphotometer measurements are used to constrain the lidar inversion. The BER is increased (decreased) if the lidar derived optical thickness is larger (smaller) than the one from the sunphotometer.

In 2014, three new LIDAR (Vaisala CL51) instruments were installed at the automatic weather stations of Zeebrugge, Humain and Diepenbeek. This network (Figure 28) is now in operational testing stage. The data are collected every 5 minutes and the data plots are available in near real time such as on this website: http://ozone.meteo.be/meteo/view/en/10860734-LIDAR+ceilometer.html.

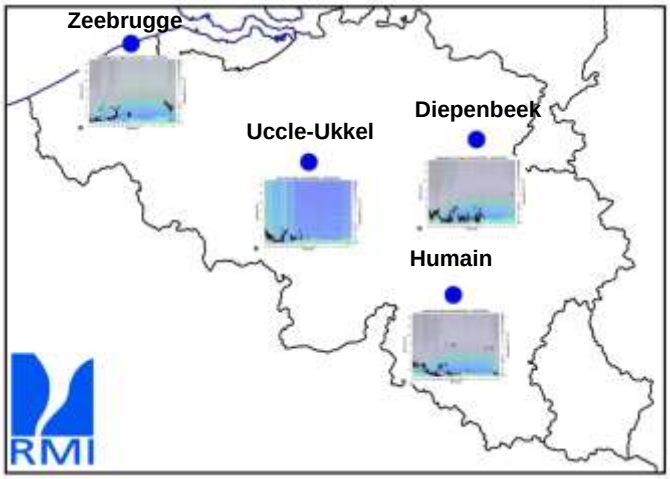

Figure 28: Map of the LIDAR network of RMI in Belgium.

On July 30th-31th 2014, the LIDAR network in Belgium detected an aerosol cloud (Figure 29) that originated from biomass burning particles released by intense and large wildfires in Northern Canada (Northwest Territories) which started in June 2014. The transport of these biomass burning aerosols over Europe was due to the production of pyrocumulonimbus clouds by these wildfires that injected the aerosols at the top of the troposphere where the configuration of the Jet Stream was suitable for blowing the aerosols across the North Atlantic. This was the case at the end of July 2014.

Figure 33 clearly shows the arrival of the smoke plume around 16:00 at Zeebrugge before it reaches Ukkel at 19:00 and Humain at 00:00. Upon its arrival and during its travel over Belgium, the front of the smoke plume was at an altitude of 2500 m but its back was located much lower than the front (between 500 and 1000 m). It is particularly visible at Ukkel with a decoupling between the smoke plume and the mixing layer characterized by an atmospheric layer poor in aerosols (low backscatter = blue). At Humain, the passage of the plume was masked by the presence of fog that blinded the LIDAR. This intercontinental smoke transport event is a remarkable case study to illustrate that a LIDAR network is more sensible and more precise (spatially and temporally) than satellite data to monitor a smoke plume. The monitoring of wildfire smoke plumes by a LIDAR network can help to validate and to improve dispersion models and global chemistry climate models for the forecast of various pollution events including aerosol plumes dangerous for aviation and health.

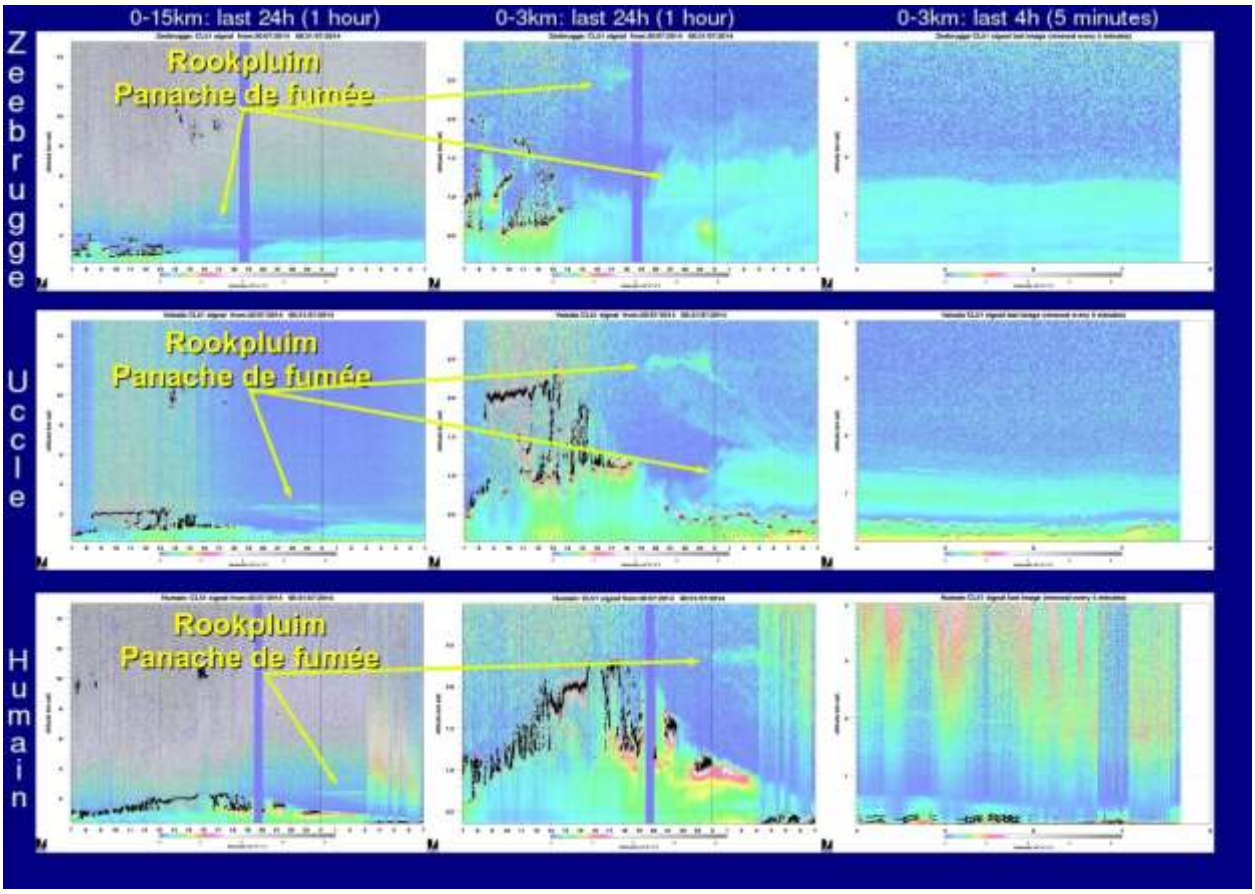

Figure 29: LIDAR plots (Zeebrugge, Ukkel and Humain) of the previous hours before 8:00 July 31, 2014. The plots in the left column and in the middle column represent respectively the last 24 hours of the backscatter signal measured between 0 and 25 000 m (above the sea level) and between 0 and 3000 m. The plots in the right column represent the last 4 hours of the backscatter signal measured between 0 and 4000 m. The color code corresponds to the intensity of the backscatter signal measured with the LIDAR and the black points correspond to the cloud base height.

Task 3.3 Aerosol data interpretation

Task 3.3.1 Exploitation of comprehensive data set of aerosol optical properties

Both KMI-IRM and BIRA-IASB have different instruments at their disposal to measure optical properties of aerosols, like an aethalometer, nephelometer, CIMEL sunphotometer, Brewer spectrophotometers, and MAX-DOAS. The measurements from these instruments have been compared, with as main objective the building of an extensive data set of aerosol optical properties at Uccle.

Aerosol optical depths (AODs) and vertical extinction profiles have been retrieved at 360 nm by applying the bePRO profiling algorithm developed at BIRA-IASB (Clémer et al., 2010; Gielen et al., 2014) to mini-MAX-DOAS O_4 measurements at Uccle, and compared to co-located AERONET data after applying the cloud-screening method (see Task 3.1.3). This has been done for the entire time series, ranging from 2011 up to now. In general, a good agreement, in both value and variation, is found between

bePRO and AERONET AODs, especially after removal of data taken under non-clear-sky conditions (see Figure 23 Left).

An extensive comparison of all available data obtained by BIRA-IASB and KMI-IRM in this workpackage has been performed. We compare in detail the retrieved aerosol extinction profiles (BIRA-IASB) with backscatter cloud profiles and mixing-layer-height values from lidar measurements (KMI-IRM). We find that in general cloud screening from BIRA-IASB corresponds to the backscatter profiles derived at KMI-IRM (see Figure 30). Also, a clear correlation between the height of the aerosol layer and the mixing-layer-height is often seen (see Figure 30/bottom plot). Both institutes are continuing their collaboration for investigating the observed trends in aerosol profiles, backscatter profiles and mixing-layer-height.

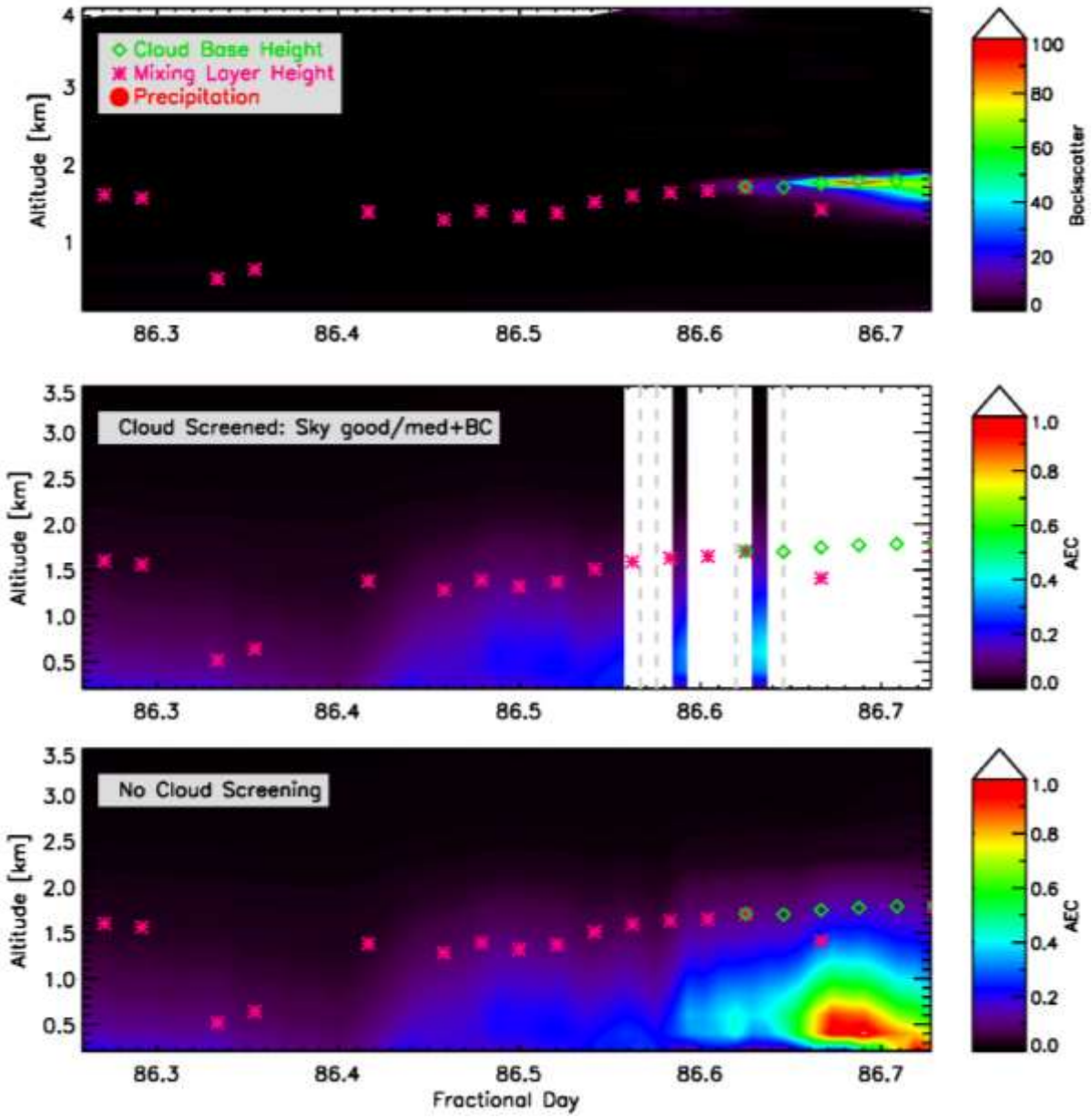

Figure 30: Comparison of the retrieved aerosol extinction coefficient (AEC) profiles (km-1) and cloud screening from BIRA-IASB (middle and bottom plot), with backscatter profiles and mixing layer height derived by KMI-IRM (top plot) for day 86

(March 27) 2013. Top: Backscatter lidar profile with the estimated cloud base heights (green) and mixing layer height (magenta). Middle: Aerosol extinction profiles retrieved by applying the bePRO profiling tool to MAX-DOAS measurements. Scans corresponding to bad sky conditions are filtered out (white areas). Bottom: MAX-DOAS aerosol profiles without cloud screening. For comparison, we also plot the cloud base height and mixing layer height derived from lidar measurements in the three plots. There is no precipitation on that day.

We have also compared MAX-DOAS AODs at Uccle to those retrieved at two other stations where BIRA is performing MAX-DOAS observations: Jungfraujoch (Swiss Alps; 3680 asl) and Xianghe (China; Beijing suburban area). Jungfraujoch is a mostly remote site while Xianghe is a highly polluted site, strongly affected by anthropogenic emissions from Beijing. Figure 31 shows that AOD values are by far the largest at Xianghe and the lowest at Jungfraujoch, as expected. This comparison illustrates the difference in the level of pollution between Europe and a region like the Beijing area known for its extreme pollution.

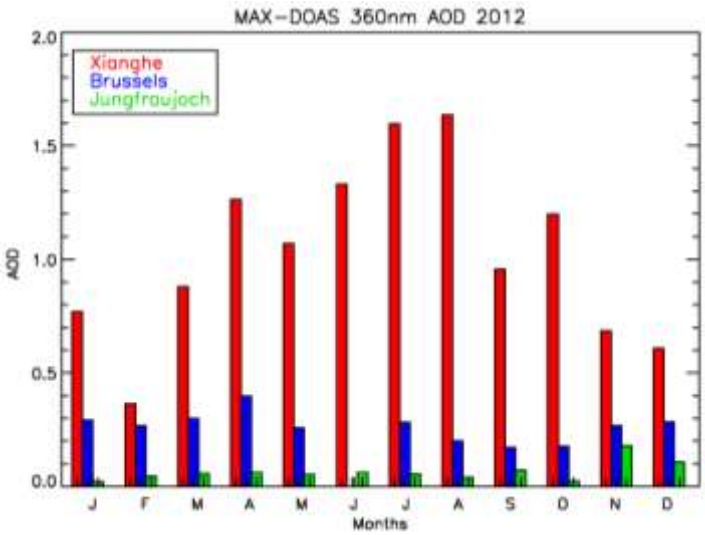

Figure 31: AOD (360 nm) monthly means retrieved from MAX-DOAS observations in Brussels (Uccle), Xianghe, and Jungfraujoch for year 2012.

Also related to WP3, it should be noted that tropospheric NO_2 columns derived from MAX-DOAS measurements in Uccle have been used to validate satellite observations, in particular GOME-2A and B data within the framework of the O3MSAF (http://cdop.aeronomie.be). As an example, comparison results between GOME-2A and MAX-DOAS for the 2011-2014 period are shown in Figure 32. Generally, a good agreement is obtained between both data sets, with similar capture of the pollution episodes and consistent seasonal variations, i.e. with high NO_2 in winter and low NO_2 in summer. However, larger differences between the monthly means are sometimes seen, like in August-September 2013. This is likely related to the location of the mini-DOAS instrument, in the city center, where the measurements are more sensitive to local pollution peaks, while these tend to be attenuated in the satellite pixel.

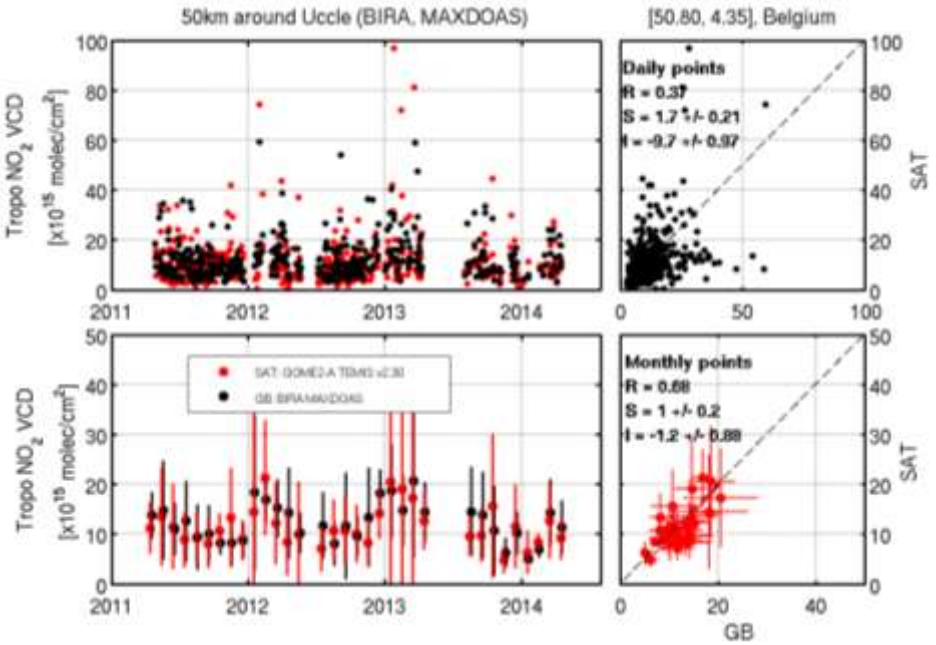

Figure 32: Time series of mini-DOAS and GOME-2A (TEMIS product v2.30; see http://www.temis.nl) tropospheric NO_2 VCD above Uccle since May 2011. The top panel presents the daily coincident points and the bottom panel presents the monthly mean values.

Task 3.3.1 demonstrate the strength of the aerosol remote sensing by exploiting the ensemble of data and by deriving the maximum of information about the aerosol optical properties at Ukkel

At Ukkel, we have different collocated instruments that are able to provide information about the optical properties of aerosol particles.
First, we have cloud-screened AOD values in the UV-B, retrieved by the ***Brewer spectrophotometers***:

- From Brewer#016: AOD at 303.3, 310.1, 313.5, 316.8 and 320.1nm from 1984
- From Brewer#178: AOD at 303.3, 310.1, 313.5, 316.8 and 320.1nm from 2002
- From Brewer#178: AOD at 340nm from 2006

These values are frequently compared with the AOD measurements from the ***Cimel sunphotometer*** (available since 2006).
Since May 2013, RMIB disposes of an ***aethalometer*** (Magee Sci.; AE31, 7 wavelengths) which measures the light absorption of aerosol particles at wavelengths covering the UV and the Near InfraRed (370, 470, 520, 590, 660, 880 and 950nm). From the instrument, the absorption coefficient (σ_a) (in Mm^{-1} where 1 $Mm=10^6$ m) and the mass concentration of light-absorbing particles (ng/m^3) can be derived. The absorption at 660 nm can be taken as absorption by soot (Black Carbon; BC) particles. In March 2014, a ***nephelometer*** (Ecotech Aurora 3000) was installed at Ukkel. This instrument is designed to measure the scattering (σ_s) and backscattering coefficient (in Mm^{-1}) of particles (at 450, 525 and 635nm), which is important for the evaluation of direct radiative forcing. The instrument has been moved to the Belgian research station in Antarctica in November 2014 and will be replaced in spring 2015 by a TSI nephelometer (which measures at slightly different wavelengths: 450, 550 and 700nm). Combining the absorption measurements of the aethalometer and the scattering measurements of the nephelometer enables us to determine the Single

Scattering Albedo (SSA). However, it should be noted that the SSA values presented below are preliminary as not all necessary corrections have been applied to the aethalometer and nephelometer data yet.

We investigated the dataset of aerosol optical properties for the year 2014. Simultaneous measurements of all above mentioned optical aerosol properties were available for 22 days between March and October 2014. The measurement period covered also a smog event on 12–14 March 2014, characterized by high amounts of pollution. Meteorological conditions were responsible for this event: stagnation, inversion and dry air in combination with a lot of sunshine created the situation in which the secondary aerosols were trapped within a stable layer where they could further accumulate. The smog period clearly distinguishes itself from the other days (Figure 33). The mass concentration of BC particles, the absorption coefficients (at all wavelengths) and the scattering coefficients (at all wavelengths) are much higher during the smog period. Whereas there seems to be a correlation (for 635, 525 and 450nm the correlation is 0.89, 0.88 and 0.87 respectively) between AOD and the scattering coefficient for most of the days – during the smog period no such correlation was seen. This shows that the relationship between AOD and total scattering is not always straightforward. Further research is needed to understand the interaction between AOD values and total scattering.
For AOD and SSA, we found no clear distinction between ‘smog’ days and ‘normal’ days. The smog days are characterized by rather low AOD values (0.2 to 0.4) and SSA values are around 0.98.

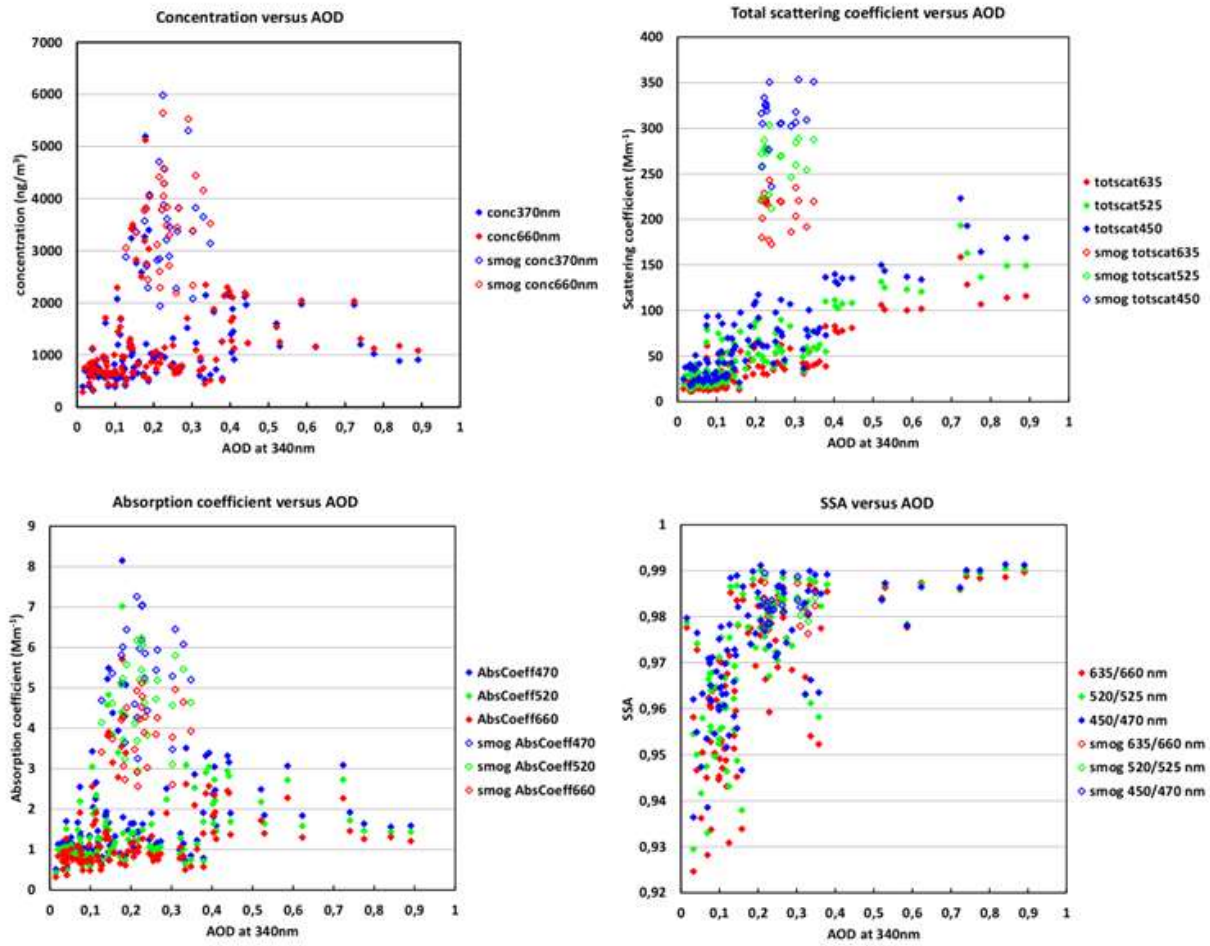

Figure 33: The upper left panel shows the aerosol concentration at 370nm (in blue) and at 660nm (in red) versus the AOD at 340nm. The upper right panel presents the total scattering coefficient at three wavelengths in function of the AOD at 340nm. The lower left panel shows the absorption coefficient at 3 wavelengths versus the AOD at 340nm. The lower right panel presents the SSA versus the AOD at 340nm. The smog days are represented by the non-filled diamonds.

Task 3.3.2 study agreement between aerosol optical properties measured with the set of instruments mentioned above and simulated with CHIMERE

The main goal is to use the output of the chemical transport model CHIMERE (Vautard et al. 2007) as input for the OPAC (Optical Properties of Aerosols and Clouds, Hess et al. 1998) software package with the aim to model the optical properties of aerosols based on their chemical composition.
The chemical transport model CHIMERE can be used to model the chemical composition (in µg/m³) of the aerosol mixture at Ukkel up to a height of 5.5km at a 50km x 50km grid resolution. In order to be able to use the output of CHIMERE as input for the OPAC software package, some adaptations were necessary. First, the output in mass density (µg/m³) had to be converted to number density (particles/cm³). Second, since the OPAC software package uses different aerosol categories, the CHIMERE components needed to be mapped onto the OPAC categories. A first mapping attempt was described in the 2013 report. Currently we apply the mapping as described in Table III. It contains three adjustable parameters, which model

uncertainties about the relative amount of optically different components in one and the same CHIMERE species:

- f_{SOA}: water-soluble and insoluble species have different optical properties. The CHIMERE species SOA represents secondary organic aerosols and contains both water solubles and insolubles. f_{SOA} denotes the mass fraction of SOA which is water-soluble.
- f_{OCAR}: idem as above but in this case concerning the CHIMERE species OCAR which represents a mix of primary organic carbon species.
- f_{DUST}: denotes the mass fraction of soil dust (as opposed to mineral dust) in the CHIMERE species DUST.

Note that the mass densities of the CHIMERE species representing complex carbon based compounds (OCAR en SOA) have been increased by an additional factor of 1.6. This is because CHIMERE only outputs the carbon masses for these species (Bessagnet et al., 2008) and the factor has been added to account for the contribution of the non-carbon atoms to the total mass of the aerosol.

Table III: Mapping of CHIMERE species into OPAC species. The meaning of f_{SOA}, f_{OCAR} and f_{DUST} is explained in the text. The size bin column denotes which of the 8 CHIMERE bins are involved in the mapping towards its corresponding OPAC equivalent. The masses of the CHIMERE species are multiplied with the corresponding factor in the third column to obtain the contribution to the equivalent OPAC species.

CHIMERE	Size bin	Factor	OPAC
SALT	1-6	1	Sea salt accumulation mode
	7-8	1	Sea salt coarse mode
NH_3	1-8	1	Water soluble
H_2SO_4	1-8	1	Water soluble
HNO_3	1-8	1	Water soluble
SOA	1-8	$1.6*f_{SOA}$	Water soluble
	1-8	$1.6*(1-f_{SOA})$	Insoluble
OCAR	1-8	$1.6*f_{OCAR}$	Water soluble
	1-8	$1.6*(1-f_{OCAR})$	Insoluble
BCAR	1-8	1	Soot
DUST	1-8	$1-f_{DUST}$	Insoluble
	1-5	f_{DUST}	Mineral dust nucleation mode
	6	f_{DUST}	Mineral dust accumulation mode
	7-8	f_{DUST}	Mineral dust coarse mode
PPM	1-8	1	insoluble

The relative contributions of the various OPAC species to the total modeled AOD have been determined. In most cases, there are 2 main contributors to the AOD: water soluble particles followed by soot. From the comparison of OPAC AOD with AERONET level 2.0 AOD (13/7/2006-31/12/2011) at 500nm (Figure 34) we could conclude that OPAC clearly underestimates the measurements, especially the largest AOD values. This underestimation occurs regardless of the parameter values f_{SOA}, f_{OCAR} and f_{DUST}. The underestimation is likely due to an underestimation of the total aerosol mass.

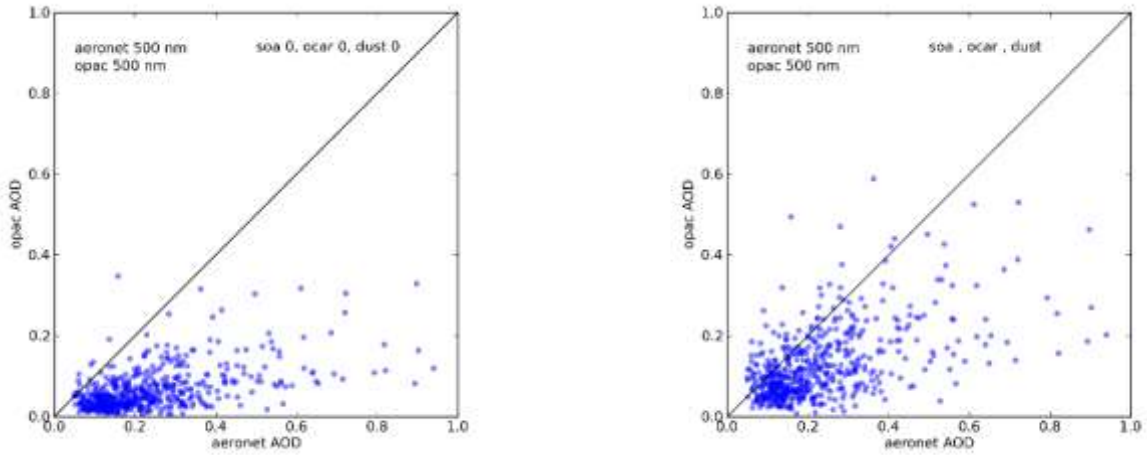

Figure 34: Comparison between observed (aeronet) and modeled (opac) AODs at 500nm at Ukkel for the period 2006-2011. Two different combinations of the parameters f_{SOA}, f_{OCAR} and f_{DUST} are shown; all zero (left panel) and all unity (right panel).

Given that CHIMERE uses a rather coarse 50km x 50km grid, it is highly plausible that soot is underestimated. To further investigate this, we made calculations in which the mass of soot is artificially increased by a factor of 4, which is the typical difference between rural and urban areas and could also be objectively observed through the measurements with our aethalometer, installed on the roof of the BIRA institute. The situation has improved somewhat even though most AODs are still underestimated by OPAC. We also decided to increase the mass of the secondary main AOD contributor (i.e. water soluble aerosols) by a factor of 4. With these adjustments, it seems that we have reached the correct order of magnitude for the amount of aerosols needed, at least for the 2 main contributors, soot and water solubles. The distribution of the dots is now fairly balanced around the one-to-one line. There is still a fraction of data points outside of the predictable range, but that fraction is now becoming a minority (Figure 35).

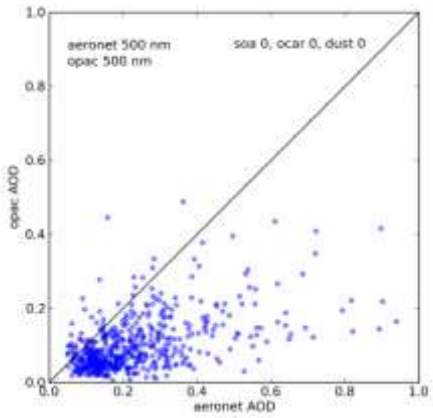

Figure 35: Comparison between observed (aeronet) and modeled (opac) aerosol AODs at 500nm at Ukkel for the period 2006-2011. The amount of soot and water solubles has been artificially increased by a factor of 4. f_{SOA}, f_{OCAR} and f_{DUST} are all zero.

There are a few other aspects that may facilitate better correspondence with the observations:

- It may prove useful to try and make simulations on a finer grid with appropriate emission sources (e.g. a 7 km x 7 km grid)
- The size bins for which CHIMERE outputs aerosol mass densities only go as far as 10µm, whereas the built-in size distribution of OPAC goes as far as 40µm. If we could provide CHIMERE output with additional two bins (eg. 10-20µm and 20-40µm), then the predicted total aerosol mass would also increase.
- One of the 2 major contributing OPAC species to the total AOD at 500nm is the water soluble species. It may be worth investigating whether splitting up CHIMERE species like NH_3, H_2SO_4 and HNO_3 into their own optical category would improve the correspondence with the observations. Performing the splitting up would involve looking up mass densities and breaking indices per wavelength and per RH for each of them, subsequently performing the necessary Mie calculations to obtain extinction and absorption coefficients for a given size distribution.

We conclude that more research is needed on this topic in order to reach the desired results.

Task 3.3.3 study correlation between observed aerosol properties and source regions, using backtrajectories and meteorological parameters

Air parcel trajectories are obtained with the APTRA model, available at the ECMWF (European Centre for Medium-range Weather Forecast) with a horizontal resolution of 1° and a time resolution of 6h. To calculate these 3D backtrajectories, data from the reanalyzed ERA-INTERIM data set have been used. The backtrajectories technique is a useful tool in tracing source regions of air pollution and determining transport patterns at receptor sites in general. Although they do not represent exactly the path of an air parcel, they are suitable to identify particular synoptic situations. For a period from 01/01/1990 till 31/12/2010, 7671 trajectories were calculated. Cluster analysis is used to identify different sources of air masses, therefore a non-hierarchical cluster routine is chosen to extract a natural number of clusters. The non-hierarchical method will sort the trajectories into groups by minimizing their geometric normalized distances (latitude, longitude and pressure level). The cluster analysis was able to divide the trajectories between 1990 and 2010 into 12 different clusters.

The distribution of the meteorological conditions (temperature, relative humidity, wind speed and wind direction) over the different clusters has been investigated. The results are presented in Figure 36 (a-e). From this figure, we can conclude that wind direction is definitely the most defining parameter. We also studied the measured Brewer AOD values (at 320 nm) in function of the different obtained clusters (Figure 36 f). If we look into the properties of each cluster, it is clear that AOD is influenced by the origin of the air masses. Clusters 1 and 8 (Figure 36-Figure 37) are characterized by more elevated AOD values (the average AOD is 0.66 and 0.48 respectively). These air masses are slow moving, local (with a slight easterly component) and therefore polluted air masses, which explains the more elevated

AOD values. A nice example of air coming from clean zones is cluster 7 (Figure 36-Figure 37), where the air masses originate in NW regions. The average AOD for this cluster is 0.26.

Finally, we applied a ***multiple linear regression technique*** (per season) to model the relation between AOD on the one hand and meteorological parameters on the other hand (eq. 1-4).

Spring (eq. 1):

$$AOD = 0.26 + 0.01\,T - 0.0002\,wind_{dir} - 0.05\,wind_{speed} + 0.005\,RH + 2.08 * 10^{-5} MLH$$

Summer (eq. 2):

$$AOD = -0.31 + 0.023\,T - 0.0002\,wind_{dir} - 0.04\,wind_{speed} + 0.008\,RH + 5.03 * 10^{-6} MLH$$

Autumn (eq. 3):

$$AOD = -0.009 + 0.01\,T - 6.27 * 10^{-5}\,wind_{dir} - 0.03\,wind_{speed} + 0.004\,RH + 8.85 * 10^{-6} MLH$$

Winter (eq. 4):

$$AOD = 0.13 + 0.0008\,T + 5.68 * 10^{-5}\,wind_{dir} - 0.02\,wind_{speed} + 0.004\,RH - 2.07 * 10^{-5} MLH$$

With T = temperature (°C), wind_dir = wind direction (°), wind_speed = wind speed (m/s), RH = relative humidity (%) and MLH = Mixing Layer Height (m).

The coefficients in red are the ones that do not significantly differ from zero. In general temperature and relative humidity have a positive effect on AOD throughout the entire year, whereas wind speed has a negative influence on AOD. The adjusted R^2 value was calculated to determine how much of the variation in AOD is explained by the meteorological parameters. In summer the highest adjusted R^2 (23%) was obtained, which means that only 23% of total AOD variation can be explained by meteorology. This value is not very high and even lower values were calculated for autumn (19%), spring (15%) and winter (7%). The results show that using meteorology alone is not enough to determine the AOD.

So we were not able to develop a model, using solely meteorological parameters, to forecast AOD.

Task 3.3.4 Improve UV index forecast using modeled AOD and SSA from CHIMERE or backtrajectories

The outcome of tasks 3.3.2 and 3.3.3 did not give us reliable and accurate enough results. Hence we were not able to improve the forecasted UV values using modeled AOD and/or SSA values. However, we were able to improve the forecast in other ways:

1) The information on the website (http://www.meteo.be/meteo/view/nl/522044-Uv.html) was adjusted so that the maximum predicted UV index value agrees with the maximum value in the graph. (This was not the case before the

adjustments.) Also, the climatological AOD, which are currently used for the UV index prediction are calculated for an extended period, from 1984 to 2014.

2) Also, we plan to use the mean AOD value (calculated based on measurements over the past 15 days) as input AOD value in the near future. The new virtual server has now become operational and we installed a new version of the radiative transfer model (TUV 5.0 instead TUV 3.0) on this server.

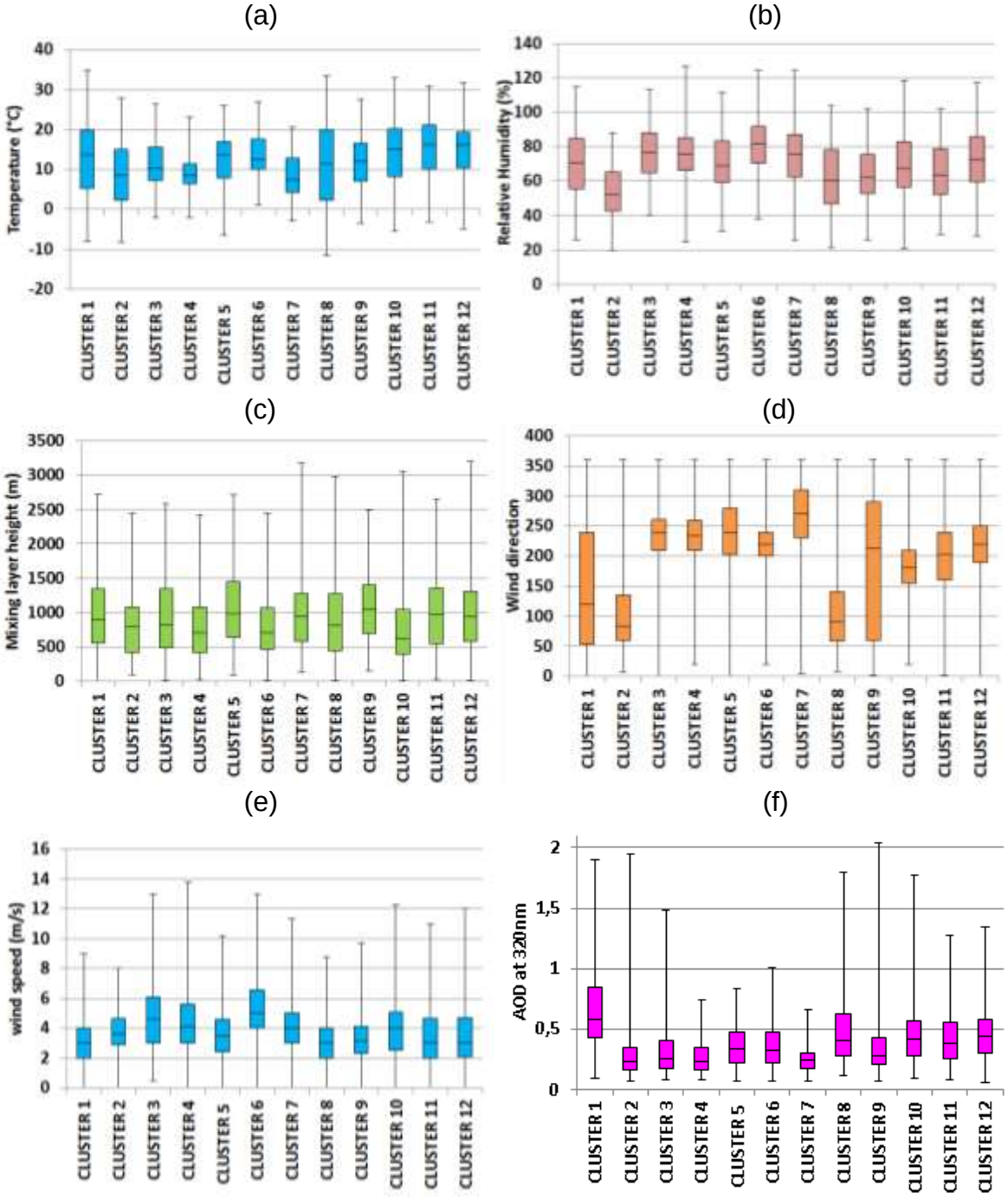

Figure 36: Boxplots of temperature (a), relative humidity (b), mixing layer height (c), wind direction (d), wind speed (e) and AOD at 320nm (f).

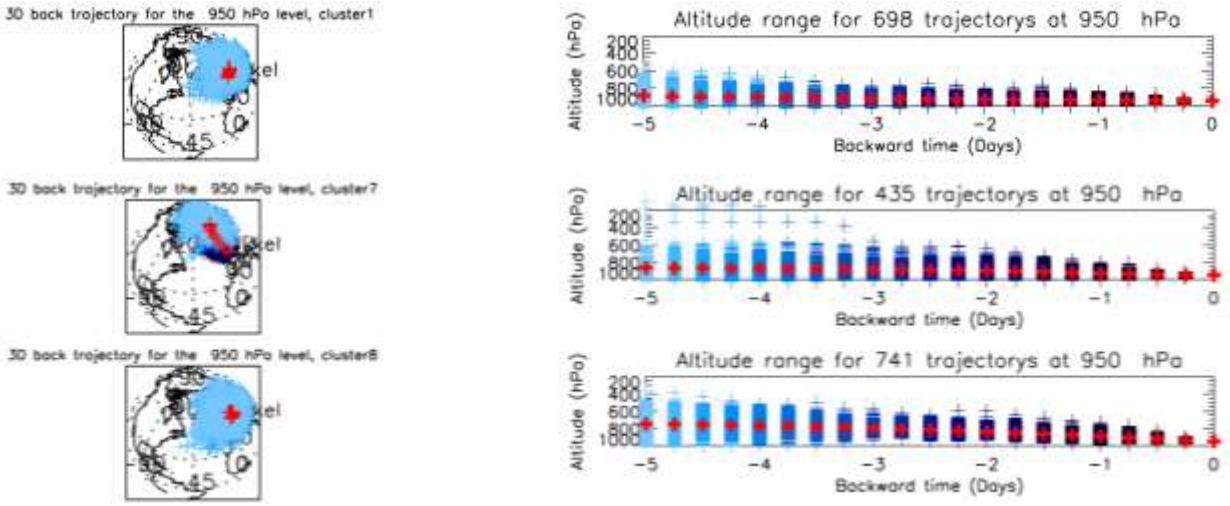

Figure 37: Detail of clusters 1, 7 and 8. The blue dots represent each individual trajectory (and its height on the right-hand figure), the red dots represent the mean of the trajectory (and the mean height on the right-hand figure).

WP 4: African emissions

The main objective of this workpackage is to study African emissions by means of complementary observations from the ground and from space. Current satellite observations indicate large uncertainties on these emissions which motivates the need for additional measurements, using reference high-precision instrumentation from the ground. We report on the installation of a scientific-grade high-performance MAX-DOAS instrument in Bujumbura (Burundi), to monitor aerosol and several key atmospheric trace gases such as formaldehyde (HCHO), nitrogen dioxide (NO_2), glyoxal (CHOCHO), ozone (O_3), and sulphur dioxide (SO_2).

Task 4.1. Installation of MAX-DOAS instrument in Burundi (Bujumbura)

In 2013, the MAX-DOAS instrument developed and assembled in late 2012 has been finalized and calibrated. This work was performed in part during the training period of Eugène Nzendako, a physicist from the University of Burundi. The training of E. Nzendako ended in February 2013. During his stay at BIRA, he contributed to the preparation and testing of the instrument including its initial calibration. He was also trained to the usage of the various control and evaluation software packages. In the period from March to late April 2013, the instrument was finalized and fully calibrated. Before its installation in Bujumbura, it was deployed in the international MADCAT intercomparison campaign which was organized at the Max Planck Institute of Mainz in June - July 2013. This campaign allowed for a complete verification and validation of the instrument against similar systems. This led to the identification of an instrumental problem which could be fixed during the summer period at BIRA-IASB. The final calibration and preparation of the instrument and the organisation of its transfer to Burundi (customs) took place in the September-October period. The instrument was finally installed in Bujumbura in the course of November 2013 (see Figure 38), together with a commercial CIMEL sunphotometer for accurate aerosol optical depth measurements as part of the AERONET network

(http://aeronet.gsfc.nasa.gov/). Both systems are operational since 25 November 2013. It should be noted the G. Pinardi (BIRA) spent three weeks in Bujumbura (18/01/2015- 06/02/2015) for the maintenance of the instruments. She also gave 30h of lectures to 2nd master physics on « introduction to physics and chemistry of the atmosphere.

Raw data (spectra) are transferred to BIRA on daily basis at night using a dedicated internet line. The overall system is highly securised by means of a dedicated room built on purpose to host the instrumentation. Also the MAX-DOAS optical head and the CIMEL system installed on the roof of the building are protected by several levels of fences, one of which is visible on Figure 38. In order to cope with the regular power failures (typically several times a day), the whole system is connected to a high capacity battery system allowing for autonomous operation of the instruments even during prolonged power failures (up to several hours).

Figure 38: MAX-DOAS instrument installed on the roof of the Physics Department building of the University of Burundi, in Bujumbura (3°S, 30°E).

Task 4.2. Data analysis for trace gases and aerosols

The instruments are completely automated using a software developed at BIRA-IASB, which controls the different devices (sun tracker, filter wheel, CCD), the sequence of measurements (elevation angles, dark currents), automatically adjust the integration time according to ambient light level, etc. The overall system can be remotely controlled from BIRA which allows to support the local operator (E. Nzendako) in case of problems or failures. Data are downloaded daily by ftp and raw data are stored at BIRA for further processing. A facility for rapid data quality control by means of a local web page has been developed at BIRA.

Vertical profiles of aerosol extinction coefficient, HCHO, NO_2 are retrieved using the bePRO profiling tool (Clémer et al., 2010; see also Hendrick et al., 2014; Gielen et al., 2014; Vlemmix et al., 2015). Figure 39 shows the current time series from November 2013 till March 2015. It is worth noting that an automated processing chain has been developed by BIRA which creates vertical profile data files in the GEOMS hdf4 format (see http://avdc.gsfc.nasa.gov/index.php?site=1876901039 for more details). So far, NO_2 and aerosol files are submitted on a daily basis to the

NDACC-RD database (ftp://ftp.cpc.ncep.noaa.gov/ndacc/RD/) within the framework of the EU FP7 project NORS (http://nors.aeronomie.be/).

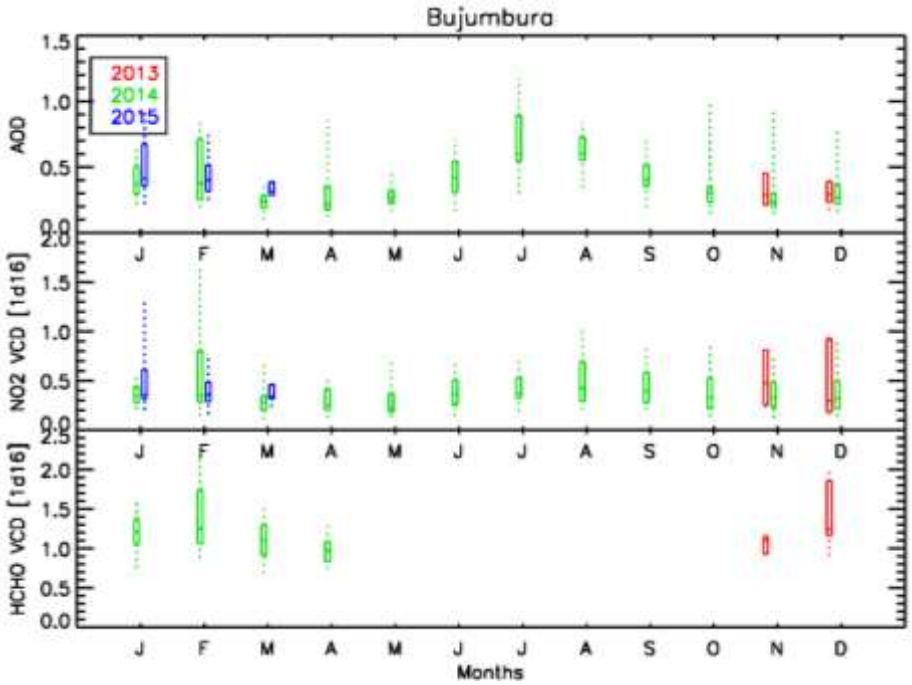

Figure 39: Time-series of AOD, NO_2 and HCHO vertical column densities (VCD; in molec/cm2) retrieved from MAX-DOAS measurements at Bujumbura. Minimum, maximum (dotted lines), 25 and 75% percentiles, and median (boxes) values are plotted. HCHO data are missing from May 2014 due to a failure of the UV CCD detector. The UV channel is operational again since April 2015.

The MAX-DOAS AODs have been compared to those measured in parallel by the CIMEL instrument, which is part of the AERONET network (http://aeronet.gsfc.nasa.gov/). A good overall agreement is obtained between both instruments as illustrated in Figure 40. As for Uccle, it can be seen that the level of agreement is significantly improved using the cloud-screened MAX-DOAS data. It should be noted that the MAX-DOAS rejected by the cloud-screening method mostly correspond to afternoon conditions when clouds appear in the pointing direction of the instrument, i.e. towards the Tanganyika lake, where an important evaporation process takes place. The impact of this process on the quality of the trace gas retrievals is under investigation.

HCHO and NO_2 vertical profiles and corresponding columns are currently used to validate satellite observations from the GOME-2A and B and OMI instruments.

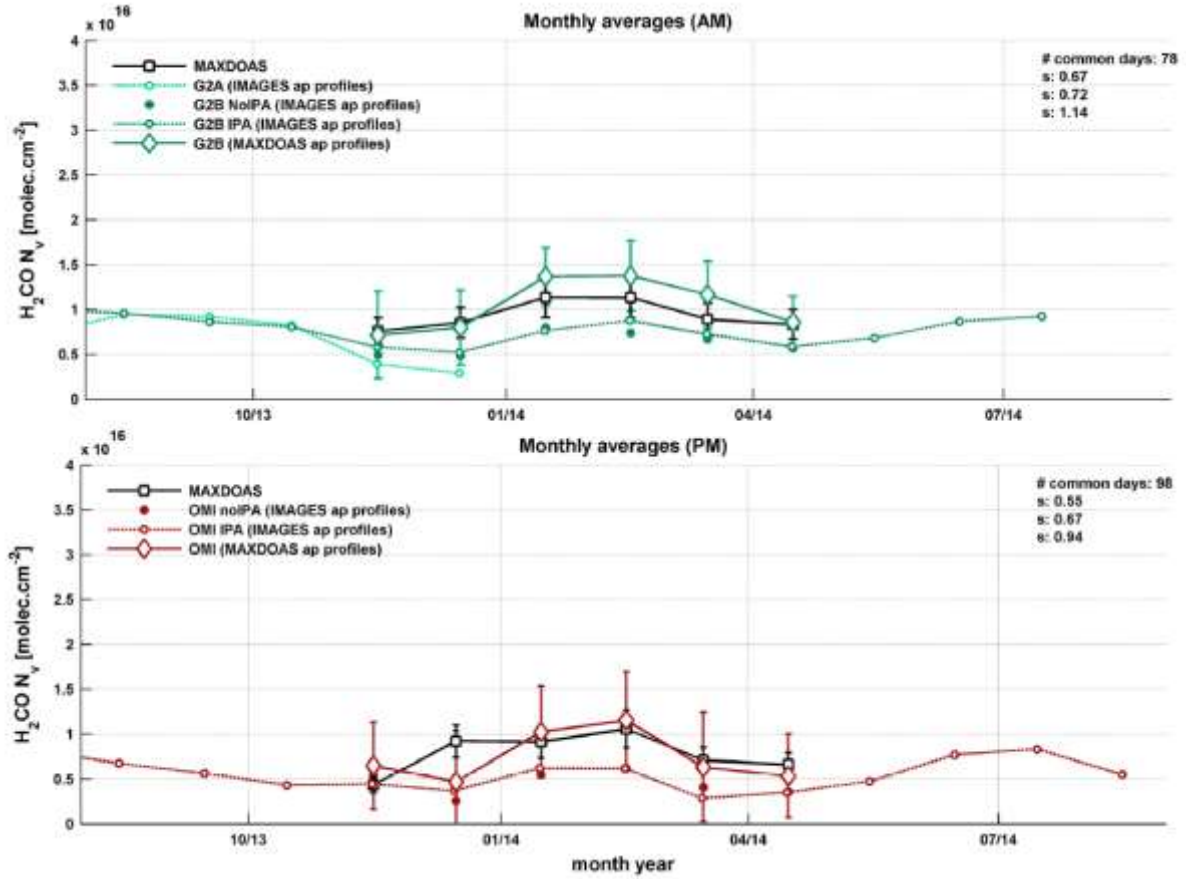

Figure 41 shows the comparison of GOME-2 and OMI HCHO vertical columns over Bujumbura with MAX-DOAS data (De Smedt et al., 2015). It is found that the choice of the a priori vertical profile for the calculation of air-mass factors (AMFs) has a significant systematic effect on the vertical columns. For both GOME-2 and OMI, switching from modelled to measured profile shapes increase the HCHO columns by 20 to 50%, bringing the satellites and ground-based observations to a satisfactory agreement within 15%. The large effect of the a priori profile shape is explained by the vertical sensitivity of the satellite measurements, decreasing strongly in the lowest atmospheric layers, and by the shape of the HCHO vertical distribution, peaking near the surface (see De Smedt et al., 2015 for more details).

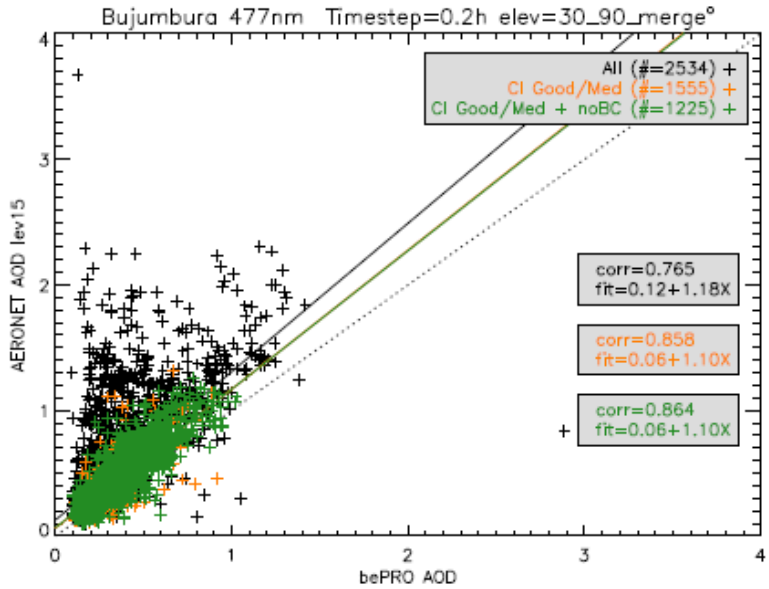

Figure 40: Correlation between MAX-DOAS and AERONET AODs at Bujumbura (11/2013-02/2015). In black the non-cloud-screened MAX-DOAS data, orange the cloud-screened data under good/mediocre conditions, green the good/mediocre data with additional removal of data hindered by broken clouds.

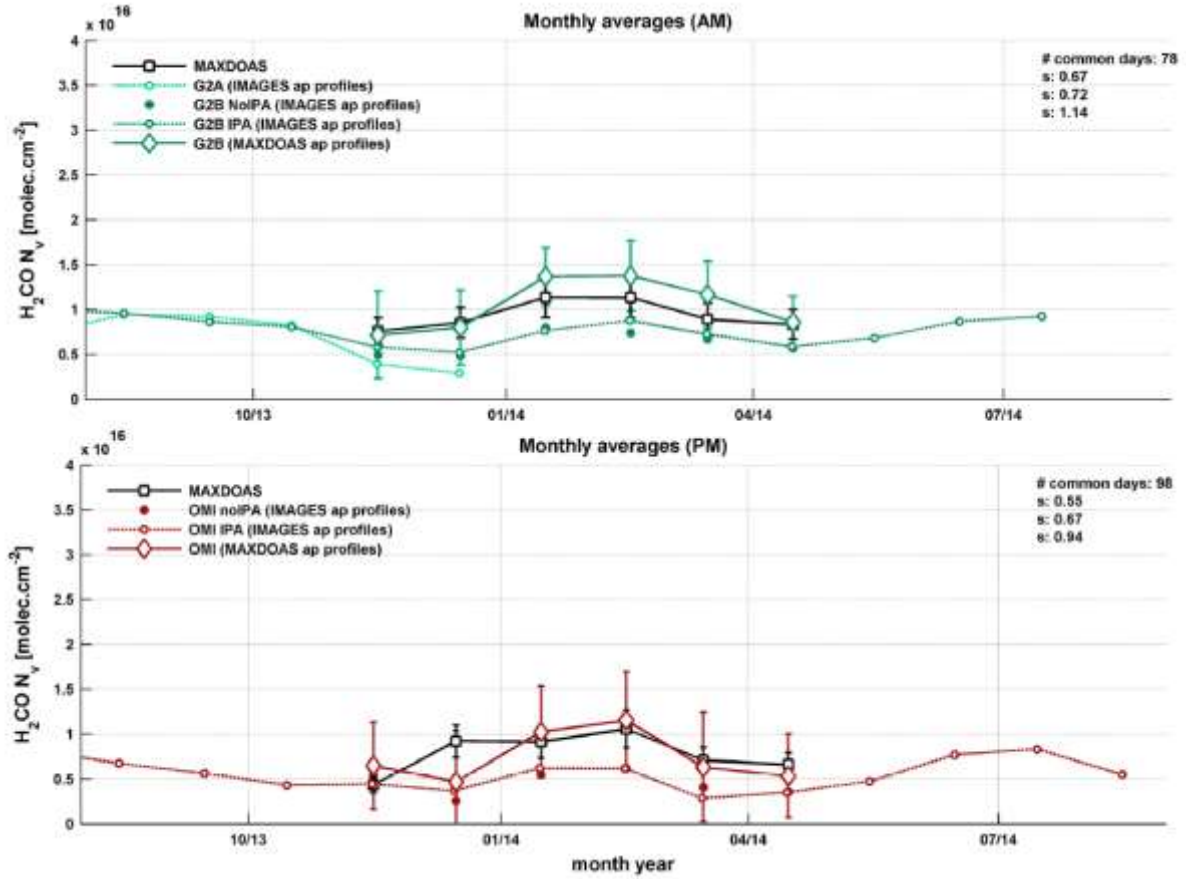

Figure 41: Validation of GOME-2A and OMI HCHO vertical columns (Nv) in Bujumbura, using MAX-DOAS retrievals (represented by black squares). Upper panel: mid-morning observations (GOME-2A and MAX-DOAS averaged over 8-11h local time). Lower panel: early afternoon observations (OMI and MAX-DOAS averaged over 12-15h local time). Observations have been averaged per month, over the period 2013-2014, selecting

correlative days between GOME-2A/OMI and the MAX-DOAS instrument. Satellite measurements have been averaged within 100km around the station. Three GOME-2A and OMI products are presented: 3D-CTM IMAGES as a priori profile/no cloud correction, 3D-CTM IMAGES as a priori profile /cloud correction (IPA), and MAX-DOAS as a priori profile/cloud correction (IPA). Slope and correlation coefficient values derived from satellite versus MAXDOAS scatterplots appear on the right upper corner of the plots. See De Smedt et al. (2015) for more details.

Another species which is relevant for investigating emissions of non-methane volatile organic compounds (NMVOCs) from biogenic, biomass burning and anthropogenic continental sources, and which can be measured by both satellite and MAX-DOAS instruments, is glyoxal (CHOCHO). Monitoring this species over Bujumbura is highly relevant since Central Africa is known to be one of the main source regions for NMVOC emissions from biomass burning and biogenic activity. An important effort has been put by BIRA in the optimization of the DOAS settings for the CHOCHO retrieval from both MAX-DOAS and satellite instruments (OMI, GOME-2). Figure 42 presents preliminary comparison results between MAX-DOAS and OMI CHOCHO vertical columns over Bujumbura for the December 2013-December 2014 period.

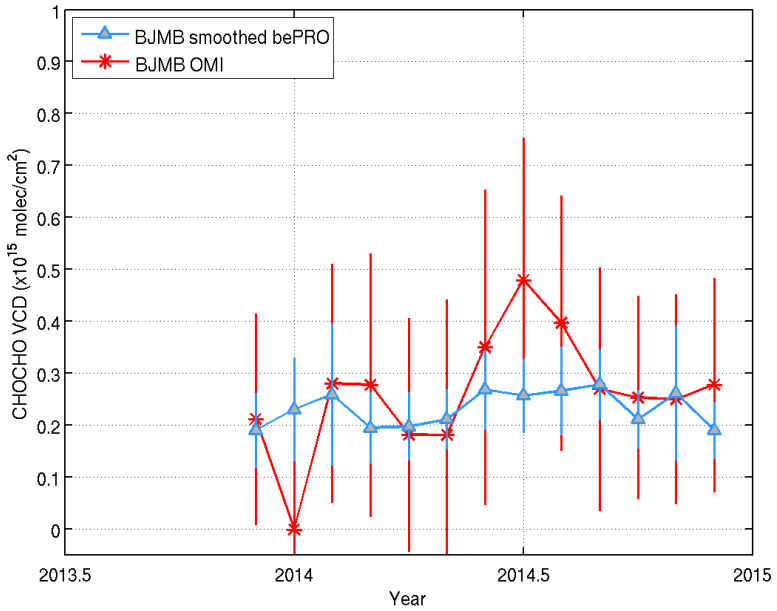

Figure 42: Validation of OMI CHOCHO vertical column (VCD) monthly means in Bujumbura using MAX-DOAS retrievals (preliminary results). OMI data are extracted from an updated version of the BIRA scientific product (Lerot et al., 2010). The MAX-DOAS columns have been smoothed using the OMI column averaging kernels. Error bars represent the 1-sigma standard deviation.

These first results are encouraging since both data sets agree within their combined error bars. However, the CHOCHO VCD seasonality is more marked for OMI than for MAX-DOAS observations. This feature is currently being investigated, as well as the daily/weekly/yearly patterns of CHOCHO and other trace gases, with focus on the impact of local sources and possible transport from other source regions.

WP 5: Outreach

Task 5.1 dissemination of results

Task 5.1.1 via publications, workshops, international symposia

The main dissemination channel of results of work carried out within AGACC-II is the peer-reviewed literature.
Another important dissemination channel of work carried out within AGACC-II involved presentations at international conferences.

All publications and communications are provided in Section 5 hereafter.

Task 5.1.2 by submitting data to international databases

The Brewer ozone and UV data are deposited in the **WOUDC database** (woudc.org) and the Brewer AOD at 340nm (from 2007 to 2011) are submitted to the **GAW World Data Centre** for aerosols, hosted by EBAS **(**http://ebas.nilu.no/Default.aspx**).**

The improved strategies which have been developed or validated within AGACC-II have been progressively implemented in the routine retrieval chain at work at ULg. This is notably true for C_2H_2, C_2H_6, HCN. As a direct result, updated time series from the mid-1990s onwards have been made available to the scientific community through the NDACC data base, using the hdf GEOMS template. Some species (e.g. CH_4) have also been delivered in near real time to support the Copernicus Atmospheric Monitoring Service (CAMS). The HCHO product from Jungfraujoch is now also ready to support this initiative.

Bujumbura MAX-DOAS data files (NO_2, aerosols) are submitted on a daily basis to the NDACC-RD database (ftp://ftp.cpc.ncep.noaa.gov/ndacc/RD/) within the framework of the NORS FP7 project (http://nors.aeronomie.be/). These data will be used in the near future for the validation of MACC models within the framework of the Copernicus Atmosphere Monitoring Service (CAMS). This is/will be also the case for the MAX-DOAS data in Xianghe, Uccle, and Jungfraujoch.

The TCCON data are submitted on a regular basis to the TCCON database at Caltech and the whole timeseries available up to now has been archived in the CDIAC data center.

The spectroscopic information to be included in the HITRAN and GEISA databases can be submitted either spontaneously or following requests by the database managers. Before inclusion in databases, submitted data is evaluated by a committee. The effort devoted to the ethylene molecule resulted in extensive spectroscopic information characterizing its 10 μm spectral region. Specifically, a list of parameters for 65420 lines of the ν_{10} / ν_7 / ν_4 / ν_{12} bands has been built, which provides a description of the 620 – 1525 cm^{-1} spectral region improved over the information currently available in the HITRAN and GEISA databases. This updated reference information will be proposed for inclusion in forthcoming updates of these databases.

3. POLICY SUPPORT

Trend results and emission determinations such as those presented in Mahieu et al. (2014) are key elements to support decision makers. Indeed, we would like to point out that our results dealing with the monitoring of halogenated source gases at the Jungfraujoch have been solicited for inclusion in the recent edition of the WMO assessment on ozone depletion (2014, see in particular Figure 1-2 and Table 1-2).

Another important result of the project is the detection of the recent increase of C_2H_6 above Jungfraujoch which is likely linked to the exploitation of shale gas and oil in the US. Impact of associated fugitive emissions (of methane and light alkanes) is the subject of follow-up studies, to evaluate with the help of model simulations the corresponding emissions and determine the impact on air quality and contribution to tropospheric ozone formation, a major pollutant, a threat for human health and a greenhouse gas. Our results relevant to these issues will be proposed as a contribution to the upcoming Tropospheric Ozone Assessment Report of GAW.

The European Copernicus initiative aims at providing user-oriented scientific information; the users are not only the scientific community but also policy makers and the public at large. Some of the AGACC-II products like the MAXDOAS aerosol extinction profiles and the FTIR HCHO and CH_4 are already or will be delivered to the Copernicus Atmospheric Monitoring Service (CAMS) for the validation of the CAMS products. They contribute to the quality assessment of the CAMS products - for ensuring that reliable information is delivered to the users.
NDACC and TCCON data will also be proposed for inclusion in the Copernicus Climate Service (C3S) Data Store.

Other data sets produced by the AGACC-II teams are also relevant for decision-making. This is e.g. the case for multidecadal ozone time series produced by KMI or stratospheric chlorine data sets derived from the long-term FTIR monitoring programme at Jungfraujoch. We are indeed solicited on a yearly basis to contribute to Regional assessments, i.e. the MIRA-T (het Milieurapport Vlaanderen) and the ICEW document (see etat.environnement.wallonie.be).

4. DISSEMINATION AND VALORISATION

In 2013, KMI-IRM started participating in a new **COST action (EUBREWNET: A European Brewer Network** – www.eubrewnet.org) which coordinates Brewer spectrophotometer measurements of ozone, spectral UV and AOD in the UV within Europe.
In the frame of the development of a coordinated system for the LIDAR observation in Europe, KMI-IRM is involved in two major European projects, with the goal to make available the measurements of its future LIDAR ceilometers network to the European meteorological community in near real time. In EUMETNET, KMI-IRM participates in the **E-PROFILE program** (http://www.eumetnet.eu/e-profile) to develop an operational LIDAR ceilometer network by the exchange of LIDAR-ceilometer backscatter data in a standard format and the maintenance of an archive of communicated data and metadata for all systems connected to the networks.
KMI-IRM also participates in a COST Action: **TOPROF** (http://www.toprof.imaa.cnr.it/). The aim of this action is to coordinate the operation of many ceilometers installed across Europe, in order to build a network and to provide quality controlled and calibrated observations of aerosols in the lowest few kilometers of the atmosphere to national meteorological services in near real time.
Quicklooks of the Lidar-ceilometer backscatter profiles are put on the ceilomaps of DWD (http://www.dwd.de/ceilomap).

Spurred on by one of the postdocs supported by AGACC-II (Tomas FOLDES), the ULB partner started to develop activities aiming to measure pollutants *in situ* using Continuous-Wave Cavity Ring-Down Spectroscopy (CW-CRDS) [see for example (von Bobrutzki et al, 2010) and (Phillips et al, 2013)]. The sensitivity of a home-made CW-CRDS spectrometer was improved (Földes, 2013), as demonstrated by application to the detection of clusters of isotopic water vapor and ammonia with argon (Didriche and Földes, 2013; Didriche *et al.*, 2013). Building upon this expertise, Tomas FOLDES developed a portable CW-CRDS-based spectrometer and demonstrated its efficiency for ***in situ*** **and on line detection and monitoring of trace pollutants in drinking water in Brussels.** This activity is at the centre of a two-years **project recently accepted bythe *Institut Bruxellois pour la Recherche et l'Innovation* (INNOVIRIS), which will start on 1 January 2016.**

BIRA initiated a collaboration with Brazilian research institutes via the international networking project BAAF, Belgian-Brazilian network for studying the Atmosphere above the Amazonian Forest, and got involved in international research projects for studying the **atmospheric composition above the Amazonian region**, together with UK and German partners. These projects will benefit form the experience acquired through AGACC-II concerning the detection of biomass burning products and BVOCs above Reunion Island, and concerning the greenhouse gas (TCCON) measurements at La Reunion.

Experience acquired in AGACC-II and the previous AGACC-I project, has lend us a good international visibility and leadership regarding some aspects. As a corollary, BIRA led the exploitation of the NDACC FTIR Ozone time series for the determination of trends – that led to a peer-reviewed publication, a contribution to **SI2N** (SPARC/IOC/IGACO-O3/NDACC initiative for assessing trends in the vertical

distribution of ozone) and the **GAW TOAR** (Tropospheric Ozone Assessement REeport), as well as contributions to the **WMO Assessment of Ozone Depletion 2014**. ULg participated in all of these studies. Moreover, ULg coordinated the investigations on the recent trend of stratospheric chlorine, involving decadal ground-based FTIR time series, satellite measurements and simulations by state-of-the-art 3D CTM models. The results from this study are now available in a paper published in Nature (Mahieu et al., 2014).

The TCCON measurements at Ile de La Réunion, initiated and maintained in the AGACC-II project, have been included in the EU FP7 Research Infrastructure project ICOS_Inwire. One of the objectives of that project is to enhance the capabilities of the ICOS atmospheric and ecosystem networks through the ICOS Thematic Centers (TC) for producing new timely delivery and near real time data products as well as of GHG surface (ICOS) and total column (TCCON) concentration, boundary layer height from lidar and eddy-covariance GHG fluxes. In the frame of ICOS_Inwire, we indeed developed a rapid-delivery system for submitting the TCCON data to the ICOS Atmospheric TC. In other words, through AGACC-II and the ICOS_Inwire project, we got connected to the **ICOS Research Infrastructure** at the Reunion Observatory. It is also in that context that we bought a PICARRO in-situ greenhouse gas analyser that is now operational at the Maido observatory.

G. Pinardi (BIRA) spent three weeks **at the University of Burundi** in Bujumbura (18/01/2015- 06/02/2015) where she gave 30h of **lectures** to 2nd master physics on "introduction to physics and chemistry of the atmosphere".

Some of the laboratory spectroscopic work carried out within AGACC-II may not necessarily result in an update of international spectroscopic databases. However, they put forward some inconsistencies and possible problems that may trigger further analysis and possible updates of the public databases. The work carried out for the ν_1+3ν_2^1 band of carbon dioxide certainly falls into that category.

5. PUBLICATIONS

Theses

Bader, W., Extension of the long-term total column time series of atmospheric methane above the Jungfraujoch station: analysis of grating infrared spectra between 1977 and 1989, master thesis, Université de Liège, 17 Allée du 6 Août, 4000-Liège, Belgium, pp. 1-95, 2011b.

Bader, W., Long-term study of methane and two of its derivatives from solar observations at the Jungfraujoch station, PhD thesis, Université de Liège, 19 Allée du 6 Août, 4000-Liège, Belgium, pp. 1-148, November 2015.

Duchatelet, P., Fluorine in the atmosphere: Inorganic fluorine budget and long-term trends based on FTIR measurements at Jungfraujoch, PhD thesis, University of Liège, 17 Allée du 6 Août, 4000-Liège, Belgium, pp. 1-182, May 2011. [http://hdl.handle.net/2268/91413]

Peer-reviewed publications

A. Alkadrou; M.-T. Bourgeois; M. Rotger; V. Boudon & J. Vander Auwera. Global frequency and intensity analysis of the v10/v7/v4/v12 band system of 12C2H4 at 10 μm using the D2h Top Data System. Journal of Quantitative Spectroscopy and Radiative Transfer, Volume 182, Pages 158-171, 2016.

Angelbratt, J., Mellqvist, J., Simpson, D., Jonson, J. E., Blumenstock, T., Borsdorff, T., Duchatelet, P., Forster, F., Hase, F., Mahieu, E., De Mazière, M., Notholt, J., Petersen, A. K., Raffalski, U., Servais, C., Sussmann, R., Warneke, T., and Vigouroux, C.: Carbon monoxide (CO) and ethane (C2H6) trends from ground-based solar FTIR measurements at six European stations, comparison and sensitivity analysis with the EMEP model, Atmos. Chem. Phys., 11, 9253-9269, 2011.

Bader, W., T. Stavrakou, J.-F. Müller, S. Reimann, C.D. Boone, J.J. Harrison, O. Flock, B. Bovy, B. Franco, B. Lejeune, C. Servais, and E. Mahieu, Long-term evolution and seasonal modulation of methanol above Jungfraujoch (46.5ºN, 8.0ºE): Optimisation of the retrieval strategy, comparison with model simulations and independent observations, Atmos. Meas. Tech., 7, 3861-3872, 2014. [http://hdl.handle.net/2268/168055]

Daneshvar L., T. Földes, J. Buldyreva, J. Vander Auwera, Infrared absorption by pure CO_2 near 3340 cm^{-1}: Measurements and analysis of collisional coefficients and line-mixing effects at subatmospheric pressures, Journal of Quantitative Spectroscopy and Radiative Transfer 149 (2014) 258-274.

De Bock, V., De Backer, H., Van Malderen, R., Mangold, A. and Delcloo, A., Relations between erythemal UV dose, global solar radiation, total ozone column and aerosol optical depth at Uccle, Belgium, Atmos. Chem. Phys., 14, 12251-12270, doi: 10.5194/acp-14-12251-2014, 2014.

De Smedt, I., Stavrakou, T., Hendrick, F., Danckaert, T., Vlemmix, T., Pinardi, G., Theys, N., Lerot, C., Gielen, C., Vigouroux, C., Hermans, C., Fayt, C., Veefkind, P., Müller, J.-F., and Van Roozendael, M.: Diurnal, seasonal and long-term variations of global formaldehyde columns inferred from combined OMI and GOME-2 observations, Atmos. Chem. Phys., 15, 12519-12545, doi:10.5194/acp-15-12519-2015, 2015.

Didriche K, T. Földes, High resolution spectroscopy of the Ar-D_2O and Ar-HDO molecular complexes in the near-infrared range, Journal of Chemical Physics 138 (2013) 104307/1-7.

Didriche K., T. Földes, T. Vanfleteren, M. Herman, Overtone (2NH) spectroscopy of NH_3–Ar, Journal of Chemical Physics 138 (2013) 181101.

Dils, B., J. Cui, S. Henne, E. Mahieu, M. Steinbacher, M. De Mazière, 1997-2007 CO trend at the high Alpine site Jungfraujoch: A comparison between NDIR surface in situ and FTIR remote sensing observations, doi:10.5194/acp-11-6735-2011, Atmos. Chem. Phys., 11, 6735–6748, 2011.

Duflot, V., Hurtmans, D., Clarisse, L., R'honi, Y., Vigouroux, C., De Mazière, M., Mahieu, E., Servais, C., Clerbaux, C., and Coheur, P.-F.: Measurements of hydrogen cyanide (HCN) and acetylene (C_2H_2) from the Infrared Atmospheric Sounding Interferometer (IASI), Atmos. Meas. Tech., 6, 917-925, doi:10.5194/amt-6-917-2013, 2013.

Duflot, V., Wespes, C., Clarisse, L., Hurtmans, D., Ngadi, Y., Jones, N., Paton-Walsh, C., Hadji-Lazaro, J., Vigouroux, C., De Mazière, M., Metzger, J.-M., Mahieu, E., Servais, C., Hase, F., Schneider, M., Clerbaux, C. and Coheur, P.-F.: Acetylene (C_2H_2) and hydrogen cyanide (HCN) from IASI satellite observations: global distributions, validation, and comparison with model, Atmospheric Chemistry and Physics, 15(18), 10509–10527, doi:10.5194/acp-15-10509-2015, 2015.

Földes T., A very simple circuit for piezo actuator pseudo-tracking for continuous-wave cavity ring-down spectroscopy, Review of Scientific Instrumentation 84 (2013) 016102/1-3.

Franco, B., W. Bader, G.C. Toon, C. Bray, A. Perrin, E.V. Fischer, K. Sudo, C.D. Boone, B. Bovy, B. Lejeune, C. Servais, and E. Mahieu, Retrieval of ethane from ground-based FTIR solar spectra using improved spectroscopy: recent burden increase above Jungfraujoch, J. Quant. Spectrosc. Radiat. Transfer, 160, 36-49, 2015. [http://hdl.handle.net/2268/175442]

Franco, B., F. Hendrick, M. Van Roozendael, J.-F. Müller, T. Stavrakou, E. A. Marais, B. Bovy, W. Bader, C. Fayt, C. Hermans, B. Lejeune, G. Pinardi, C. Servais, and E. Mahieu, Retrievals of formaldehyde from ground-based FTIR and MAX-DOAS observations at the Jungfraujoch station and comparisons with GEOS-Chem and IMAGES model simulations, Atmos. Meas. Tech., 8, 1733-1756, 2015. [http://hdl.handle.net/2268/174025]

Franco, B., Marais, E. A., Bovy, B., Bader, W., Lejeune, B., Roland, G., Servais, C. and Mahieu, E.: Diurnal cycle and multi-decadal trend of formaldehyde in the remote atmosphere near 46° N, Atmospheric Chemistry and Physics Discussions, 15(21), 31287–31333, doi:10.5194/acpd-15-31287-2015, 2015.

Gielen, C., M. Van Roozendael, F. Hendrick, G. Pinardi, T. Vlemmix, V. De Bock, H. De Backer, C. Fayt, C. Hermans, D. Gillotay, and P. Wang, A simple and versatile cloud-screening method for MAX-DOAS retrievals, Atmos. Meas. Tech., 7, 3509-3527, doi: 10.5194/amt-7-3509-2014, 2014.

Hendrick, F., E. Mahieu, G. E. Bodeker, K. F. Boersma, M. P. Chipperfield, M. De Mazière, I. De Smedt, P. Demoulin, C. Fayt, C. Hermans, K. Kreher, B. Lejeune, G. Pinardi, C. Servais, R. Stübi, R. van der A, J.-P. Vernier, and M. Van Roozendael, Analysis of stratospheric NO2 trends above Jungfraujoch using ground-based UV-visible, FTIR, and satellite nadir observations, Atmospheric Chemistry and Physics, 12, 8851-8864, 2012.

Hendrick, F., J.-F. Müller, K. Clémer, M. De Mazière, C. Fayt, C. Gielen, C. Hermans, J. Z. Ma, G. Pinardi, T. Stavrakou, T. Vlemmix, P. Wang, and M. Van Roozendael, Four

Years of Ground-based MAX-DOAS Observations of HONO and NO_2 in the Beijing Area, Atmospheric Chemistry and Physics, 14, 765-781, 2014.

Kohlhepp, R., Ruhnke, R., Chipperfield, M. P., De Mazière, M., Notholt, J., Barthlott, S., Batchelor, R. L., Blatherwick, R. D., Blumenstock, Th., Coffey, M. T., Demoulin, P., Fast, H., Feng, W., Goldman, A., Griffith, D. W. T., Hamann, K., Hannigan, J. W., Hase, F., Jones, N. B., Kagawa, A., Kaiser, I., Kasai, Y., Kirner, O., Kouker, W., Lindenmaier, R., Mahieu, E., Mittermeier, R. L., Monge-Sanz, B., Morino, I., Murata, I., Nakajima, H., Palm, M., Paton-Walsh, C., Raffalski, U., Reddmann, Th., Rettinger, M., Rinsland, C. P., Rozanov, E., Schneider, M., Senten, C., Servais, C., Sinnhuber, B.-M., Smale, D., Strong, K., Sussmann, R., Taylor, J. R., Vanhaelewyn, G., Warneke, T., Whaley, C., Wiehle, M., and Wood, S. W.: Observed and simulated time evolution of HCl, $ClONO_2$, and HF total column abundances, Atmos. Chem. Phys., 12, 3527-3556, doi:10.5194/acp-12-3527-2012, 2012

Lamouroux J., L. Régalia, X. Thomas, J. Vander Auwera, R.R. Gamache, J.-M. Hartmann, CO_2 line-mixing database and software update and its tests in the 2.1 and 4.3 μm regions, Journal of Quantitative Spectroscopy and Radiative Transfer 151 (2015) 88-96.

Lattanzi F., C. di Lauro, J. Vander Auwera, Toward the understanding of the high resolution infrared spectrum of C_2H_6 near 3.3 μm, Journal of Quantitative Spectroscopy and Radiative Transfer 267 (2011) 71-79.

Mahieu, E., R. Zander, G.C. Toon, M.K. Vollmer, S. Reimann, J. Mühle, W. Bader, B. Bovy, B. Lejeune, C. Servais, P. Demoulin, G. Roland, P.F. Bernath, C.D. Boone, K.A. Walker, and P. Duchatelet, Spectrometric monitoring of atmospheric carbon tetrafluoride (CF_4) above the Jungfraujoch station since 1989: evidence of continued increase but at a slowing rate, Atmos. Meas. Tech., 7, 333-344, 2014. [http://hdl.handle.net/2268/154767]

Paulot, F., Wunch, D., Crounse, J. D., Toon, G. C., Millet, D. B., DeCarlo, P. F., Vigouroux, C., Deutscher, N. M., González Abad, G., Notholt, J. Warneke, T., Hannigan, J. W., Warneke, C., de Gouw, J. A., Dunlea, E. J., De Mazière, M., Griffith, D. W. T., Bernath, P., Jimenez, J. L., and Wennberg, P. O.: Importance of secondary sources in the atmospheric budgets of formic and acetic acids, Atmos. Chem. Phys., 11, 1989-2013, 2011.

Pinardi, G., M. Van Roozendael, N. Abuhassan, C. Adams, A. Cede, K. Clémer, C. Fayt, U. Frieß, M. Gil, J. Herman, C. Hermans, F. Hendrick, H. Irie, A. Merlaud, M. Navarro Comas, E. Peters, A. J. M. Piters, O. Puentedura, A. Richter, A. Schönhardt, R. Shaiganfar, E. Spinei, K. Strong, H. Takashima, M. Vrekoussis, T. Wagner, F. Wittrock, and S. Yilmaz, MAXDOAS formaldehyde slant column measurements during CINDI: intercomparison and analysis improvement, Atmospheric Measurement Techniques, 6, 167-185, 2013.

Rinsland, C.P., E. Mahieu, P. Demoulin, R.Zander, C. Servais, and J.-M. Hartmann, Decrease of the Carbon Tetrachloride (CCl_4) Loading above Jungfraujoch, based on High Resolution Infrared Solar Spectra recorded between 1999 and 2011, J. Quant. Spectrosc. Radiat. Transfer, 113, 1322-1329, 10.1016/j.jqsrt.2012.02.016, 2012. [http://hdl.handle.net/2268/121150]

Senten, C., De Mazière, M., Vanhaelewyn, G., and Vigouroux, C.: Information operator approach applied to the retrieval of the vertical distribution of atmospheric constituents from ground-based high-resolution FTIR measurements, Atmos. Meas. Tech., 5, 161-180, doi:10.5194/amt-5-161-2012, 2012.

Stavrakou, T., Guenther, A., Razavi, A., Clarisse, L., Clerbaux, C., Coheur, P.-F., Hurtmans, D., Karagulian, F., De Mazière, M., Vigouroux, C., Amelynck, C., Schoon, N., Laffineur, Q., Heinesch, B., Aubinet, M., Rinsland,. C., and Müller, J.-F.: First space-based derivation of the global atmospheric methanol emission fluxes, Atmos. Chem. Phys., 11, 4873-4898, 2011.

Stavrakou, T., J-F. Müller, J. Peeters, A. Razavi, L. Clarisse, C. Clerbaux, P.-F. Coheur, D. Hurtmans, M. De Mazière, C. Vigouroux, N. M. Deutscher, D. W. T. Griffith, N. Jones, C. Paton-Walsh, Satellite evidence for a large source of formic acid from boreal and tropical forests, Nature Geosci., 5, 26-30, doi: 10.1038/ngeo1354, 2012.

Tack, F., F. Hendrick, F. Goutail, C. Fayt, A. Merlaud, G. Pinardi, C. Hermans, J.-P. Pommerau, and M. Van Roozendael., Tropospheric nitrogen dioxide column retrieval from ground-based zenith-sky DOAS observations, Atmos. Meas. Tech. Discuss., 8, 936-985, 2015.

Theys, N., I. De Smedt, J. van Gent, T. Danckaert, T. Wang, F. Hendrick, T. Stavrakou, S. Bauduin, L. Clarisse, C. Li, N. Krotkov, H. Yu, H. Brenot, M. Van Roozendael, Sulphur dioxide vertical column DOAS retrievals from the Ozone Monitoring Instrument: global observations and comparison to ground-based and satellite data, J. Geophys. Res., 120, doi:10.1002/2014JD022657, 2015.

Vander Auwera, J., A. Fayt, M. Tudorie, M. Rotger, V. Boudon, B. Franco, and E. Mahieu, Self-broadening coefficients and improved line intensities for the ν_7 band of ethylene near 10.5 μm, and impact on ethylene retrievals from Jungfraujoch solar spectra, J. Quant. Spectrosc. Radiat. Transfer, 148, 177-185, 10.1016/j.jqsrt.2014.07.003, 2014. [http://hdl.handle.net/2268/169909]

van Geffen, J. H. G. M., K. F. Boersma, M. Van Roozendael, F. Hendrick, E. Mahieu, I. De Smedt, M. Sneep, and J. P. Veefkind, Improved spectral fitting of nitrogen dioxide from OMI in the 405–465nm window, Atmos. Meas. Tech., 8, 1685–1699, 2015.

Vigouroux, C., T. Stavrakou, C. Whaley, B. Dils, V. Duflot, C. Hermans, N. Kumps, J.-M. Metzger, F. Scolas, G. Vanhaelewyn, J.-F. Müller, D. B. A. Jones, Q. Li, and M. De Mazière, FTIR time-series of biomass burning products (HCN, C_2H_6, C_2H_2, CH_3OH, and HCOOH) at Reunion Island (21°S, 55°E) and comparisons with model data, Atmos. Chem. Phys., 12, 10367-10385, doi:10.5194/acp-12-10367-2012, 2012.

Vigouroux, C., Blumenstock, T., Coffey, M., Errera, Q., García, O., Jones, N. B., Hannigan, J. W., Hase, F., Liley, B., Mahieu, E., Mellqvist, J., Notholt, J., Palm, M., Persson, G., Schneider, M., Servais, C., Smale, D., Thölix, L., and De Mazière, M.: Trends of ozone total columns and vertical distribution from FTIR observations at eight NDACC stations around the globe, Atmos. Chem. Phys., 15, 2915-2933, doi:10.5194/acp-15-2915-2015, 2015.

Vlemmix, T., F. Hendrick, G. Pinardi, I. De Smedt, C. Fayt, C. Hermans, A. Piters, P. Levelt, and M. Van Roozendael, MAX-DOAS observations of aerosols, formaldehyde and nitrogen dioxide in the Beijing area: comparison of two profile retrieval approaches, Atmospheric Measurement Techniques, 8, 941-963, 2015.

Wang, T., F. Hendrick, P. Wang, G. Tang, K. Clémer, H. Yu, C. Fayt, C. Hermans, C. Gielen, J.-F. Müller, G. Pinardi, N. Theys, H. Brenot, and M. Van Roozendael, Evaluation of tropospheric SO2 retrieved from MAX-DOAS measurements in Xianghe, China, Atmospheric Chemistry and Physics, 14, 11149-11164, 2014.

Other publications

De Mazière, M., H. De Backer, E. Mahieu, J. Vander Auwera, W. Bader, V. De Bock, F. Desmet, T. Földes, C. Gielen, F. Hendrick, C. Hermans, B. Langerock, B. Lejeune, A. Mangold, M. Tudorie, R. Van Malderen, M. Van Roozendael et C. Vigouroux, Pas d'image fiable de notre terre sans mesures depuis le sol, Science Connection n°44, août-septembre 2014.

Pinardi, G., M. Van Roozendael, J.-C. Lambert, K. Clemer, I. De Smedt, F. Hendrick, C. Lerot, N. Theys, J. van Gent, T. Vlemmix, M. De Maziere, H. De Backer, A. Delcloo, and H. Yu, Integrated trace gas validation and quality assessment system for the EUMETSAT polar system, Proceedings of the EUMETSAT conference, Sopot, Poland, 3-7 September 2014.

Pinardi, G., M. Van Roozendael, J.C. Lambert, J. Granville, F. Hendrick, F. Tack, H. Yu, A. Cede, Y. Kanaya, H. Irie, F. Goutail, J.-P. Pommereau, F. Wittrock, T. Wagner, U. Friess, T. Vlemmix, A. Piters, N. Hao, M. Tiefengraber, J. Herman, N. Abuhassan, A. Bais, N. Kouremeti, J. Hovila, R. Holla, GOME-2 total and tropospheric NO2 validation based on ZenithSky, DirectSun and MAXDOAS network observations, Proceedings of the EUMETSAT conference, Geneva, Switzerland, 22-26 September 2014.

Stavrakou, T., Müller, J.-F., Bauwens, M., De Smedt, I., Van Roozendael, M., De Mazière, M., Vigouroux, C., Hendrick, F., George, M., Clerbaux, C., Coheur, P.-F., and Guenther, A.: How consistent are top-down hydrocarbon emissions based on formaldehyde observations from GOME-2 and OMI?, Atmos. Chem. Phys., 15, 11861-11884, doi:10.5194/acp-15-11861-2015, 2015.

Vigouroux, C.: Ground-based FTIR measurements of volatile organic compounds: precious data for model and satellite validation, NDACC newsletter, vol. 5, September 2013. http://www.ndsc.ncep.noaa.gov/news/archives/ (See Annex, publication No. 11)

Communications

Oral:

Bader, W., B. Bovy, B. Franco, B. Lejeune, E. Mahieu, S. Conway, K. Strong, I. Murata, D. Smale, A. Turner, P. Bernath, and E. Buzan, Recent changes of CH_4 since 2005 from FTIR observations and GEOS-CHEM simulation, oral presentation at the *2015 NDACC-IRWG meeting*, June 8-12, 2015, University of Toronto, Toronto, ON, 2015.

Bourgeois M.-T., M. Rotger, M. Tudorie, J. Vander Auwera, V. Boudon, Frequency analysis of the 10 μm region of the ethylene spectrum using the D_{2h} Top Data System, Oral presentation at the 68th Ohio State University International Symposium on Molecular Spectroscopy, Columbus, Ohio, USA, 17-21 June 2013

Buldyreva J., J. Vander Auwera, A theoretical model for wide-band infrared-absorption molecular spectra at any presssure: fiction or reality?, Oral presentation at the 69th International Symposium on Molecular Spectroscopy, Champaign-Urbana, Illinois, USA, 16-20 June 2014

Dammers E. , C. Vigouroux, M. Palm, M. Van Damme, D. Smale, N.B.Jones, H. Nakajima, G.C. Toon, J. Notholt, C. Petri, J.W. Erisman: Retrival of ammonia from FTIR measurements and a first comparison with IASI-NH3, oral presentation, IRWG annual meeting, Bad-Sulza, Germany, 12-15 June, 2014.

Daneshvar L., T. Földes, S. Léonis, J. Buldyreva, J. Vander Auwera, Infrared absorption by pure CO_2 near 3300 cm^{-1}: measurements of collisional broadening and shift coefficients and analysis of line-mixing effects at subatmospheric pressures, Oral presentation at the 2014 GEISA Workshop « Towards a new vision of spectroscopic databases », Paris, France, 3-4 June 2014

De Bock, V., Aerosol optical depth measurements at 340 nm with a Brewer spectrophotometer and comparison with Cimel sunphotometer observations at Ukkel, Belgium, presentatie op het KMI, 5 oktober 2011.

De Bock, V., "AGACC-II: Advanced exploitation of Ground based measurements for Atmospheric Chemistry and Climate Applications - II: RMI project results, conference at RMI, 10 December 2014, Uccle, Belgium.

De Bock, V., “Brewer AOD retrieval at RMI using DS measurements”, COST ES1207 - Eubrewnet WG2-WG3 meeting, 27-28 January 2015, Santa Cruz de Tenerife, Spain.

De Mazière, M., Site Report for Ile de la Réunion, oral presentation at the TCCON/IRWG Meeting, Wengen, Switzerland, June 11-15, 2012.

De Mazière, M., C. Hermans, Atmospheric composition monitoring using infrared spectrometry, seminar for the Instituto Federal De Educação Ciencia E Tecnologia De Rondonia (IFECTR) - Campus Porto Velho, February, 26, 2014.

De Mazière, Martine & T. Warneke, Planned FTIR solar absorption measurements of atmospheric short-lived and carbon gases at Porto Velho, oral presentation at the Amazonian Carbon Observatory (ACO) Workshop, (Keswick, UK), Sept. 16-17, 2014.

De Mazière, Martine, Filip Desmet, Christian Hermans, Jean-Marc Metzger, Jean-Pierre Cammas: The Belgian Institute for Space Aeronomy and ICOS (oral presentation), ICOS Belgium Study Day, Antwerp, Belgium, April 22 2015.

Demoulin, P., G. Roland, W. Bader, B. Lejeune, P. Duchatelet, E. Mahieu, C. Servais, and R. Zander, Analysis of historical grating spectra : Jungfraujoch atmospheric database extended back to 1977, oral presentation at the *2011 NDACC Symposium*, 7-10 November 2011, Saint Paul, La Réunion, France, 2011.

De Smedt, I., M. Van Roozendael, T. Danckaert, T. Vlemmix, G. Pinardi, F. Hendrick, H. Yu, T. Stavrakou, J.-F. Müller, On the formaldehyde diurnal variation as observed with GOME-2 and OMI, ground-based measurements and model simulations, Oral presentation at the 6th International DOAS Workshop, Boulder, USA, 12-14 August 2013

De Smedt, I., M. Van Roozendael, T. Stavrakou, J.-F. Müller, G. Pinardi, and F. Hendrick, Satellite observations of tropospheric formaldehyde combining GOME-2 and OMI measurements, Oral presentation at the General Assembly of the European Geosciences Union, Vienna, Austria, 27 April-2 May 2014

Desmet, F., M. De Mazière, C. Hermans, F. Scolas, N. Kumps, TCCON Site Report for Île de la Réunion, oral presentation at TCCON/IRWG Meeting, Wengen, Switzerland, June 11-15, 2012.

Desmet, Filip, Christian Hermans, Nicolas Kumps, Francis Scolas, Corinne Vigouroux, Bavo Langerock, Martine De Mazière, Jean-Marc Metzger, Jean-Pierre Cammas, Reunion Island site report, oral presentation by F. Desmet at the NDACC IRWG Annual meeting, Bad Sulza, Germany, May 12-15, 2014.

Desmet, F., B. Langerock, C. Vigouroux, N. Kumps, C. Hermans, M. De Mazière, J.-M. Metzger, J.-P. Cammas, The Fourier Transform InfraRed (FTIR) measurements at La Réunion - Maido & Results of the ACTRIS TNA missions, oral presentation by M. De Mazière at the ACTRIS 4th General Assembly, Clermont-Ferrand, June 10-13, 2014.

Desmet, Filip, Christian Hermans, Martine De Mazière, Huilin Chen, Bert Kers, Marcel de Vries, Rigel Kivi, Pauli Heikinnen, Juha Hatakka, Tuomas Laurila, Florin Mingireanu, Aurel Chirila: Greenhouse Gas Measurements at La Réunion in the frame of TCCON and ICOS (oral presentation), ICOS Science Conference, Brussels, Belgium, September 24 2014.

Dils, B., J. Cui, S. Henne, E. Mahieu, M. Steinbacher, M. De Mazière, NDIR surface in situ and FTIR remote sensing measurements at the Jungfraujoch see different CO trends, oral presentation at the EGU General Assembly 2011, Vienna, Austria, 6-8 April 2011.

Dils, B., J. Cui, S. Henne, E. Mahieu, M. Steinbacher, M. De Mazière, 1997-2007 CO at the high Alpine site Jungfraujoch: A comparison between NDIR surface in situ and FTIR remote sensing observations, Seminar at BIRA, Brussels, 24 June 2011.

De Mazière, M., and M. Van Roozendael, Spectrometry and atmospheric research: a fruitful marriage, invited lecture at the 25 Spektrometertagung (25th Conference of Spectrometry), Schaffhausen, 26-28/9/2011.

Duflot V., Clarisse L., Coheur P. F., Wespes C., Murphy C., Jones N., Hurtmans D., Hadji-Lazaro J., Ngadi Y., R'honi Y., Vigouroux C., De Mazière M., Metzger J.-M., Mahieu E.,Servais C., Blumenstock T., Hase F., Schneider M., and Clerbaux C.: Near-real-time measurements of acetylene (C2H2) and hydrogen cyanide (HCN) from IASI: method, validation, global distribution and comparison with model, oral presentation, IASI Conference, Hyères, France, 4 – 8 Feb, 2013.

Fissiaux L., T. Földes, F. Kwabia Tchana, L. Daumont, M. Lepère, J. Vander Auwera, Infrared line intensities for formaldehyde from simultaneous measurements in the infrared and far infrared spectra ranges, Oral presentation at the 66th Ohio State University International Symposium on Molecular Spectroscopy, Columbus, Ohio, USA, 20-24 juin 2011.

Franco, B., W. Bader, B. Bovy, E. Mahieu, E.V. Fischer, K. Strong, S. Conway, J.W. Hannigan, E. Nussbaumer, P.F. Bernath, C.D. Boone, and K.A. Walker, Recent increase of ethane detected in the remote atmosphere of the Northern Hemisphere, oral and PICO presentations at the *"EGU 2015 General Assembly"*, 12-17 April 2015, Vienna, Austria, 2015.

Franco, B., W. Bader, E. Mahieu, B. Bovy, E.V. Fischer, Z.A. Tzompa-Sosa, K. Strong, S. Conway, J.W. Hannigan, E. Nussbaumer, K. Sudo, P.F. Bernath, C.D. Boone, and K.A. Walker, Recent ethane increase above North America: comparison between FTIR measurements and model simulations, oral presentation at the *2015 NDACC-IRWG meeting*, June 8-12, 2015, University of Toronto, Toronto, ON, 2015.

Franco, B., F. Hendrick, M. Van Roozendael, J.-F. Müller, T. Stavrakou, E. Marais, B. Bovy, W. Bader, C. Fayt, C. Hermans, B. Lejeune, G. Pinardi, C. Servais, and E. Mahieu, Retrievals of formaldehyde from ground-based FTIR and MAX-DOAS observations at the Jungfraujoch station and comparisons with GEOS-Chem and IMAGES model simulations, oral presentation at the "NORS/NDACC/GAW workshop", 5-7 November 2014, Brussels, Belgium, 2014.

Gebhardt, C., A. Rozanov, R. Hommel, M. Weber, J. P. Burrows, F. Hendrick, and M. Van Roozendael, Linear changes/trends of stratospheric BrO as seen by SCIAMACHY limb for the decade 2002-12, PICO presentation at the General Assembly of the European Geosciences Union, Vienna, Austria, 27 April-2 May 2014

Gielen, C., M. Van Roozendael, F. Hendrick, C. Fayt, C. Hermans, G. Pinardi, and T. Vlemmix, Development of a cloud-screening method for MAX-DOAS observations, Oral presentation at the 6th International DOAS Workshop, Boulder, USA, 12-14 August 2013

Gielen, C., M. Van Roozendael, F. Hendrick, G. Pinardi, I. De Smedt, C. Hermans, C. Fayt, Y. Hu, E. Ndenzako, P. Nzohabonayo, R. Akimana, A first look at African aerosol and trace-gas emissions from the Bujumbura station, Oral presentation at the NORS/NDACC/GAW workshop, Brussels, Belgium, 5-7 November 2014

Goutail, F., A. Pazmino, J.-P. Pommereau, D. Ionov, F. Hendrick, R. D. Evans, E. Kyrö, and M. Van Roozendael, SAOZ total ozone measurements: Application of the new NDACC settings and comparisons to correlative ground-based and satellite observations, Oral presentation at the 2011 NDACC Symposium, Reunion Island, France, 7-10 November 2011

Gu, M., C.-F. Enell, F. Hendrick, J. Pukite, M. Van Roozendael, U. Platt, U. Raffalski, and T. Wagner, Stratospheric NO2 vertical profile retrieved from ground-based Zenith-Sky DOAS observations at Kiruna, Sweden, PICO presentation at the General Assembly of the European Geosciences Union, Vienna, Austria, 27 April-2 May 2014

Hannigan, J.W., M. Palm, S. Conway, E. Mahieu, D. Smale, E. Nussbaumer, K. Strong, and J. Notholt, Current trend in carbon tetrachloride from several NDACC FTIR stations, oral presentation at the "*Solving the mystery of carbon tetrachloride*" workshop, 4-6 October 2015, Empa Akademie, Duebendorf, Switzerland, 2015.

Hao, N., M. Van Roozendael, A. Ding, B. Zhou, F. Hendrick, Y. Shen, T. Wang, and P. Valks, Retrieval of tropospheric NO2 vertical column densities and aerosol optical properties form MAX-DOAS measurements in Yangtze River Delta, China, Oral presentation at the General Assembly of the European Geosciences Union, Vienna, Austria, 27 April-2 May 2014

Hendrick, F., Y. Kasai, P. Baron, K. Kreher, M. De Mazière, A. Rozanov, and M. Van Roozendael, Validation of JEM-SMILES BrO scientific and operational products using ground-based zenith-sky UV-visible observations, Oral presentation at the SMILES International Workshop 2011 Spring, Kyoto, Japan, 14-15 March 2011

Hendrick, F., P. Demoulin, K. Kreher, M. De Mazière, P. Duchâtelet, C. Fayt, C. Hermans, B. Lejeune, E. Mahieu, G. Pinardi, C. Servais, and M. Van Roozendael, Trend analysis of stratospheric NO2 above Jungfraujoch (46.5°N, 8.0°E) using long-term ground-based UV-visible, FTIR, and satellite observations, Oral presentation at the General Assembly of the European Geosciences Union, Vienna, Austria, 3-8 April 2011

Hendrick, F., P. Demoulin, K. Kreher, G. Bodeker, M. De Mazière, P. Duchâtelet, C. Fayt, C. Hermans, B. Lejeune, E. Mahieu, G. Pinardi, C. Servais, and M. Van Roozendael, Trend analysis of stratospheric NO2 above Jungfraujoch (46.5°N, 8.0°E) using long-term ground-based UV-visible, FTIR, and satellite observations, Oral presentation at the 5th International DOAS Workshop, Mainz, Germany, 13-15 July 2011

Hendrick, F., P. Demoulin, G. Bodeker, K. F. Boersma, M. P. Chipperfield, E. Mahieu, M. De Mazière, P. Duchâtelet, C. Fayt, C. Hermans, K. Kreher, B. Lejeune, E. Mahieu, G. Pinardi, C. Servais, and M. Van Roozendael, Trend analysis of stratospheric NO2 above Jungfraujoch (46.5°N, 8.0°E) using long-term ground-based UV-visible, FTIR, and satellite nadir observations, Oral presentation at the 2011 NDACC Symposium, Reunion Island, France, 7-10 November 2011

Hendrick, F., J.-F. Müller, M. De Mazière, C. Fayt, C. Hermans, T. Stavrakou, P. Wang, and M. Van Roozendael, Four Years of Ground-based MAX-DOAS Observations of HONO and NO2 in the Beijing Area, Oral presentation at the General Assembly of the European Geosciences Union, Vienna, Austria, 07-12 April 2013

Hendrick, F., J.-F. Müller, M. De Mazière, C. Fayt, C. Gielen, C. Hermans, G. pinardi, T. Stavrakou, P. Wang, and M. Van Roozendael, Four Years of Ground-based MAX-

DOAS Observations of HONO and NO2 in the Beijing Area, Oral presentation at the 6th International DOAS Workshop, Boulder, USA, 12-14 August 2013

Hendrick, F., J.-F. Müller, M. De Mazière, C. Fayt, C. Gielen, C. Hermans, G. pinardi, T. Stavrakou, P. Wang, and M. Van Roozendael, Four Years of Ground-based MAX-DOAS Observations of HONO and NO2 in the Beijing Area, BIRA Seminar, 30 August 2013

Hendrick, F., C. Fayt, B. Franco, C. Gielen, C. Hermans, E. Mahieu, J.-F. Müller, G. Pinardi, T. Stavrakou, and M. Van Roozendael, Retrieval of HCHO from MAX-DOAS measurements at the high-altitude alpine station of Jungfraujoch (46.5°N, 8.0°E), Oral presentation at the General Assembly of the European Geosciences Union, Vienna, Austria, 27 April-2 May 2014

Hendrick, F., C. Fayt, B. Franco, C. Gielen, C. Hermans, E. Mahieu, J.-F. Müller, G. Pinardi, T. Stavrakou, and M. Van Roozendael, Retrieval of HCHO from MAX-DOAS measurements at the high-altitude alpine station of Jungfraujoch (46.5°N, 8.0°E), Oral presentation at the ACTRIS VOCs/NOx Workshop, Dübendorf, Switzerland, 2-5 June 2014.

Hendrick, F., I. Boyd, M. De Mazière, C. Fayt, U. Friess, M. Gil, F. Goutail, C. Hermans1, C. Gielen, L. Gomez, B. Langerock, M. Navarro Comas, S. Niemeijer, A. Pazmino, G. Pinardi, J.-P. Pommereau, O. Puentedura, J. Remmers, A. Richter, C. Robles González, F. Tack, T. Vlemmix, T. Wagner, F. Wittrock, M. Yela, and M. Van Roozendael, Overview of the progress made by the NDACC UV-vis Working Group during the NORS project, Oral presentation at the NORS/NDACC/GAW workshop, Brussels, Belgium, 5-7 November 2014

Hendrick, F., C. Gielen, C. Lerot, T. Stavrakou, I. De Smedt, C. Fayt, C. Hermans, J.-F. Müller, G. Pinardi, R. Volkamer, P. Wang, and M. Van Roozendael, Retrieval of CHOCHO from MAX-DOAS measurements in the Beijing area, Oral presentation at the 7th International DOAS Workshop, Brussels, Belgium, 6-8 July 2015.

Keppens A., D. Hubert, J. Granville, J.-C. Lambert, B. Dils, M. De Mazière, C. Vigouroux, and (Multi-)TASTE GHG Team: (Multi-)TASTE: NDACC-based Validation Of Envisat Greenhouse Gas Data Products And Their Evolution, oral presentation, IWGGMS-10, ESA-ESTEC, Noordwijk, Netherlands, May 5-7, 2014.

Kolonjari, F., K.A. Walker, E. Mahieu, C.D. Boone, S. Strahan, C. McLinden, G.L. Manney, W.H. Daffer, and P.F. Bernath, Measurements of HCFC-22 and validation update, oral presentation at the “ACE Science Team Meeting”, 23-24 May 2012, University of Waterloo, Waterloo, ON, Canada, 2012.

Kolonjari, F., K.A. Walker, C.D. Boone, S. Strahan, E. Mahieu, C. McLinden, G.L. Manney, W.H. Daffer, and P.F. Bernath, Assessing the losses of HCFC-22 using ACE-FTS measurements, oral presentation at the “Canadian Network for the Detection of Atmospheric Change (CANDAC) Workshop/CREATE-Arctic Atmospheric Science Research Symposium”, 8-9 November 2012, Toronto, ON, Canada, 2012.

Kurylo, M., and NDACC contributors: Long term changes in the stratosphere and upper stratosphere: NDACC, oral presentation at the 2nd SI2N workshop, Columbia, Maryland, 16 -18 April 2012.

Laffineur Q., De Backer H., Nemeghaire J., and Debal F., "Illustration of physical processes with LIDAR ceilometer measurements", Third Joint Meeting on meteorological applications and forecasts including warnings, Brussels, Belgium, 21-22 November 2013.

Laffineur, Q. and Haeffelin, M. (given by M. Haeffelin), "Investigate fog prediction capabilities of ALC profiles", TOPROF meeting, Roskilde, Denmark, 19 November 2014.

Langerock, B., SFIT uncertainty computations at BIRA-IASB, oral presentation at the IRWG/NORS Workshop on uncertainties, (Boulder, Co), Jan. 28-Feb. 1, 2013.

Lerot**,** C., T. Stavrakou, F. Hendrick, I. De Smedt, J.-F. Müller, R. Volkamer, and M. Van Roozendael, Global observations of glyoxal columns from OMI/Aura and GOME-2/Metop-A sensors and comparison with multi-year simulations by the IMAGES model, Oral presentation at the General Assembly of the European Geosciences Union, Vienna, Austria, 12 April-17 April 2015.

Mahieu, E., Recent results from long-term FTIR monitoring activities at Jungfraujoch: some unexpected trends and new target species, oral presentation at the meeting "Spawning the atmosphere measurements of Jungfraujoch, Schneefernerhaus and Sonnblick", 22-23 January 2014, Bern, Switzerland, 2014.

Mahieu, E., W. Bader, B. Bovy, B. Franco, B. Lejeune, C. Servais, J. Notholt, M. Palm, and G.C. Toon, Halogenated source gases measured by FTIR at the Jungfraujoch station: updated trends and new target species, oral and PICO presentations at the *"EGU 2015 General Assembly"*, 12-17 April 2015, Vienna, Austria, 2015.

Merlaud, A., C. Fayt, J. Van Gent, X. Toledo, O. Ronveaux, F. Hendrick, and M. Van Roozendael, DOAS measurements of NO2 from an ultralight aircraft during the Earth Challenge Expedition, Oral presentation at the Sino-German Workshop on Remote Sensing of Atmospheric Pollutants in Chinese Megacities, Hefei, China, 31 May-3 June 2011. Chairman of the session on Retrieval of trace gas and aerosol vertical profiles from MAX-DOAS.

Merlaud, A., C. Fayt, J. Van Gent, F. Hendrick, X. Toledo, O. Ronveaux, and M. Van Roozendael, DOAS measurements of NO2 from an ultralight aircraft during the Earth Challenge Expedition, Oral presentation at the 5th International DOAS Workshop, Mainz, Germany, 13-15 July 2011

Merlaud, A., C. Fayt, G. Pinardi, F. Tack, F. Hendrick, A.-L. Le Roux, D.-E. Constantin, M. Voiculescu, R. Shaiganfar, T. Wagner, and M. Van Roozendael, Five years of NO2 Mobile-DOAS measurements in Europe: an overview, Oral presentation at the General Assembly of the European Geosciences Union, Vienna, Austria, 27 April-2 May 2014

Pinardi, G., M. Van Roozendael, J.C. Lambert, J. Granville, F. Hendrick, F. Tack, H. Yu, A. Cede, Y. Kanaya, H. Irie, F. Goutail, J.-P. Pommereau, F. Wittrock, T. Wagner, U. Friess, T. Vlemmix, A. Piters, N. Hao, M. Tiefengraber, J. Herman, N. Abuhassan, GOME-2 total and tropospheric NO2 validation based on ZenithSky, DirectSun and MAXDOAS network observations, Oral presentation at the EUMETSAT conference, Geneva, Switzerland, 22-26 September 2014

Pinardi, G., M. Van Roozendael, J.C. Lambert, J. Granville, F. Hendrick, F. Tack, H. Yu, A. Cede, Y. Kanaya, H. Irie, F. Goutail, J.-P. Pommereau, F. Wittrock, T. Wagner, U. Friess, T. Vlemmix, A. Piters, N. Hao, M. Tiefengraber, J. Herman, N. Abuhassan, A. Bais, N. Kouremeti, J. Hovila, R. Holla, GOME-2 total and tropospheric NO2 validation based on ZenithSky, DirectSun and MAXDOAS network observations, Oral presentation at the NORS/NDACC/GAW workshop, Brussels, Belgium, 5-7 November 2014

Pommereau, J.-P., F. Goutail, A. Pazmino, D. Ionov, F. Hendrick, and M. Van Roozendael, Evaluation of satellite total ozone and NO2 columns using the SAOZ UV-vis network, Oral presentation at the ESA Atmospheric Science Conference 2012, Bruges, Belgium, 18-22 June 2012

Pommereau, J.-P., F. Goutail, A. Pazmino, D. Ionov, F. Hendrick, and M. Van Roozendael, Evaluation of Satellites NO2 Columns using the SAOZ UV-Vis Network, Oral presentation at the ESA ACVE conference, Frascati, Italy, 13-15 March 2013

Senten, C., M. De Mazière, G. Vanhaelewyn, and C. Vigouroux, Information operator approach applied to ground-based FTIR measurements at Ile de La Réunion and compared with optimal estimation approach, oral presentation at the NDACC Infrared Working Group Meeting, NCAR, Boulder, CO, May 23-25, 2011.

Theys, N., M. Van Roozendael, F. Hendrick, X. Yang, I. De Smedt, A. Richter, M. Begoin, P. V. Johnston, K. Kreher, and M. De Mazière, Global observations of tropospheric BrO columns using GOME-2, Oral presentation at the 5th International DOAS Workshop, Mainz, Germany, 13-15 July 2011

Theys, N., I. De Smedt, M. Van Roozendael, L. Froidevaux, L. Clarisse, and F. Hendrick, Satellite detection of volcanic halogens (OClO, BrO and HCl) after the eruption of Puyehue-Cordón Caulle, Oral presentation at the General Assembly of the European Geosciences Union, Vienna, Austria, 27 April-2 May 2014

Tudorie M., C. di Lauro, F. Lattanzi, J. Vander Auwera, An improved rotational analysis of the ν_7 band of ethane, Oral presentation at the International workshop on the spectroscopy of methane and derived molecules for atmospheric and planetary applications, Dole, France, 26-28 November 2012

Vander Auwera J., J. Buldyreva, Collisional line-shape and line-mixing parameters for CO_2 absorption near 3340 cm^{-1}: measurements and modeling, Oral presentation at the 13th Biennial HITRAN Conference, Harvard, Massachussetts, USA, 23-25 June 2014

Vander Auwera J, FTIR laboratory spectroscopy and reference data, Oral presentation at the 6th meeting of the NOMAD science working team, Centre Spatial de Liège, April 20-22, 2015.

Vanhaelewyn, G., C. Vigouroux, M. De Mazière, Systematic error due to the choice in a priori profile, oral presentation by M. De Mazière at the NDACC Infrared Working Group Meeting, NCAR, Boulder, CO, May 23-25, 2011.

Van Roozendael, M., A. Rozanov, P. V. Johnston, M. De Mazière, C. Fayt, C. Hermans, K. Kreher, and F. Hendrick, Trend analysis of stratospheric BrO using long-term ground-based UV-visible and satellite limb observations, Oral presentation at the 2011 NDACC Symposium, Reunion Island, France, 7-10 November 2011.

Vigouroux, C., T. Stavrakou, C. Whaley, B. Dils, V. Duflot, C. Hermans, N. Kumps, J.-M. Metzger, F. Scolas, G. Vanhaelewyn, J.-F. Müller, D. B. A. Jones, Q. Li, and M. De Mazière: Measurements of biomass burning products at Reunion Island ; comparisons with Chemistry-Transport models, oral presentation at AGACC-II meeting, Brussels, 29th September 2011.

Vigouroux, C., T. Stavrakou, C. Whaley, B. Dils, V. Duflot, C. Hermans, N. Kumps, J.-M. Metzger, F. Scolas, G. Vanhaelewyn, J.-F. Müller, D. B. A. Jones, Q. Li, and M. De Mazière: Time-series of biomass burning products from ground-based measurements at Reunion Island and comparisons with model data, oral presentation at NDACC symposium, Saint-Paul, 7-10th November 2011.

Vigouroux, C., T. Stavrakou, C. Whaley, B. Dils, V. Duflot, C. Hermans, N. Kumps, J.-M. Metzger, F. Scolas, G. Vanhaelewyn, J.-F. Müller, D. B. A. Jones, Q. Li, and M. De Mazière: Time-series of biomass burning products products (HCN, C2H6, C2H2, CH3OH, and HCOOH) at Reunion Island and comparisons with model data, oral presentation at IRWG meeting, Wengen, 11-15th June 2012.

Vigouroux C., M. De Mazière, P. Demoulin, C. Servais, T. Blumenstock, F. Hase, R. Kohlhepp, S. Barthlott, O. García, M. Schneider, J. Mellqvist, G. Personn, M. Palm, J. Notholt, J. Hannigan, M. Coffey, D. Smale, B. Liley, V. Sherlock, N. Jones, R. Kivi: Ozone variability and trends from ground-based FTIR network observations, oral presentation at IRWG annual meeting, 10-14 June, Abashiri, Japan, 2013.

Vigouroux, C., M. De Mazière, F. Desmet, B. Dils, C. Hermans, N. Kumps, B. Langerock, F. Scolas, J.-M. Metzger, M. Mahieu, T. Stavrakou J.-F. Müller : WP2 of AGACCII: Retrievals of CH3OH, CH3Cl, and C2H4, AGACCII meeting, oral presentation, Brussels, 18th December, 2013.

Vlemmix, T., F. Hendrick, I. De Smedt, G. Pinardi, A. Piters, and M. Van Roozendael, MAX-DOAS observations of formaldehyde, nitrogen dioxide, and aerosols in the Beijing area: Comparison of two profile retrieval approaches, Oral presentation at the ESA ACVE conference, Frascati, Italy, 13-15 March 2013

Vlemmix, T., F. Hendrick, G. Pinardi, I. De Smedt, C. Fayt, C. Hermans, C. Gielen, A. Piters, P. Levelt, and M. Van Roozendael, Comparison of two profile retrieval algorithms for MAX-DOAS: tropospheric profiles of NO2, HCHO and aerosols obtained from four years of observations in China, Oral presentation at the General Assembly of the European Geosciences Union, Vienna, Austria, 27 April-2 May 2014

Poster:

Alkadrou A., M.-T. Bourgeois, M. Rotger, M. Tudorie, J. Vander Auwera, V. Boudon, Modeling the 10 μm region of the ethylene spectrum using the D_{2h} Top Data System : Frequency and intensity analysis, Poster presentation at the 23rd International Conference on High Resolution Molecular Spectroscopy, Bologna, Italy, 1-6 September 2014

Alkadrou A., M.-T. Bourgeois, M. Rotger, M. Tudorie, J. Vander Auwera, V. Boudon, Modeling the 10 μm region of the ethylene spectrum using the D_{2h} Top Data System : Frequency and intensity analysis, Poster presentation at the *Colloque commun de la division de Physique Atomique, Moléculaire et Optique de la Société française de Physique et des Journées de Spectroscopie Moléculaire* (PAMO-JSM), Reims, France, 7-10 July 2014

Alkadrou A., M. Rotger, V. Boudon, J. Vander Auwera, Global frequency and intensity analysis of the $\nu_{10}/\nu_7/\nu_4/\nu_{12}$ band systemof $^{12}C_2H_4$ at 10 μm region using the D_{2h} Top Data System, Poster presentation at the 24th Colloquium on High Resolution Molecular Spectroscopy, Dijon, France, 24-28 August 2015.

Bader, W., B. Lejeune, P. Demoulin, P. Duchatelet, G. Roland, K. Sudo, H. Yashiro, and E. Mahieu, Extension of the long-term total column time series of atmospheric methane above the Jungfraujoch station: analysis of grating infrared spectra between 1976 and 1989, poster presentation at the *"EGU 2011 General Assembly"*, 3-8 April 2011, Vienna, Austria, 2011a.

Bader, W., E. Mahieu, B. Bovy, B. Lejeune, P. Demoulin, and C. Servais, First retrievals of methanol (CH3OH) above Jungfraujoch (46.5ºN): Optimization fo the retrieval strategy and information content, poster presentation at the "Journée des doctorants UNITER", 10 December 2012, Université Libre de Bruxelles, Belgique, 2012.

Bader, W., A. Perrin, D. Jacquemart, J.J. Harrison, G.C. Toon, K. Sudo, O.A. Søvde, P. Demoulin, C. Servais, and E. Mahieu, Retrievals of ethane from ground-based high-resolution FTIR solar observations with updated line parameters: determination of the optimum strategy for the Jungfraujoch station, poster presentation at the "11th Atmospheric Spectroscopy Applications" meeting (ASA2012), united with the "12th HITRAN Conference", 29 – 31 August 2012, Reims, France, 2012.

Bader, W., A. Perrin, D. Jacquemart, K. Sudo, H. Yashiro, M. Gauss, P. Demoulin, C. Servais, and E. Mahieu, Retrievals of ethane from ground-based high-resolution FTIR solar observations with updated line parameters: determination of the optimum strategy for the Jungfraujoch station, poster presentation at the "EGU 2012 General Assembly",

22-27 April 2012, Vienna, Austria and at the 4th Symposium on METEOrology and CLIMatology for PhD students - MeteoClim2012, 2012.

Bader, W., A. Perrin, D. Jacquemart, K. Sudo, H. Yashiro, O.E. Søvde, P. Demoulin, C. Servais, and E. Mahieu, Retrievals of ethane from ground-based high-resolution FTIR solar observations with updated line parameters: determination of the optimum strategy for the Jungfraujoch station, poster presentation at the "NDACC-IRWG Annual Meeting", 11-15 June 2012, Wengen, Switzerland, 2012.

Bader, W., E. Mahieu, B. Bovy, B. Lejeune, P. Demoulin, C. Servais, and J.J. Harrison, Evolution of methanol (CH_3OH) above the Jungfraujoch station (46.5ºN): variability, seasonal modulation and long-term trend, poster presentation at the "EGU 2013 General Assembly", 07-12 April 2013, Vienna, Austria, 2013.

Bader, W., B. Bovy, K. Wecht, F. Hase, and E. Mahieu, Seeking for causes of recent methane increase: comparison between GEOS-Chem tagged simulations and FTIR column measurements above Jungfraujoch, poster presentation at the joint NDACC-IRWG and TCCON meeting, 12 – 16 May 2014, Bad Sulza, Germany, 2014.

Bader, W., T. Stavrakou, J.-F. Müller, S. Reimann, C.D. Boone, J.J. Harrison, O. Flock, B. Bovy, B. Franco, B. Lejeune, C. Servais, and E. Mahieu, Long-term evolution and seasonal modulation of methanol above Jungfraujoch (46.5ºN, 8.0ºE): Optimisation of the retrieval strategy, comparison with model simulations and independent observations, poster presentation at the joint NDACC-IRWG and TCCON meeting, 12 – 16 May 2014, Bad Sulza, Germany, 2014.

Bourgeois M.-T., M. Rotger, V. Boudon, J. Vander Auwera, Frequency analysis of the 10 and 3 μm regions of the ethylene spectrum using the D_{2h} Top Data System, Poster presentation at the *Colloque commun de la Division de Physique Atomique, Moléculaire et Optique de la Société française de Physique et des Journées de Spectroscopie Moléculaire*, Metz, France, 3-6 July 2012

Bourgeois M.-T., M. Rotger, V. Boudon, J. Vander Auwera, Frequency analysis of the 10 and 3 μm regions of the ethylene spectrum using the D_{2h} Top Data System, Poster presentation at the 11th ASA Conference united with the 12th HITRAN Conference, Reims, France, 29-31 August 2012

Bourgeois M.-T., M. Rotger, V. Boudon, J. Vander Auwera, Frequency analysis of the 10 and 3 μm regions of the ethylene spectrum using the D_{2h} Top Data System, Poster presentation at the 22nd International Conference on High Resolution Molecular Spectroscopy, Prague, République tchèque, 4-8 September 2012

Bourgeois M.-T., M. Rotger, M. Tudorie, J. Vander Auwera, V. Boudon, Frequency analysis of the 10 μm region of the ethylene spectrum using the D_{2h} Top Data System, Poster presentation at the 23rd Colloquium on High Resolution Molecular Spectroscopy, Budapest, Hungary, 25-30 August 2013

Daneshvar L., T. Földes, S. Léonis, J. Buldyreva, J. Vander Auwera, Infrared absorption by pure CO_2 near 3300 cm^{-1}: measurements of collisional broadening and shift coefficients and analysis of line-mixing effects at subatmospheric pressures, Poster presentation at the 23rd Colloquium on High Resolution Molecular Spectroscopy, Budapest, Hungary, 25-30 August 2013

De Bock, V., H. De Backer and A. Mangold, Improved cloud screening for Aerosol Optical Depth measurements with a Brewer spectrophotometer, European Aerosol Conference, Manchester, United Kingdom, September 4-9, 2011.

De Bock, V., H. De Backer, R. Van Malderen, Analysis of an extensive time series of UV irradiation and AOD measurements in the UV-B region at Uccle, Belgium, International Radiation Symposium 2012, Berlin, Germany, 6-10 August 2012.

De Bock, V., H. De Backer, R. Van Malderen, Analysis of an extensive time series of UV irradiation and AOD measurements in the UV-B region at Uccle, Belgium, Quadrennial Ozone Symposium 2012, Toronto, Canada, 26-31 August 2012.

De Bock, V., H. De Backer, A. Mangold, Retrieval of Single Scattering Albedo values from Brewer spectrophotometer irradiance measurements at Uccle, Belgium, European Aerosol Conference 2012, Granada, Spain, 2-7 September 2012.

De Bock, V., Delcloo, A., Mangold, A. and De Backer, H., Modeling of aerosol optical properties with CHIMERE and OPAC and validation with Brewer and Cimel measurements at Brussels, Belgium, European Aerosol Conference 2013, Prague, Czech Republic, 1-6 September 2013.

De Bock, V., De Backer, H. and Mangold, A., "Aerosol Optical Depth retrieval from Brewer spectrophotometers at Uccle, Belgium", Eubrewnet open congres/14th WMO-GAW Brewer Users Group Meeting, Tenerife, 24-28 March, 2014 .

De Bock, V., Mangold, A., De Backer, H. and Delcloo, A., Aerosol optical properties during a 2014 smog period at Uccle, Belgium, European Aerosol Conference, Milan, Italy, 6-11 September 2015.

De Mazière M. , C. Hermans, F. Desmet, C. Vigouroux, B. Langerock, B. Dils, C. Bauer Aquino, L. Gatti : Belgian-Brazilian network for studying the Atmosphere above the Amazonian Forest (BAAF), poster presentation, IRWG annual meeting, Bad-Sulza, Germany, 12-15 June, 2014.

Demoulin, P., E. Mahieu, C. Servais, B. Lejeune, W. Bader, G. Roland, R. Zander, K. Walker, P. Bernath, M. Van Roozendael, and F. Hendrick, Long-term trends of NOy, Cly, and Fy above northern mid-latitude as inferred from Jungfraujoch, HALOE, and ACE-FTS infrared solar observations, Poster presentation at the Quadrennial Ozone Symposium 2012, Toronto, Canada, 27-31 August 2012

Desmet, F., C. Hermans, M. De Mazière, N. Kumps, F. Scolas, J-L. Baray, J-M. Metzger, The First Results from the New TCCON Station at Reunion Island, poster presentation at the EGU General Assembly, Vienna, April 2012.

Desmet, Filip, Christian Hermans, Corinne Vigouroux, Bavo Langerock, Francis Scolas, Nicolas Kumps, Martine De Mazière, Jean-Marc Metzger, Thierry Gaudo, Jean-Luc Baray: Reunion Island Site Report (poster presentation), TCCON/NDACC IRWG Meeting, June 10-14, 2013, Abashiri, Japan.

Duchatelet, P., R. Zander, E. Mahieu, J. Mühle, P. Demoulin, B. Lejeune, G. Roland, C. Servais, and O. Flock, First retrievals of carbon tetrafluoride (CF_4) from ground-based FTIR measurements: production and analysis of the two-decadal time series above the Jungfraujoch, poster presentation at the “EGU 2011 General Assembly”, 3-8 April 2011, Vienna, Austria, 2011.

Fissiaux L., T. Földes, F. Kwabia Tchana, L. Daumont, M. Lepère, J. Vander Auwera, Infrared line intensities for formaldehyde from simultaneous measurements in the infrared and far infrared spectra ranges, Poster presentation at the 22nd Colloquium on High Resolution Molecular Spectroscopy, Université de Bourgogne, Dijon, France, 29 August – 2 September 2011

Gielen, C., M. Van Roozendael, F. Hendrick, C. Fayt, C. Hermans, G. Pinardi, and T. Vlemmix, Development of a cloud-screening method for MAX-DOAS observations,

Poster presentation at the General Assembly of the European Geosciences Union, Vienna, Austria, 07-12 April 2013

Gielen, C., M. Van Roozendael, F. Hendrick, C. Fayt, C. Hermans, G. Pinardi, H. De Backer, V. De Bock, Q. Laffineur, and T. Vlemmix, The effect of cloud screening on MAX-DOAS aerosol retrievals, Poster presentation at the General Assembly of the European Geosciences Union, Vienna, Austria, 27 April-2 May 2014

Gielen, C., M. Van Roozendael, F. Hendrick, G. Pinardi, I. De Smedt, C. Fayt, C. Hermans, E. Ndenzako, P. Nzohabonayo, and R. Akimana, African aerosol and trace-gas emissions from the Central-African Bujumbura station, Poster presentation at the General Assembly of the European Geosciences Union, Vienna, Austria, 12 April-17 April 2015

Gil-Ojeda, M., M. Navarro-Comas, A. Redondas, O. Puentedura, F. Hendrick, M. Van Roozendael, J. Iglesias, E. Cuevas, Total ozone measurements from the NDACC Izaña subtropical station: Visible Spectroscopy versus Brewer and satellite instruments, Poster presentation at the Quadrennial Ozone Symposium 2012, Toronto, Canada, 27-31 August 2012

Gu, M., C.-F. Enell, J. Pukite, S. Kühl, F. Hendrick, M. Van Roozendael, U. Platt, U. Raffalski, Long-term variation of stratospheric NO2 from ground-based zenith-sky DOAS observations at Kiruna, Sweden, Poster presentation at the 6th International DOAS Workshop, Boulder, USA, 12-14 August 2013

Hannigan, J., M. De Maziere, Characterization of recent advances in vertical profile retrievals from the Fourier-transform infrared spectrometers in the NDACC IRW, poster presentation at the NDACC Symposium, St. Paul, La Réunion, Nov. 7-10, 2011.

Hendrick, F., D. Ionov, F. Goutail, C. Hermans, C. Fayt, E. Kyrö, A. Pazmino, J.-P. Pommereau, and M. Van Roozendael, New NDACC recommendations for the retrieval of total ozone columns from ground-based zenith-sky UV-visible observations, Poster presentation at the 2011 NDACC Symposium, Reunion Island, France, 7-10 November 2011

Hendrick, F., D. Ionov, F. Goutail, A. Pazmino, U. Friess, M. Gil, J.-C. Lambert, M. Navarro, M. Pastel, J.-P. Pommereau, A. Richter, T. Wagner, F. Wittrock, and M. Van Roozendael, New NDACC recommendations for the retrieval of stratospheric NO2 from ground-based zenith-sky UV-visible observations, Poster presentation at the General Assembly of the European Geosciences Union, Vienna, Austria, 22-27 April 2012

Hendrick, F., E. Mahieu, A. Rozanov, K. F. Boersma, M. De Mazière, P. Demoulin, C. Fayt, C. Hermans, G. Pinardi, and M. Van Roozendael, Trend analysis of stratospheric NO2 above Jungfraujoch (46.5°N, 8°E) and Harestua (60°N, 11°E) using long-term ground-based UV-visible, FTIR, and satellite observations, Poster presentation at the ESA Atmospheric Science Conference 2012, Bruges, Belgium, 18-22 June 2012

Hendrick, F., J.-F. Müller, K. Clémer, M. De Mazière, C. Fayt, C. Hermans, T. Stavrakou, T. Vlemmix, P. Wang, and M. Van Roozendael, Four years of ground-based MAX-DOAS observations of HONO and NO2 in the Beijing area, Poster presentation at the American Geophysical Union Fall Meeting, San Francisco, USA, 3-7 December 2012

Kolonjari, F., E. Mahieu, K.A. Walker, Y. Kasai, A. Kagawa, R. Lindenmaier, R.L. Batchelor, K. Strong, C.D. Boone, and P.F. Bernath, Validation of ACE-FTS using ground-based FTIR measurements of CFC-11, CFC-12 and HCFC-22, poster presentation at the 2012 Summer School in Arctic Atmospheric Science, 23-27 July 2012, Alliston, Canada, 2012.

Kolonjari, F., K.A. Walker, E. Mahieu, R.L. Batchelor, P.F. Bernath, C.D. Boone, S. Conway, L. Dan, D. Griffin, A. Harrett, Y. Kasai, A. Kagawa, R. Lindenmaier, K. Strong, and C.

Whaley, Validation of ACE-FTS measurements of CFC-11, CFC-12 and HCFC-22 using ground-based FTIRs, poster presentation at the “AGU Fall Meeting 2013”, 09-13 December 2013, San Fransisco, CA, USA, 2013.

Lamouroux J., L. Régalia, J. Vander Auwera, R.R. Gamache, J.-M. Hartmann, An update of the CO_2 line-mixing database and software and its tests in the 2.1 and 4.3 μm regions, Poster presentation at the 23rd International Conference on High Resolution Molecular Spectroscopy, Bologna, Italy, 1-6 September 2014

Laffineur Q., De Backer H., Delcloo A., Nemeghaire J., and Debal. F., Quality control on the retrieval of mixing layer height by LIDAR-ceilometer, European Geoscience Union General Assembly 2013, Vienna, 7-12 April 2013.

Laffineur, Q., Delcloo, A., De Backer, H., Adam, M. and Klugmann, D., "Observation of an intercontinental smoke plume over Europe on June 2013: some ambiguity in the determination of the source", European Geosciences Union, General Assembly 2014, Vienna, 27 April-2 May 2014.

Lambert, J., D. Hubert, J. Granville, O. Aulamo, T. Blumenstock, J. Burrows, H. De Backer, M. De Mazière, M. Gil, F. Goutail, F. Hase, F. Hendrick, G. Held, D. Ionov, P. Johnston, R. Kivi, G. Kopp, K. Kreher, E. Kyrö, E. Mahieu, S. Mikuteit, M. Navarro Comas, J. Notholt, A. Pazmiño, A. Piters, J.-P. Pommereau, O. Puentedura, A. Richter, R. Susmann, Y. Timofeyev, M. Van Roozendael, C. Vigouroux, T. Warneke, F. Wittrock, S. Wood, M. Yela Gonzalez, (Multi-)TASTE: Ten years of quality tasting of Envisat and TPM atmospheric composition retrievals with the NDACC network, Poster presentation at the ESA Living Planet Symposium, Edinburgh, UK, 9-13 September 2013

Maasakkers, J. D., K. F. Boersma, J. E. Williams, J. van Geffen, G. C. M. Vinken, M. Sneep, F. Hendrick, M. van Roozendael, and J. P. Veefkind, Vital improvements to the retrieval of tropospheric NO2 columns from the Ozone Monitoring Instrument, Poster presentation at the General Assembly of the European Geosciences Union, Vienna, Austria, 07-12 April 2013

Mahieu, E., J. Harrison, P.F. Bernath, G.C. Toon, C.P. Rinsland, P. Demoulin, P. Duchatelet, B. Lejeune, C. Servais, and M. De Mazière, First retrievals of methyl chloride from ground-based high-resolution FTIR solar observations, poster presentation at the “EGU 2011 General Assembly”, 3-8 April 2011, Vienna, Austria, 2011.

Mahieu, E., P. Duchatelet, R. Zander, B. Lejeune, W. Bader, P. Demoulin, G. Roland, C. Servais, C.P. Rinsland, M.J. Kurylo, and G.O. Braathen, Changes in atmospheric composition discerned from long-term NDACC measurements: trends in direct greenhouse gases derived from infrared solar absorption spectra recorded at the Jungfraujoch station, poster presentation at the World Climate Research Programme Open Science Conference, 24-28 October 2011, Denver, CO, USA, 2011.

Mahieu, E., P. Duchatelet, R. Zander, B. Lejeune, W. Bader, P. Demoulin, C. Servais, M. Schneider, S. Barthlott, and C.P. Rinsland, Long-term trends of a dozen direct greenhouse gases derived from infrared solar absorption spectra recorded at the Jungfraujoch station, poster presentation at the 2011 NDACC Symposium, 7-10 November 2011, Saint Paul, La Réunion, France, 2011.

Mahieu, E., W. Bader, B. Lejeune, C. Vigouroux, P. Demoulin, C. Servais, G. Roland, and R. Zander, Seeking for the optimum retrieval strategy of methanol (CH_3OH) using ground-based high-resolution FTIR solar observations recorded at the high-altitude Jungfraujoch station (46.5ºN), poster presentation at the “EGU 2012 General Assembly”, 22-27 April 2012, Vienna, Austria, 2012.

Mahieu, E., W. Bader, B. Bovy, B. Lejeune, C. Vigouroux, P. Demoulin, C. Servais, G. Roland, and R. Zander, Retrieval of methanol (CH_3OH) from the high-altitude

Jungfraujoch station (46.5ºN): preliminary total column time series, long-term trend and seasonal modulation, poster presentation at the "NDACC-IRWG Annual Meeting", 11-15 June 2012, Wengen, Switzerland, 2012.

Mahieu, E., S. O'Doherty, S. Reimann, M. Vollmer, W. Bader, B. Bovy, B. Lejeune, P. Demoulin, G. Roland, C. Servais, and R. Zander, First retrievals of HCFC-142b from ground-based high-resolution FTIR solar observations: application to high-altitude Jungfraujoch spectra, poster presentation at the "EGU 2013 General Assembly", 07-12 April 2013, Vienna, Austria, 2013.

Mahieu, E., B. Bovy, W. Bader, P. Demoulin, B. Franco, B. Lejeune, C. Servais, and C. Vigouroux, Overview of the geophysical data derived from long-term FTIR monitoring at the Jungfraujoch NDACC site (46.5°N), poster presented at the 6th International GEOS-Chem Meeting, 6-9 May 2013, Harvard University, Cambridge, MA, 2013.

Mahieu, E., B. Bovy, W. Bader, B. Franco, B. Lejeune, E.V. Fischer, E.A. Marais, A.J. Turner, J.W. Hannigan, E. Nussbaumer, K. Strong, and S. Conway, Use of GEOS-Chem for the interpretation of long-term FTIR measurements at the Jungfraujoch and other NDACC sites, poster presented at the *7th International GEOS-Chem Meeting*, 4-7 May 2015, Harvard University, Cambridge, MA, 2015.

Mahieu, E., W. Bader, B. Franco, B. Bovy, B. Lejeune, C. Servais, G. Roland, and R. Zander, Overview of the recent results derived from the Jungfraujoch observational database, poster presented at the *2015 NDACC-IRWG meeting*, June 8-12, 2015, University of Toronto, Toronto, ON, 2015.

Mahieu, E., P.F. Bernath, C.D. Boone, and K.A. Walker, Decrease of carbon tetrachloride (CCl_4) over 2004-2013 as inferred from global occultation measurements with ACE-FTS, poster presentation at the "*Solving the mystery of carbon tetrachloride*" workshop, 4-6 October 2015, Empa Akademie, Duebendorf, Switzerland, 2015.

Mangold, A., De Backer, H., Delcloo, A., De Bock, V., Hermans, C., Gorodetskaya, I., and W. Maenhaut, Seasonal physical and optical properties of atmospheric aerosol at Princess Elisabeth station, East Antarctica, European Aerosol Conference 2013, 1-6 September 2013, Prague, Czech Republic.

Mangold, A., Van Malderen, R., De Backer, H., Delcloo, A., De Bock, V., Gorodetskaya, I., Wex, H., and Hermans, C., "Observations of atmospheric composition, clouds and precipitation in Dronning Maud Land, East Antarctica", MOZAIC–IAGOS Scientific Symposium on Atmospheric Composition Observations by Commercial Aircraft: 20th Anniversary, Toulouse, 12-15 May 2014.

Nikitidou, E., V. De Bock, H. De Backer and A. Kazantzidis, Estimation of aerosol optical properties and their effect on UV irradiance at Ukkel, Belgium, 11th EMS Annual Meeting / 10th European Conference on Applications of Meteorology (ECAM), Berlin, Germany, September 12-16, 2011.

Nikitidou, E., V. De Bock, H. De Backer, A. Kazantzidis, Aerosols optical properties and their effect on the UV solar irradiance at Uccle, Belgium, International Radiation Symposium 2012, Berlin, Germany, 6-10 August 2012.

Pinardi, G., Huan Yu, F. Hendrick, F. Tack, J. Granville, J.-C. Lambert, and M. Van Roozendael, End-to-end validation of total and tropospheric NO2 columns from atmospheric composition satellite sensors, Poster presentation at the ESA ACVE conference, Frascati, Italy, 13-15 March 2013.

Pinardi, G. , M. Van Roozendael, J.-C. Lambert , J. Granville, M. De Mazière, H. De Backer, A. Delcloo , I. De Smedt, F. Hendrick , H. Yu , T. Wang, C. Lerot, N. Theys , J. van Gent , F. Tack, and C. Gielen, Trace gas validation and quality assessment system for

atmospheric sensors on METOP, Poster presentation at the 2013 EUMETSAT Meteorological Satellite Conference, Vienna, Austria, 16-20 September 2013

Pinardi**,** G., M. Van Roozendael, J.-C. Lambert, F. Hendrick, J. Granville, F. Tack, F. Goutail, J.-P. Pommereau, A. Pazmino, F. Wittrock, A. Richter, T. Wagner, M. Gu, U. Friess, M. Navarro, and O. Puentedura, Assessment of the stratospheric NO_2 column using long-term ground-based UV-visible and satellite nadir observations, PICO presentation at the General Assembly of the European Geosciences Union, Vienna, Austria, 12 April-17 April 2015

Plass-Dülmer, C., S. Reimann, M. Wallasch, S. Solberg, D. Klemp, P. Coddeville, and E. Mahieu, NMHC Climatology from Central European Mountain Observatories, poster presentation at the "EGU 2011 General Assembly", 3-8 April 2011, Vienna, Austria, 2011.

Pommereau, J.-P., F. Goutail, A. Pazmino, D. Ionov, F. Hendrick, and M. Van Roozendael, Evaluation of satellite total ozone retrievals using the NDACC-SAOZ UV-vis network, Poster presentation at the Quadrennial Ozone Symposium 2012, Toronto, Canada, 27-31 August 2012

Rotger M., M.A. Lorono, A. Alkadrou, J. Vander Auwera, V. Boudon, Frequency and intensity analysis of the 3 μm region of the ethylene spectrum using the D_{2h} Top Data System, Poster presentation at the 24th Colloquium on High Resolution Molecular Spectroscopy, Dijon, France, 24-28 August 2015.

Rozanov, A., C. Gebhardt, F. Hendrick, M. Weber, H. Bovensmann, W. Lotz, M. Van Roozendael, and J. P. Burronws, Stratospheric BrO trends observed from SCIAMACHY limb and ground-based UV-visible observations, Poster presentation at the Quadrennial Ozone Symposium 2012, Toronto, Canada, 27-31 August 2012

Schibig, M., M. Leuenberger, P. Nyfeler, and E. Mahieu, Comparison of continuous background in-situ and column integrated CO_2 observations at Jungfraujoch with an urban site in the city of Bern, poster presentation at the "EGU 2014 General Assembly", 27 April - 02 May 2014, Vienna, Austria, 2014.

Stavrakou, T., J.-F. Müller, M. Bauwens, I. De Smedt, M. Van Roozendael, M. De Mazière, C. Vigouroux: Hydrocarbon emissions constrained by formaldehyde column measurements from GOME-2 and OMI, poster presentation at AGU Fall meeting 2014, San Francisco, 10-12 December 2014.

Suleiman, R., K. Chance, T. Kurosu, G. Mount, E. Spinei, W. Simpson, K. Kreher, D. Donohoue, R. Salawitch, and F. Hendrick, Improved OMI BrO and OClO algorithms and BrO validation, Poster presentation at the American Geophysical Union Fall Meeting, San Francisco, USA, 5-9 December 2011

Tack, F., F. Hendrick, F. Goutail, C. Fayt, A. Merlaud, G. Pinardi, J.-P. Pommereau, and M. Van Roozendael, Tropospheric nitrogen dioxide column retrieval based on ground-based zenith-sky DOAS observations, Poster presentation at the General Assembly of the European Geosciences Union, Vienna, Austria, 27 April-2 May 2014

Tudorie M., C. di Lauro, F. Lattanzi, J. Vander Auwera, A new analysis of the ν_7 band of ethane, Poster presentation at the Solvay workshop on femto-, astro-, spectro-ethyne, Université Libre de Bruxelles, 2-5 May 2012

Tudorie M., C. di Lauro, F. Lattanzi, J. Vander Auwera, A new analysis of the ν_7 band of ethane, Poster presentation at the *Colloque commun de la Division de Physique Atomique, Moléculaire et Optique de la Société française de Physique et des Journées de Spectroscopie Moléculaire*, Metz, France, 3-6 July 2012

Tudorie M., C. di Lauro, F. Lattanzi, J. Vander Auwera, A new analysis of the ν_7 band of ethane, Poster presentation at the 11th ASA Conference united with the 12th HITRAN Conference, Reims, France, 29-31 août 2012

Tudorie M., C. di Lauro, F. Lattanzi, J. Vander Auwera, A new analysis of the ν_7 band of ethane, Poster presentation at the 22nd International Conference on High Resolution Molecular Spectroscopy, Prague, République tchèque, 4-8 September 2012

Vander Auwera, J., A. Fayt, M. Tudorie, M. Rotger, V. Boudon, B. Franco, and E. Mahieu, Self broadening coefficients and improved line intensities for the υ_7 band of ethylene near 10.5 µm, and impact on ethylene retrievals from Jungfraujoch spectra, poster presentation at the PAMO-JSM meeting, 7-10 July 2014, Reims, France, 2014.

Vander Auwera, J., A. Fayt, M. Tudorie, M. Rotger, V. Boudon, B. Franco, and E. Mahieu, Self broadening coefficients and improved line intensities for the υ_7 band of ethylene near 10.5 µm, and impact on ethylene retrievals from Jungfraujoch spectra, poster presentation at the 23rd International Conference on High Resolution Molecular Spectroscopy, 2-6 September 2014, Bologna, Italy, 2014.

Vigouroux, C., M. De Mazière, P. Demoulin, C. Servais, T. Blumenstock, M. Schneider, F. Hase, R. Kohlhepp, S. Barthlott, J. Klyft, J. Mellqvist, M. Palm, J. Notholt, J. Hannigan, M. Coffey, R. Batchelor, Ozone tropospheric and stratospheric trends (1995-2011) at six ground-based FTIR stations (28°N to 79°N), poster presentation at the NDACC symposium, St. Paul, La Réunion, Nov. 7-10, 2011.

Vigouroux, C., M. De Mazière, P. Demoulin, C. Servais, F. Hase, T. Blumenstock, M. Schneider, R. Kohlhepp, S. Barthlott, O. García, J. Mellqvist, G. Personn, M. Palm, J. Notholt, J. Hannigan, M. Coffey: Ozone tropospheric and stratospheric trends (1995-2011) at six ground-based FTIR stations (28°N to 79°N), poster presentation at QOS symposium, Toronto, 27-31st August 2012.

Vigouroux C., M. De Mazière, P. Demoulin, C. Servais, T. Blumenstock, F. Hase, R. Kohlhepp, S. Barthlott, O. García, M. Schneider, J. Mellqvist, G. Personn, M. Palm, J. Notholt, J. Hannigan, M. Coffey: Ozone tropospheric and stratospheric trends (1995-2012) at six ground-based FTIR stations (28°N to 79°N), poster presentation, EGU 2013 General Assembly, 7-12 April, Vienna, Austria, 2013.

Vigouroux C., De Mazière, M., Desmet, F., Hermans, C., Langerock., B., Scolas, F., Van Damme, M., L. Clarisse, Coheur, P.-F. : Ground-based FTIR measurements of NH3 total columns and comparison with IASI data, poster presentation, EGU 2013 General Assembly, 7-12 April, Vienna, Austria, 2013.

Vigouroux C., De Mazière, M., Desmet, F., Hermans, C., Langerock., B., Scolas, F., Van Damme, M., L. Clarisse, Coheur, P.-F. : Ground-based FTIR measurements of NH3 total columns and comparison with IASI data, poster presentation, IRWG annual meeting, 10-14 June, Abashiri, Japan, 2013.

Vigouroux C., M. De Mazière, P. Demoulin, C. Servais, T. Blumenstock, F. Hase, R. Kohlhepp, S. Barthlott, O. García, M. Schneider, J. Mellqvist, G. Personn, M. Palm, J. Notholt, J. Hannigan, M. Coffey, D. Smale, B. Liley, V. Sherlock, N. Jones, R. Kivi: Vertical ozone trends from NDACC FTIR observations, poster presentation, SI2N meeting, 18-19 September, Helsinki, Finland, 2013.

Wang, T., M. Van Roozendael, P. Wang, F. Hendrick, C. Fayt, H. Yu, C. Gielen, G. Pinardi, and C. Hermans, SO2 Validation of GOME-2, OMI and SCIAMACHY by Ground-based MAX-DOAS Measurements in the Beijing Area, Poster presentation at the ESA Living Planet Symposium, Edinburgh, UK, 9-13 September 2013

Wang, T., F. Hendrick, P. Wang, G. Tang, K. Clémer, H. Yu, C. Fayt, C. Hermans, C. Gielen, G. Pinardi, N. Theys, H. Brenot, and M. Van Roozendael, Evaluation of tropospheric

SO2 retrieved from MAX-DOAS measurements in Xianghe, China, Poster presentation at the General Assembly of the European Geosciences Union, Vienna, Austria, 27 April-2 May 2014

Zhao, X. C. Adams, K. Strong, R. L. Batchelor, P. F. Bernath, S. Brohede, D. Degenstein, W. H. Daffer, J. R. Drummond, P. F. Fogal, E. Farahani, C. Fayt, A. Fraser, F. Goutail, F. Hendrick, F. Kolonjari, R. Lindenmaier, G. Manney, C. T. McElroy, C. A. McLinden, J. Mendonca, J. H. Park, B. Pavlovic, A. Pazmino, C. Roth, V. Savastiouk, K. A. Walker, and D. A. Weaver, Validation of ACE and OSIRIS ozone measurements sung using ground-based instruments at 80°N, Poster presentation at the Quadrennial Ozone Symposium 2012, Toronto, Canada, 27-31 August 2012

6. REFERENCES

Bessagnet, B., Menut, L., Curci, G., Hodzic, A., Guillaume, B., Liousse, C., Moukhtar, S., Pun, B., Seigneur, C. and Schulz, M., Regional modeling of carbonaceous aerosols over Europe – focus on secondary organic aerosols, J. Atmos. Chem., 61(3), 175-202, doi: 10.1007/s10874-009-9129-2, 2008.

Blass W.E. et al., Absolute intensities in the ν_7 band of ethylene: tunable laser measurements used to calibrate FTS broadband spectra, Journal of Quantitative Spectroscopy and Radiative Transfer 68 (2001) 467-472.

Brannon J.F. Jr, P. Varanasi, Tunable diode laser measurements on the 951.7393 cm–1 line of 12C2H4 at planetary atmospheric temperatures, Journal of Quantitative Spectroscopy and Radiative Transfer 47 (1992) 237-242 & Corrigenda, Journal of Quantitative Spectroscopy and Radiative Transfer 49 (1993) 695-696.

Clémer, K., M. Van Roozendael, C. Fayt, F. Hendrick, C. Hermans, G. Pinardi, R. Spurr, P. Wang, and M. De Mazière, Multiple wavelength retrieval of tropospheric aerosol optical properties from MAXDOAS measurements in Beijing, Atmospheric Measurement Techniques, 3, 863-878, 2010.

Crisp D et al., The Orbiting Carbon Observatory (OCO) mission, Advanced Space Research 34 (2004) 700-709.

Crisp D et al., The need for atmospheric carbon dioxide measurements from space: Contributions from a rapid reflight of the Orbiting Carbon Observatory, http://www.nasa.gov/pdf/363474main_OCO_Reflight.pdf.

Daneshvar L., T. Földes, J. Buldyreva, J. Vander Auwera, Infrared absorption by pure CO_2 near 3340 cm^{-1}: Measurements and analysis of collisional coefficients and line-mixing effects at subatmospheric pressures, Journal of Quantitative Spectroscopy and Radiative Transfer 149 (2014) 258-274.

De Bock, V., De Backer, A., Mangold, A. and Delcloo, A., Aerosol Optical Depth measurements at 340 nm with a Brewer spectrophotometer and comparison with Cimel observations at Uccle, Belgium, Atmos. Meas. Tech., 3, 1577-1588, doi: 10.5194/amt-3-1577-2010, 2010.

De Bock, V., De Backer, H., Van Malderen, R., Mangold, A. and Delcloo, A.: Relations between erythemal UV dose, global solar radiation, total ozone column and aerosol optical depth at Uccle, Belgium, Atmos. Chem. Phys., 14, 12251-12270, doi: 10.5194/acp-14-12251-2014, 2014

Didriche K, T. Földes, High resolution spectroscopy of the Ar-D2O and Ar-HDO molecular complexes in the near-infrared range, Journal of Chemical Physics 138 (2013) 104307/1-7.

Didriche K., T. Földes, T. Vanfleteren, M. Herman, Overtone (2NH) spectroscopy of NH3–Ar, Journal of Chemical Physics 138 (2013) 181101.

Fabricant B., Krieger, D., Muenter, J.S., Molecular beam electric resonance study of formaldehyde, thioformaldehyde and ketene, Journal of Chemical Physics 67 (1977) 1576-1586.

Földes T., A very simple circuit for piezo actuator pseudo-tracking for continuous-wave cavity ring-down spectroscopy, Review of Scientific Instrumentation 84 (2013) 016102/1-3.

Gielen, C., M. Van Roozendael, F. Hendrick, G. Pinardi, T. Vlemmix, V. De Bock, H. De Backer, C. Fayt, C. Hermans, D. Gillotay, and P. Wang, A simple and versatile

cloud-screening method for MAX-DOAS retrievals, Atmospheric Measurement Techniques, 7, 3509-3527, 2014.

Gillotay, D., Besnard, T., and Zanghi, F.: A systematic approach of the cloud cover by thermic infrared measurements, Proceedings of 18th Conference on Weather Analysis and Forecasting, Fort Lauderdale, Fl, USA, 30 July–2 August 2001, 292–295, 2001.

Glatthor, N., von Clarmann, T., Fischer, H., Funke, B., Grabowski, U., Höpfner, M., Kellmann, S., Kiefer, M., Linden, A., Milz, M., Steck, T., and Stiller, G. P.: Global peroxyacetyl nitrate (PAN) retrieval in the upper troposphere from limb emission spectra of the Michelson Interferometer for Passive Atmospheric Sounding (MIPAS), Atmos. Chem. Phys., 7, 2775-2787, doi:10.5194/acp-7-2775-2007, 2007.

Harrison J.J., N.D.C. Allen, P.F. Bernath, Infrared absorption cross sections for ethane (C_2H_6) in the 3 μm region, Journal of Quantitative Spectroscopy and Radiative Transfer 111 (2010) 357-363.

Hendrick, F., J.-F. Müller, K. Clémer, M. De Mazière, C. Fayt, C. Gielen, C. Hermans, J. Z. Ma, G. Pinardi, T. Stavrakou, T. Vlemmix, P. Wang, and M. Van Roozendael, Four Years of Ground-based MAX-DOAS Observations of HONO and NO2 in the Beijing Area, Atmospheric Chemistry and Physics, 14, 765-781, 2014.

Hess, M., Koepke, P. and Schult, I., Optical Properties of Aerosols and Clouds: The software package OPAC, Bulletin of the American Meteorological Society, 79(5), 831-844, 1998.

Jacquinet-Husson N. et al., The 2009 edition of the GEISA spectroscopic database, Journal of Quantitative Spectroscopy and Radiative Transfer 112 (2011) 2395-2445.

Lamouroux J., L. Régalia, X. Thomas, J. Vander Auwera, R.R. Gamache, J.-M. Hartmann, CO_2 line-mixing database and software update and its tests in the 2.1 and 4.3 μm regions, Journal of Quantitative Spectroscopy and Radiative Transfer 151 (2015) 88-96.

Lattanzi F., C. di Lauro, J. Vander Auwera, Toward the understanding of the high resolution infrared spectrum of C_2H_6 near 3.3 μm, Journal of Quantitative Spectroscopy and Radiative Transfer 267 (2011) 71-79.

Lerot, C., T. Stavrakou, I. De Smedt, J.-F. Müller, and M. Van Roozendael, Glyoxal vertical columns from GOME-2 backscattered light measurements and comparisons with a global model, Atmospheric Chemistry and Physics, 10, 12059-12072, 2010.

Liang, Q., Newman, P. A., Daniel, J. S., Reimann, S., Hall, B. D., Dutton, G. and Kuijpers, L. J. M.: Constraining the carbon tetrachloride (CCl_4) budget using its global trend and inter-hemispheric gradient, Geophysical Research Letters, 41(14), 5307–5315, doi:10.1002/2014GL060754, 2014.

Madronich, S.: UV radiation in the natural and perturbed atmosphere, in: Teveni, M. (Ed.), Environmental Effects of Ultraviolet Radiation, Lewis, Boca Raton, FL., 17-69, 2003.

Mahieu, E., Chipperfield, M. P., Notholt, J., Reddmann, T., Anderson, J., Bernath, P. F., Blumenstock, T., Coffey, M. T., Dhomse, S. S., Feng, W., Franco, B., Froidevaux, L., Griffith, D. W. T., Hannigan, J. W., Hase, F., Hossaini, R., Jones, N. B., Morino, I., Murata, I., Nakajima, H., Palm, M., Paton-Walsh, C., Russell, J. M., Schneider, M., Servais, C., Smale, D. and Walker, K. A.: Recent Northern Hemisphere stratospheric HCl increase due to atmospheric circulation changes, Nature, 515(7525), 104–107, doi:10.1038/nature13857, 2014.

Perrin A., D. Jacquemart, F. Kwabia Tchana, N. Lacome, Absolute line intensities measurements and calculations for the 5.7 and 3.6 μm bands of formaldehyde, Journal of Quantitative Spectroscopy and Radiative Transfer 110 (2009) 700-716.

Phillips N.G. et al., Mapping urban pipeline leaks: Methane leaks across Boston, Environmental Pollution 173 (2013) 1-4.

Pine A.S., S.C. Stone, Torsional tunneling and A_1–A_2 splittings and air broadening of the $^rQ_0$ and $^pQ_3$ subbranches of the ν_7 band of ethane, Journal of Molecular Spectroscopy 175 (1996) 21-30.

Reinsel, G. C., Miller, A. J., Weatherhead, E. C., Flynn, L. E., Nagatani, R. M., Tiao, G. C., and Wuebbles, D. J.: Trend analysis of total ozone data for turnaround and dynamical contributions, J. Geophys. Res., 110, D16306, doi: 10.1029/2004JD004662, 2005.

Reuter D.C., J.M. Sirota, Absolute intensities and foreign gas broadening coefficients of the $1_{11,10}$– $1_{12,10}$ and $18_{0,18}$ – $11_{1,18}$ lines in the ν_7 band of C_2H_4, Journal of Quantitative Spectroscopy and Radiative Transfer 50 (1993) 477-482.

Rinsland C.P., E. Mahieu, R. Zander, P. Demoulin, J. Forrer, B. Buchmann, Free tropospheric CO, C2H6, and HCN above central Europe: recent measurements from the Jungfraujoch station including the detection of elevated columns during 1998, J. Geophys. Res. 105 (2000) 24235-24249.

Rinsland, C. P., G. Dufour, C. D. Boone, P. F. Bernath, L. Chiou, P.-F. Coheur, S. Turquety, and C. Clerbaux (2007), Satellite boreal measurements over Alaska and Canada during June–July 2004: Simultaneous measurements of upper tropospheric CO, C2H6, HCN, CH3Cl, CH4, C2H2, CH3OH, HCOOH, OCS, and SF6 mixing ratios, Global Biogeochem. Cycles, 21, GB3008, doi:10.1029/2006GB002795, 2007.

Rinsland, C. P., E. Mahieu, L. Chiou, and H. Herbin (2009), First ground-based infrared solar absorption measurements of free tropospheric methanol (CH3OH): Multidecade infrared time series from Kitt Peak (31.9°N 111.6°W): Trend, seasonal cycle, and comparison with previous measurements, J. Geophys. Res., 114, D04309, doi:10.1029/2008JD011003, 2009.

Rothman L.S. et al., The HITRAN 2012 molecular spectroscopic database, Journal of Quantitative Spectroscopy and Radiative Transfer 130 (2013) 4-50.

Rusinek E., H. Fichoux, F. Herlemont, J. Legrand, A. Fayt, SubDoppler study of the ν7 band of C2H4 with a CO2 laser sideband spectrometer, Journal of Molecular Spectroscopy 189 (1998) 64-73.

Santee, M.L., N. J. Livesey, N.J., G. L. Manney, A. Lambert, W. G. Read: Methyl Chloride from the Aura Microwave Limb Sounder: First Global Climatology and Assessment of Variability in the Upper Troposphere and Stratosphere, J. Geophys. Res., Accepted Article, doi: 10.1002/2013JD020235, 2013.

Stavrakou, T., A. Guenther, A. Razavi, L. Clarisse, C. Clerbaux, P.-F. Coheur, D. Hurtmans, F. Karagulian, M. De Mazière, C. Vigouroux, C. Amelynck, N. Schoon, Q. Laffineur, B. Heinesch, M. Aubinet, C. Rinsland, and J.-F. Müller, First space-based derivation of the global methanol emission fluxes, Atmos. Chem. Phys., 11, 4873–4898, 2011.

Stavrakou, T., J-F. Müller, J. Peeters, A. Razavi, L. Clarisse, C. Clerbaux, P.-F. Coheur, D. Hurtmans, M. De Mazière, C. Vigouroux, N. M. Deutscher, D. W. T. Griffith, N. Jones, C. Paton-Walsh, Satellite evidence for a large source of formic acid from boreal and tropical forests, Nature Geosci., 5, 26-30, doi: 10.1038/ngeo1354, 2012.

Stavrakou, T., Müller, J.-F., Bauwans, M., De Smedt, I., Van Roozendael, M., De Mazière, M., Vigouroux, C., Georges, M., Clerbaux, C., Coheur, P.-F., and Guenther, A.: How consistent are top-down hydrocarbon emissions based on formaldehyde observations from GOME-2 and OMI ?, submitted to ACP, 2015.

Steinbrecht, W., Claude, H., Schönenborn, F., McDermid, I. S., Leblanc, T., Godin, S., Song, T., Swart, D. P. J., Meijer, Y. J., Bodeker, G. E., Connor, B. J., Kämpfer, N., Hocke, K.,

Calisesi, Y., Schneider, N., de la Noë, J., Parrish, A. D., Boyd, I. S., Brühl, C., Steil, B., Giorgetta, M. A., Manzini, E., Thomason, L. W., Zawodny, J. M., McCormick, M. P., Russell III, J. M., Bhartia, P. K., Stolarski, R. S., and Hollandsworth-Frith, S. M.: Long-term evolution of upper stratospheric ozone at selected stations of the Network for the Detection of Stratospheric Change (NDSC), J. Geophys. Res., 111, D1027, doi: 10.1029/2005JD006454, 2006.

van der Werf, G. R., Randerson, J. T., Giglio, L., Collatz, G. J., Mu, M., Kasibhatla, P. S., Morton, D. C., DeFries, R. S., Jin, Y., and van Leeuwen, T. T.: Global fire emissions and the contribution of deforestation, savanna, forest, agricultural, and peat fires (1997–2009), Atmos. Chem. Phys., 10, 11707-11735, doi:10.5194/acp-10-11707-2010, 2010.

Vander Auwera J., A. Fayt, M. Tudorie, M. Rotger, V. Boudon, B. Franco, E. Mahieu, Self-broadening coefficients and improved line intensities for the $\nu 7$ band of ethylene near 10.5 mm, and impact on ethylene retrievals from Jungfraujoch solar spectra, Journal of Quantitative Spectroscopy and Radiative Transfer 148 (2014) 177-185.

Vautard, R., M. Beekmann, B. Bessagnet and L. Metut, Chimere – Un simulateur numérique de la quantité de l'air. (http://www.lmd.polytechnique.fr/chimere/docs/chimere-info20070131.pdf), 2007.

Vigouroux, C., Hendrick, F., Stavrakou, T., Dils, B., De Smedt, I., Hermans, C., Merlaud, A., Scolas, F., Senten, C., Vanhaelewyn, G., Fally, S., Carleer, M., Metzger, J.-M., Müller, J.-F., Van Roozendael, M., and De Mazière, M.: Ground-based FTIR and MAX-DOAS observations of formaldehyde at Réunion Island and comparisons with satellite and model data, Atmos. Chem. Phys., 9, 9523-9544, 2009.

Vlemmix, T., F. Hendrick, G. Pinardi, I. De Smedt, C. Fayt, C. Hermans, A. Piters, P. Levelt, and M. Van Roozendael, MAX-DOAS observations of aerosols, formaldehyde and nitrogen dioxide in the Beijing area: comparison of two profile retrieval approaches, Atmospheric Measurement Techniques, 8, 941-963, 2015.

Von Bobrutzki K. et al., Field inter-comparison of eleven atmospheric ammonia measurement techniques, Atmospheric Measurement Techniques 3 (2010) 91-112.

Wenger, C., Raballand, W., Rotger, M., Boudon, V., D2h Top Data System (D2h TDS) software for spectrum simulation of X2Y4 asymmetric molecules, Journal of Quantitative Spectroscopy and Radiative Transfer 95 (2005) 521-538.

Wenny, B. N., Saxena, V. K., and Frederick, J. E.: Aerosol optical depth measurements and their impact on surface levels of ultraviolet-B radiation, J. Geophys. Res., 106, 17311–17319, doi: 10.1029/2001JD900185, 2001.

ANNEX 1: COPY OF THE PUBLICATIONS

Only copies of peer reviewed publications have been included in this section. Copies of the other publications (conference proceedings, poster presentations, etc.) can be provided in addition, if requested.

ANNEX 2: MINUTES OF THE FOLLOW-UP COMMITTEE MEETINGS

The annexes are available on our website

http://www.belspo.be/belspo/SSD/science/pr_climate_en.stm